

Aus der Hals-Nasen-Ohren-Klinik der Universität Heidelberg
(Geschäftsführender Direktor: Prof. Dr. Dr. h.c. Peter Plinkert)
Abteilung Experimentelle und Translationale Kopf-Hals Onkologie
(Direktor: Prof. Dr. rer. nat. Jochen Hess)

**Estrogen receptor-related signaling networks as
prognostic biomarkers and therapeutic targets in head
and neck squamous cell carcinoma**

Inauguraldissertation
zur Erlangung des Doctor scientiarum humanarum (Dr.sc.hum)
an der
Medizinischen Fakultät Heidelberg
der Ruprecht-Karls-Universität

vorgelegt von
Chao Rong

aus
Hefei, China

2017

Dekan: Herr Prof. Dr. med. Wolfgang Herzog

Doktorvater: Herr Prof. Dr. rer. nat. Jochen Hess

To my parents and beloved wife

Table of contents

List of Figures	1
List of Tables	3
Abbreviations	4
1. Introduction	8
1.1 Epidemiological and clinical features of head and neck squamous cell carcinoma	8
1.2 Molecular mechanisms of HNSCC pathogenesis	12
1.2.1 Cellular proliferation and tumor suppressor genes.....	13
1.2.2 Overexpression of EGFR in HNSCC.....	14
1.2.3 PI3K-AKT-mTOR pathway.....	16
1.2.4 Ras-Raf-MEK-MAPK pathway	18
1.2.5 JAK-STAT pathway	18
1.2.6 Additional cancer-related genes and pathways.....	19
1.3 Preclinical mouse model for tumor recurrence	19
1.4 The opiorphin gene family	21
1.4.1 The pathophysiological function of opiorphin genes.....	21
1.4.2 Opiorphin genes in HNSCC	21
1.5 Aims of the study	22
2. Materials	23
2.1 Equipment and consumables	23
2.2 Chemicals	25
2.3 Molecular biological reagents	27
2.4 Antibodies	27
2.5 Buffers and solutions	28
2.6 Cell lines	29
2.7 Softwares	30
3. Methods	31
3.1 Cell culture	31
3.1.1 Cultivation of cell lines and treatment.....	31

3.1.2	Colony forming Assay	32
3.1.3	Immunofluorescence (IF)	33
3.1.4	Senescence-associated β -galactosidase (SA- β -gal) staining.....	34
3.2	Protein biochemistry methods	34
3.2.1	Protein extraction and determination of protein concentration.....	34
3.2.2	SDS polyacrylamide gel electrophoresis (SDS-PAGE)	35
3.2.3	Western bolt	35
3.3	Immunohistochemistry(IHC) with TSA.....	36
3.4	Tissue microarray (TMA).....	37
3.4.1	TMA production	37
3.4.2	TMA scoring	38
3.4.3	Statistical analysis	39
4.	Results.....	41
4.1	Co-expression of ESR2 and SMR3A in HNSCC and correlation with clinical features	41
4.2	Co-expression of OPRPN and SMR3A in HNSCC cell lines and response to fractionated irradiation	44
4.3	Expression of OPRPN in primary OPSCC and correlation with clinic-pathological features	45
4.4	Correlation of OPRPN and SMR3A expression with disease-specific and progression-free survival.....	49
4.5	Inhibition of ESR2 signaling sensitizes HNSCC cell lines to irradiation	51
4.6	Regulation of ESR2 and pERK1/2 in FaDu cells upon fractionated-IR and MEK1/2 inhibitor treatment.....	53
4.7	Impact of MEK1/2 inhibitor on the radiosensitivity of FaDu and Cal27 cells	55
4.8	Sensitivity of 6 HNSCC cell lines to MEK1/2 inhibitor.....	56
4.9	Regulation of ESR2 in FaDu and Cal27 cells after cetuximab treatment	57
4.10	Sensitivity of 6 HNSCC cell lines to cetuximab.....	59
4.11	Regulation of pERK1/2 and PD-L1 by cetuximab treatment.....	61
4.12	Impact of MEK1/2 inhibitor treatment and fractionated IR on PD-L1 expression in FaDu cells	64

4.13	Regulation of p-ERK1/2 and PD-L1 by MEK1/2 inhibitor treatment.	66
4.14	Effects of MEK1/2 inhibitor on p-Akt and p-Histone H2AX in HNSCC cell lines.	68
4.15	MEK1/2 inhibitor induced cellular senescence in HNSCC cell lines.....	70
5.	Discussion.....	72
5.1	Opiorphin genes serve as a surrogate marker for radioresistance.	72
5.2	Distinct functions of ESR subtypes in cancer.....	74
5.3	Targeting the ESR signaling for cancer therapy	77
5.4	Interaction of ESR with EGFR signaling	80
5.5	Effects of EGFR-MAPK pathway on PD-L1 expression in HNSCC.....	84
5.6	Conclusion and perspective.....	87
6.	Summary	89
7.	Bibliography.....	91
8.	Supplements	113
9.	Curriculum vitae.....	116
10.	Acknowledgements	117

List of Figures

Figure 1-1: Anatomical structure and subunits of the head and neck.	8
Figure 1-2: Incidence and mortality of HNSCC in the world and western Europe.	10
Figure 1-3: Progression model of phenotypical and genetic alterations in HNSCC.	13
Figure 1-4: Major signaling pathways involved in head and neck cancer.	16
Figure 1-5: Preclinical murine model for tumor relapse after surgery.	20
Figure 3-1: Schematic protocol of the colony forming Assay	33
Figure 3-2: Schematic diagram of wet electro-transfer technique.	36
Figure 4-1: SMR3A and ESR2 expression in HNSCC patients.	42
Figure 4-2: Co-expression of OPRPN and SMR3A in HNSCC cell lines in response to fractionated irradiation.	45
Figure 4-3: OPRPN protein expression in normal mucosa and primary tumors of OPSCC patients.	46
Figure 4-4: Progression-free survival and disease-specific survival in the cohort of OPSCC patients depending on OPRPN expression	49
Figure 4-5: Combinatorial analysis of progression-free survival and disease-specific survival in the cohort of OPSCC patients depending on OPRPN and SMR3A expression	50
Figure 4-6: Combinatorial analysis of progression-free survival and disease-specific survival in the subgroup of OPSCC patients with radiotherapy depending on OPRPN and SMR3A expression.	51
Figure 4-7: Impact of fulvestrant or TAM treatment on FaDu and Cal27 with fractionated IR.	53
Figure 4-8: Effect of fractionated-IR and MEK1/2 inhibitor treatment on ESR2 and phospho-ERK1/2 protein levels in FaDu cells.	54
Figure 4-9: PD-901 treatment sensitizes HNCC cell lines to fractionated IR.	56
Figure 4-10: Sensitivity of 6 HNSCC cell lines to MEK1/2 inhibitor PD-901.	57
Figure 4-11: Regulation of ESR2 by cetuximab in single dose treatment.	58
Figure 4-12: Regulation of ESR2 by cetuximab in three times-repeated treatment.	59
Figure 4-13: Sensitivity of 6 HNSCC cell lines to cetuximab.	60
Figure 4-14: Regulation of P-ERK1/2 and PD-L1 by cetuximab in single dose treatment.	62
Figure 4-15: Regulation of P-ERK1/2 and PD-L1 by cetuximab in three times-repeated treatment.	64
Figure 4-16: Impact of MEK1/2 inhibitor and fractionated IR on PD-L1 expression	

in FaDu cells.....	65
Figure 4-17: Regulation of P-ERK1/2 and PD-L1 by PD-901 in single dose treatment.	67
Figure 4-18: Regulation of P-ERK1/2 and PD-L1 by PD-901 in three times-repeated treatment.....	68
Figure 4-19: Effects of MEK1/2 inhibitor on p-AKT and p-Histone H2AX in HNSCC cell lines.....	69
Figure 4-20: Long-term treatment of PD-901 induced marker of cellular senescence in HNSCC cell lines.....	71
Figure 5-1. Structural composition of ESR1 and ESR2	75
Figure 5-2. Structure of 4-hydroxtamoxifen (A) and fulvestrant (B).....	79
Figure 5-3. Mechanism of the steroidal ER α antagonist, fulvestrant, at the level of transcriptional regulation.....	80
Figure 5-4. Schematic model for mechanisms on how the estrogen receptor (ESR) interacts with the epidermal growth factor receptor (EGFR) to influence the cellular signaling even and cells growth in the Lung cancer.	83

List of Tables

Table 2-1: Equipment and consumables	23
Table 2-2: Chemicals	25
Table 2-3: Molecular biological reagents	27
Table 2-4: Primary antibodies.....	27
Table 2-5: Secondary Antibodies.....	28
Table 2-6: Buffers and solutions	28
Table 2-7: Cell lines.....	29
Table 2-8: Softwares	30
Table 3-1: Substances used for cell treatment.....	32
Table 4-1: Correlation of ESR2 expression with histopathological and clinical characteristics.....	43
Table 4-2: Correlation analysis for OPRPN expression and clinic-pathological features in the OPSCC patients Cohort	48

Abbreviations

°C	degree Celsius
µg	microgram
µM	micromole
4-OH-TAM	4-Hydroxytamoxifen
aa	amino acids
ADCC	antibody dependent cellular cytotoxicity
AJCC	American Joint Committee on Cancer
AML	acute myeloid leukemia
APL	acute promyelocyte leukemia
APN	aminopeptidase N
APS	ammonium persulfate
Asp	aspartic acid
ATCC	American Type Culture Collection
BCA	bicinchoninic acid
BSA	albumin from bovine serum
CaCl ₂	calcium chloride
cAMP	cyclic adenosine monophosphate
CDK2	cyclin-dependent kinase 2
CDKN2A	cyclin-dependent kinase Inhibitor 2A
cDNA	complementary deoxyribonucleic acid
cetux	cetuximab
cm	centimetre
CO ₂	carbon dioxide
CTLA4	cytotoxic T lymphocyte-associated antigen 4
Ctrl	control
DAB	3,3'-diaminobenzidine
DBD	DNA-binding domain
ddH ₂ O	double distilled water
DKFZ	German Cancer Research Center
DMBA	7,12-Dimethylbenz(a)anthracene
DMEM	Dulbecco's Modified Eagle Medium
DMSO	dimethyl sulfoxide
DNA	deoxyribonucleic acid
DSS	disease-specific survival
DTT	dithiothreitol
ECL	enhanced chemiluminescence
ED	erectile dysfunction
EDTA	ethylenediaminetetraacetic acid
EGFR	epidermal growth factor receptor

EMT	epithelial-to-mesenchymal-transition
ERK	extracellular signal-regulated kinases
estrogen receptor	ESR
EtOH	ethanol
FBS	fetal bovine serum
FDA	Food and Drug Administration
g	gramm
Gy	gray
h	hour
H ₂ O	water
H ₂ O ₂	hydrogen peroxide
HCl	hydrochloric acid
Her2	human epidermal growth factor receptor 2
HGF	hepatocyte growth factor
HNSCC	head and neck squamous cell carcinoma
HPV	human papilloma virus
HRP	horseradish peroxidase
IHC	immunohistochemistry
IR	irradiation
ISH	in-situ hybridization
JAK	Janus kinase
kDa	kiloDalton
KH ₂ PO ₄	potassium dihydrogen phosphate
LBD	ligand-binding domain
LSCC	laryngeal squamous cell carcinoma
mAbs	monoclonal antibodies
MAPK	mitogen activated protein kinase
MDM2	mouse double minute 2 homolog
MET	mesenchymal-to-epithelial-transition
mg	milligramm
MgCl ₂	magnesium chloride
min	minute
ml	millilitre
mM	millimol per litre
mm	millimetre
MMPs	matrix metalloproteinases
MnCl ₂	manganese (II) chloride
mTOR	mammalian target of rapamycin
mTORC2	mTOR complex 2
Na ₂ HPO ₄	disodium phosphate
NaCl	sodium chloride

NaHCO ₃	sodium bicarbonate
NCT	National Center for Tumor Disease
NEP	neutral endopeptidase
NK	natural killer
NSCLC	non-small cell lung carcinoma
OPN	osteopontin
OPSCC	oropharyngeal squamous cell carcinoma
OS	overall survival
OSCC	oral cavity squamous cell carcinoma
p	p-value, significant level
PBS	phosphate-buffered saline
PD-1	Programmed death-1
PDK1	phosphoinositide-dependent kinase 1
PD-L1	programmed death ligand 1
pERK1/2	ERK1/2 phosphorylation
PFA	paraformaldehyde
PFS	progression free survival
pH	potentia hydrogenii
pH2A.X	phosphorylation of Histone H2A.X
PI3K	phosphatidylinositol-3-kinase
PIP ₂	phosphorylates phosphatidylinositol 1,4-bisphosphate
PIP ₃	phosphatidylinositol 1,4,5-bisphosphate
PKA	protein kinase A
PSA	prostate-specific antigen
PTEN	Phosphatase and tensin homolog
PVDF	polyvinylidene difluoride
Rb	retinoblastoma
RIPA	radioimmunoprecipitation assay buffer
RNA	ribonucleic acid
rpm	revolutions per minute
RT	room temperature
RTKs	receptor tyrosine kinases
SCC	squamous cell carcinoma
SDS	sodium dodecylsulfate
SDS-PAGE	sodium dodecylsulfate-polyacrylamide gel electrophoresis
SEM	standard error of mean
Ser	serine; amino acid
SMR3A	submaxillary gland androgen-regulated protein 3A
Src	steroid receptor coactivator
STAT	signal transducer and activator transcription
TAM	tamoxifen
TBS	tris-buffered saline

TEMED	N,N,N',N',Tetramethyl-ethylenediamine
TGF- α	transforming growth factor- α
TGF- β	transforming growth factor- β
TIL	tumor infiltrating lymphocytes
TMA	tissue microarray
TNB	tris-NaCl-blocking buffer
TNF	tumour necrosis factor
	TNM Classification of Malignant Tumours (tumour, nodes, metastasis)
TNM	
TNT	Tris/HCl-NaCl-Tween
Treg	regulatory T cells
TSA	Tyramide Signal Amplification
UICC	Union International Cancer Control
V	volt
VEGF	vascular endothelial growth factor
β -gal	β -galactosidase

1. Introduction

1.1 Epidemiological and clinical features of head and neck squamous cell carcinoma

Accounting for about 4% of all carcinomas worldwide and 5% mortality of all malignancies, head and neck cancer represents the sixth most prevalent carcinoma in humans. Head and neck squamous cell carcinoma (HNSCC), which arises from the mucosal epithelia of upper aerodigestive tract, occupies more than 90% of all head and neck tumors (Bose *et al.*, 2013; Rothenberg and Ellisen, 2012). Anatomically, HNSCC principally occurs in the oral cavity, larynx and pharynx (Figure 1-1). Different tumor subsites reveal distinct microscopic features and severity of tumor progression. Consequently, therapeutic schemes and clinical prognosis vary significantly among various localizations (Molinolo *et al.*, 2009).

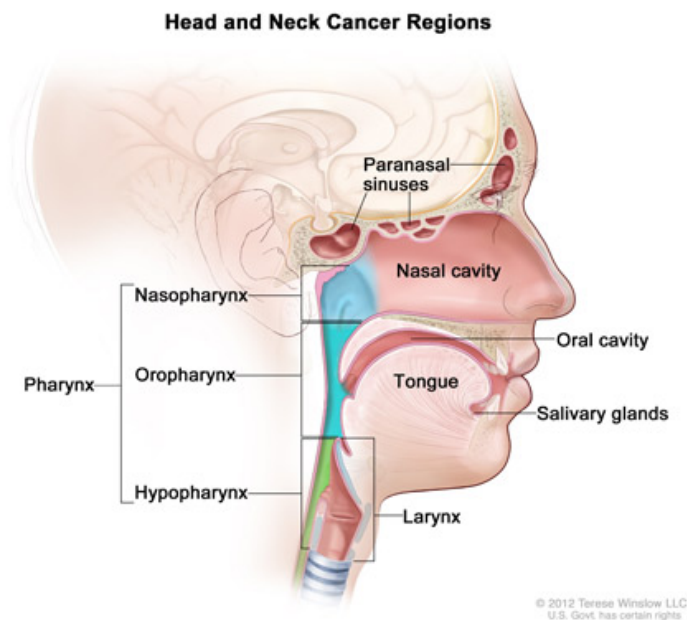


Figure 1-1: Anatomical structure and subunits of the head and neck.

Head and neck region consists of paranasal sinuses, nasal cavity, oral cavity, larynx and pharynx (consisting of the nasopharynx, oropharynx and hypopharynx). Image source:

<https://www.cancer.gov>

The use of tobacco and excess consumption of alcohol are so far identified as main risk factors which synergistically account for HNSCC occurrence (Leemans *et al.*, 2011). Added risk factor caused by betel quid chewing has been identified in south-east Asia and India area (Chen *et al.*, 2008; Jeng *et al.*, 2001; Wang *et al.*, 2017). In a subgroup of HNSCC patients, high-risk human papillomavirus (HPV) infection accounts for development of the oropharyngeal squamous cell carcinoma (OPSCC) particularly, which is also considered as an independent prognostic factor (Marur *et al.*, 2010; Syrjanen, 2005). Although certain inherited diseases (e.g. Fanconi anemia) reveal similarly genetic susceptibility to HNSCC, they have a minor role as risk factors (Alter *et al.*, 2005; Rosenberg *et al.*, 2005). In the western states, public health measures have been carried out to reduce the use of tobacco and consumption of alcohol, hence the incidence of HNSCC in specific sites has been decreasing during the past several years. However, the incidence rates of oropharyngeal cancers are increasing dramatically, which is related to a high-risk HPV infection. Currently, approximately 70% of OPSCC and 25% of all HNSCC are caused by HPV infections (Deschler *et al.*, 2014; Kostareli *et al.*, 2012; Lewis *et al.*, 2015).

Worldwide, over 550,000 new patients are diagnosed with HNSCC and 380,000 deaths annually. However, incidence rates of HNSCC show significant differences across the globe (Figure 1-2). In Europe, HNSCC accounts for 4% of the cancer incidence, there were approximately 250,000 cases and 63,500 deaths in 2012 (Gatta *et al.*, 2015). Whereas, in India, HNSCC represents the most common malignance accounting for 40% of all cancers (Warnakulasuriya, 2009). In Germany, oral and pharyngeal malignances are the 5th most common cancer in the male population. The age standardized rate per 100,000 inhabitants of HNSCC was 21.7 for male and 5.2 for female (Figure 1-2).

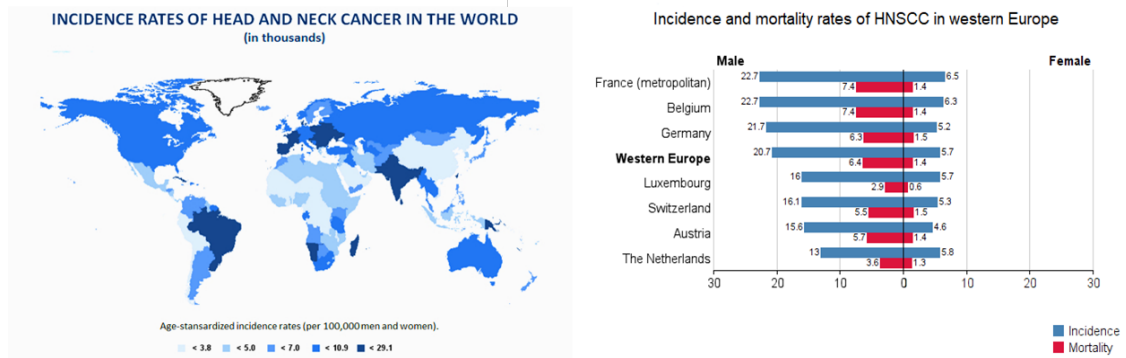


Figure 1-2: Incidence and mortality of HNSCC in the world and Western Europe.

Incidence and mortality of HNSCC in Western Europe are age standardized and calculated per 100,000 inhabitants. Tumors of the lip, oral cavity, nasopharynx, other pharynx and larynx were included. Data and image were derived from database of World Health Organization and (Ferlay *et al.*, 2010).

Unfortunately, less than 50% of newly diagnosed cases with HNSCC will survive for five years. The prognosis of patients with HNSCC is mainly dependent on the stage of the primary diagnosed tumor, which is estimated by physical examination, Imaging diagnosis, cytology of lymph nodes and pathological evaluation (Argiris *et al.*, 2008). Recently, HPV status has been identified as a prognostic factor in oropharyngeal malignances, as well as the traditional tumor, node, metastasis (TNM) staging system. Until now approximately 100 subtypes of HPV have been recognized, but HPV type-16 (HPV16) is identified as high-risk oncogenic subtype, which accounts for more than 90% of HPV-related HNSCC (de Villiers *et al.*, 2004; Gillison *et al.*, 2008). Clinically, Oncogenic HPV subtypes can be evaluated with viral DNA in-situ hybridization (ISH) and p16 immunohistochemistry (IHC) (Venuti and Paolini, 2012). Approximately 25% HNSCCs contain HPV genomic DNA, encoding the viral oncoprotein, E6 and E7, expression of which inactivate the tumor-suppressor gene p53 and retinoblastoma (Rb), respectively (Stransky *et al.*, 2011). In the infected cells unrest of cell cycle regulation is triggered, which is deemed to be the initiation of HPV-induced carcinogenesis. In the past, our lab demonstrated that the viral load and the presence of viral RNA patterns, which was better suited than p16 expression by IHC, identified a subpopulation of HPV16-induced OPSCC patient with a better clinical outcome (Holzinger *et al.*, 2013;

Holzinger *et al.*, 2012).

Generally, HPV-related OPSCCs have a more favorable prognosis as compared to the HPV-unrelated tumors. Underlying reasons may conclude two major mechanisms. First, host-intrinsic factors, since HPV-related OPSCCs are more prominent in younger and healthier patients with fewer complications. Second, tumor-intrinsic factors of different OPSCCs reveal distinct genetic pathway alterations yielding increased therapeutic sensitivity (Burtneess *et al.*, 2013; Swanson *et al.*, 2016). The favorable clinical outcome associated with HPV-related OPSCC has caused the conception of therapy alteration for the low risk subgroup patients. Clinically, it is emphasized on protocol of de-escalation of standard treatment with more local resection, a lower dose of irradiation, or de-intensified chemotherapy for HPV-related OPSCCs. In several trials, traditional cytotoxic drugs are replaced with targeted therapy to evaluate whether alternative schemes could be applied effectively to patients with HPV-related OPSCC (Bose *et al.*, 2013).

The detailed treatment scheme of an individual HNSCC is principally determined in a multidisciplinary combination, which include surgical techniques, irradiation delivery, chemotherapy, and targeted therapy (Argiris *et al.*, 2008). About 35% of patients suffer from early-stage tumor, and as a result they are treated with either surgery or radiation therapy and reveal the potential to be cured with rates of 70-90%. However, the majority of patients with locally advanced stage tumor require multimodality treatment with surgery, combined adjuvant radiotherapy with or without chemotherapy (Argiris *et al.*, 2008; Suh *et al.*, 2014). Despite considerable development in both surgical resection and irradiation techniques, up to half of locally advanced HNSCC evolve to locoregional or distant recurrence within the first two years post treatment. Salvage surgery, re-irradiation alone or combination with chemotherapy have been applied for patients with recurrent or metastatic HNSCC, with response rates of approximately 20%

and median overall survival of 10-12 months (Brockstein, 2011). Recently, immunotherapy approaches, especially immune checkpoint inhibitors, have obtained a large amount of excitement and prosperity on the second line treatment of recurrent and (or) metastatic HNSCC. The next step will be to enlarge the immune-based therapy benefit to the first line treatment and to combine conventional therapy for favorable clinical response in HNSCC (Gotwals *et al.*, 2017; Szturz and Vermorken, 2017).

1.2 Molecular mechanisms of HNSCC pathogenesis

Although over 95% of head and neck cancers are squamous cell carcinomas, heterogeneity is a significant attribute of HNSCC. The heterogeneous feature not only complicates accurate prognostication and effective therapy, but also hampering the identification of pathogenic gene and signaling cascades (Leemans *et al.*, 2011). However, preliminary studies show the existence of various molecular classifications of HNSCC, such as basal, mesenchymal, atypical and classical, which are depending on the biological properties of differentially expressed genes in each subtype. A great deal of genetic and molecular studies have revealed characteristic changes in cancer-related genes and signaling cascades in pathogenesis and progression of HNSCC, most of those at chromosomes 3p, 8p, 9p, 11q,13q and 18q (Bernstein *et al.*, 2013; Deshpande and Wong, 2008; Pai and Westra, 2009). Accumulation of genetic and epigenetic alterations in genes functioning in carcinogenic signaling pathways, can lead to the formation of malignant phenotypes, which consisting of limitless replicative potential, sufficiency growth signal, ability to evade apoptosis, invasion, metastasis, angiogenesis and immune escape (Ferris, 2015; Hanahan and Weinberg, 2011; Negrini *et al.*, 2010; Whiteside, 2017).

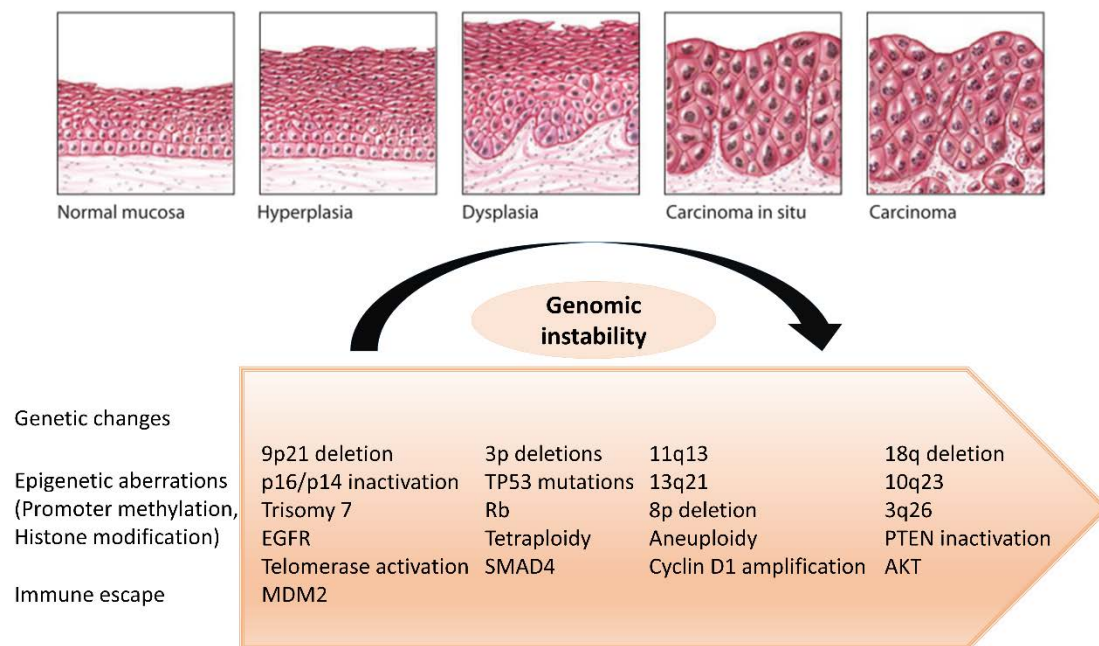


Figure 1-3: Progression model of phenotypic and genetic alterations in HNSCC.

Head and neck carcinogenesis is a multistep clinical and histological progression from normal mucosa through the squamous dysplasia to invasive malignancy, which is triggered by the accumulation of genetic alterations. Involved genomic instability and alternative signaling pathways are depicted. Adapted from (Argiris *et al.*, 2008; Pai and Westra, 2009).

1.2.1 Cellular proliferation and tumor suppressor genes

The TP53 and retinoblastoma (Rb) pathways are mutated in nearly all of HNSCCs leading to unending replicative capacity and immortalization. Somatic mutations in TP53 are observed in approximately 60%-80% of cases with HNSCC (Poeta *et al.*, 2007). An elevated rate of TP53 mutations in HNSCC is related to alcohol consumption and smoking history (Brennan *et al.*, 1995). In tumors with wild-type p53, the abrogation of p53 function may be caused by other mechanism including expression of HPV viral oncoprotein E6, overexpression or amplification of mouse double minute 2 homolog (MDM2) and deletion of cyclin-dependent kinase Inhibitor 2A (CDKN2A) and p14/ARF (Carroll *et al.*, 1999; Denaro *et al.*, 2011; Vogelstein *et al.*, 2000). Together with p53, other family members, p63 and p73, have been demonstrated to exert significant

functions in carcinogenesis of HNSCC (Ratovitski *et al.*, 2006; Rocco *et al.*, 2006). In HNSCCs, pRb is targeted early through deactivation of CDKN2A, encoding the cell cycle modulators p16/INK4A and p14/Arf/INK4B. Inactivation of p16/INK4A has been demonstrated consistently to associate with clinical poor outcome (Reed *et al.*, 1996; Smeets *et al.*, 2009). Nevertheless, the correlation of p14/Arf/INK4B with HNSCC prognosis remains controversial (Dominguez *et al.*, 2003; Sailasree *et al.*, 2008). CDKN2A mutations were observed in 7-9% of cases by whole-exome sequencing, with copy number variants in a further 25% of tumors (Agrawal *et al.*, 2011; Stransky *et al.*, 2011). In HPV-related HNSCC, HPV E7 protein can inactivate the Rb pathway and bind RB1, result in up-regulation of p16/INK4A, which is a cyclin dependent kinase inhibitor. This HPV-related activation of p16 has been considered clinically as a functional surrogate marker for evaluation of HPV status (Schache *et al.*, 2011).

1.2.2 Overexpression of EGFR in HNSCC

The epidermal growth factor receptor (EGFR) belongs to the ErbB family of transmembrane receptor tyrosine kinases. Overexpression of EGFR is claimed to be an early and common event in HNSCC (Grandis and Twardy, 1993; Hama *et al.*, 2009; Ozanne *et al.*, 1986). Both gene mutations and amplification have been reported, however, amplification of EGFR is not indicated as a reason for high EGFR protein expression or related-poor clinical outcome in HNSCC (Grandis and Twardy, 1993; Licitra *et al.*, 2011). Generally, EGFR overexpression triggers the activation of kinase activity through spontaneous dimerization of receptors. Constitutive activity of EGFR is driven by autocrine signaling via the co-expression of EGFR and its ligand transforming growth factor- α (TGF- α), which is regularly found in HNSCC and associated with an unfavorable clinical outcome (Quon *et al.*, 2001; Zhu *et al.*, 2013). However, reports on correlations between EGFR overexpression and clinical prognosis reveal conflicting data. In general, about 60% of the reports show a correlation between EGFR

overexpression and unfavorable prognosis, whereas 40% of those studies a negative consequence (Leemans *et al.*, 2011). This may be due to the heterogeneity of HNSCC. Distinct downstream signaling pathways are activated in various tumors, which is attributed to inconsistent function of EGFR and anti-EGFR therapy resistance. The signaling pathways stimulated by EGFR include phosphatidylinositol-3-kinase (PI3K)/AKT/mammalian target of rapamycin (mTOR), Ras/Raf/mitogen activated protein kinase (MAPK), Janus kinase(JAK)/signal transducer and activator transcription (STAT) (Figure 1-4) (Choong and Cohen, 2006; Hynes and Lane, 2005; Yarden and Sliwkowski, 2001). Potentially, such complexity affects the EGFR function in tumor cells, therapeutic effects and the clinical outcome of patients. Furthermore, different subsites in HNSCC reveal various EGFR expression levels, for instance, tumors in the oral cavity and pharynx tend to possess elevated EGFR expression than carcinomas of the larynx. Targeted therapy of EGFR can be achieved by inhibition of extracellular ligand binding with specific monoclonal antibodies (mAbs) such as cetuximab (cetux), or by inhibition of the tyrosine kinase domain using a small molecule compound. So far, cetux serves as the only FDA-approved and European Medicines Agency-approved targeted therapy in HNSCC and is employed with no correlation with EGFR status.

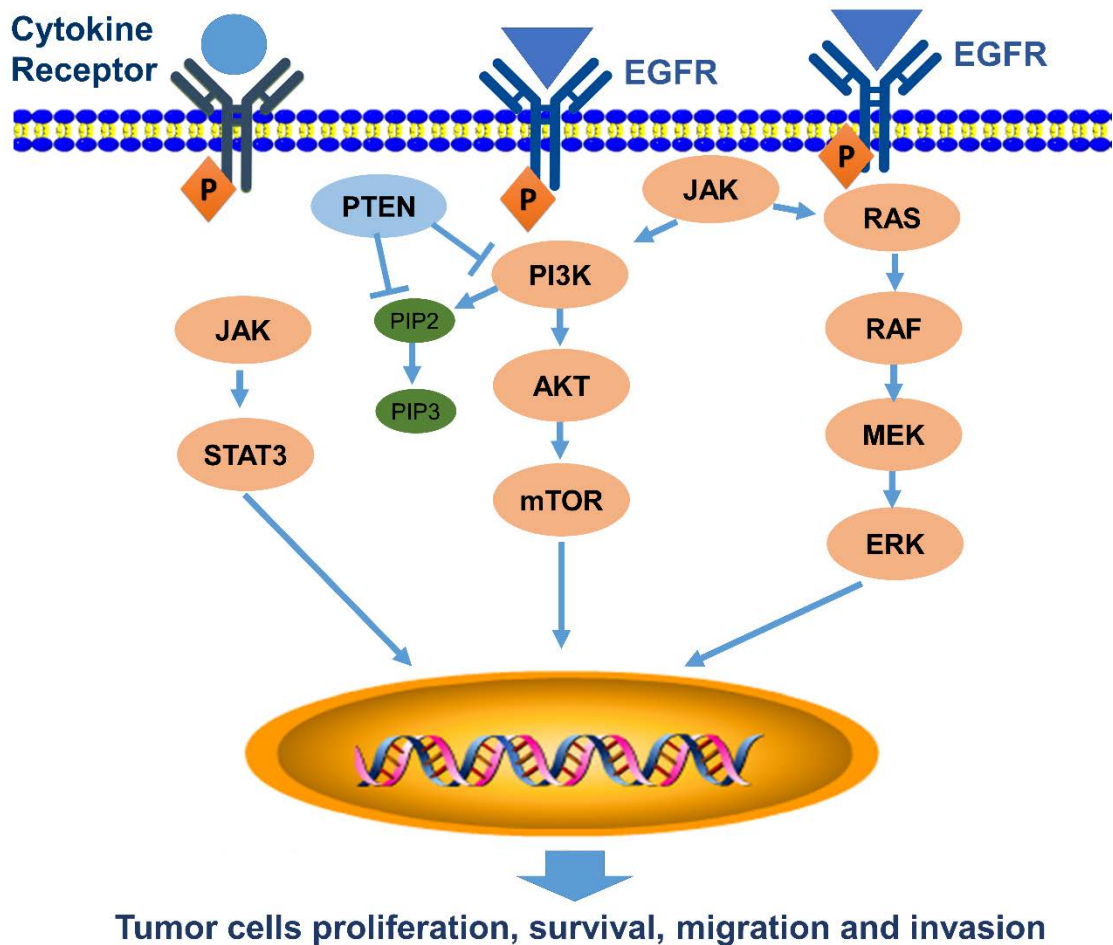


Figure 1-4: Major signaling pathways involved in head and neck cancer.

EGFR, PI3K, RAS and JAK-STAT pathways are presented as examples for the main signaling pathways contributing to the pathogenesis of head and neck cancer. Ligand binding to EGFR triggers receptor dimerization and activation of downstream signaling pathways such as RAS/RAF/MEK/ERK, PI3K/AKT/mTOR, and JAK/STAT. PTEN is a negative modulator of the PI3K pathway. JAKs are activated by binding to cytokine receptors. PI3K and RAS signaling cascades are also triggered by activated JAKs.

1.2.3 PI3K-AKT-mTOR pathway

One of the major downstream targets of EGFR is the PI3K signaling pathway, which has been demonstrated as one of the most commonly activated pathways in human cancer. Genomic alterations including mutation, amplification and rearrangements in multiple components of the PI3K signaling route, lead to the dysregulation of cellular proliferation, differentiation, migration and survival (Cancer Genome Atlas, 2015).

Thereupon, those contribute to an uncontrolled growth, metastatic capacity and resistance to treatment. There are three classes of PI3Ks with each own specific substrates. The class I PI3Ks are activated by growth factor tyrosine kinase receptor such as EGFR, and the catalytic subunit phosphorylates phosphatidylinositol 1,4-bisphosphate (PIP₂) to form phosphatidylinositol 1,4,5-bisphosphate (PIP₃). PIP₃ belongs to the inner leaflet of the plasma membrane and interact with the Pleckstrin Homology domain of AKT and phosphoinositide-dependent kinase 1 (PDK1), which results in phosphorylation of AKT proteins within their catalytic domains T-loop (Thr308 in AKT1). Another specific site of phosphorylation by the mTOR complex (mTORC2), which belongs to one of distinct complexes of mTOR is at Ser473 in AKT1. Activation of the PI3K-AKT pathway can be achieved via various mechanisms including mutation or amplification of PI3K, amplification of AKT, activation of oncogenes such as RAS, or mutation of tumor suppressor protein Phosphatase and tensin homolog (PTEN) (Bauman *et al.*, 2012). PTEN suppresses signal transduction through the PI3K signaling pathway by converting PIP₃ to PIP₂. Loss of PTEN expression can be found in approximately 30% of HNSCCs and serves as an independent unfavorable prognostic factor. Furthermore, activating mutations of oncogene PIK3CA can be observed in a small subpopulation (10%-20%) of HNSCC patients, particularly through the mechanisms of gene amplification and low-level copy number augment (Cancer Genome Atlas, 2015; Murugan *et al.*, 2008; Qiu *et al.*, 2006). Whole exome sequencing studies show an elevated incidence of PIK3CA mutations in HPV-related HNSCC, suggesting PIK3CA mutations may interact synergistically with HPV E6 and E7 proteins in the progress of invasive OPSCC. All in all, the PI3K-AKT-mTOR axis plays a significant role in the carcinogenesis of HNSCC, implying a potentially consequential clinical implication. Therapies targeting the PI3K and related signaling pathway have been assessed in various phases of clinical trials (Bossi and Alfieri, 2016; Horn *et al.*, 2015; Isaacsson Velho *et al.*, 2015; Swick *et al.*, 2017).

1.2.4 Ras-Raf-MEK-MAPK pathway

The extracellular signal-regulated kinases (ERK) / mitogen-activated protein kinase (MAPK) pathway (also known as the Ras-Raf-MEK-MAPK pathway) consists of small GTPases of the RAS family (HRAS, KRAS, NRAS) and members of RAF, MEK and ERK kinase (ARAF, BRAF, CRAF, MEK1/2 and ERK1/2) families, which are key regulators in the communication from the cell surface to the nucleus and regulate the progression of various carcinomas. Members of the Ras oncogene family are some of the most commonly mutated genes in human malignance. Activating mutations of HRAS occur in 4-5% of HNSCC cases and the other Ras genes are infrequently mutated in HNSCC (Agrawal *et al.*, 2011; Stransky *et al.*, 2011). Particularly in oral cancer of areca quid chewing patients, the Ras-Raf-MAPK signaling pathway can be triggered sequentially owing to gain of function mutations in Ras genes. Several reports show the MEK-ERK cascade can be activated in radioresistant cells of HNSCC (Affolter *et al.*, 2017; Drigotas *et al.*, 2013). Observations suggest that targeting ERK-MAPK pathway may sensitize the treatment of irradiation to HNSCC.

1.2.5 JAK-STAT pathway

JAKs are part of a family of non-receptor tyrosine kinases that are triggered by cell surface cytokine receptors through transphosphorylation. STATs, which were phosphorylated by activated JAKs, dimerize and translocate to the nucleus where they can activate transcription of the target genes. Similarly, JAKs can be activated directly by receptor tyrosine kinases (RTKs) such as EGFR, triggering the RAS-MEK-MAPK and PI3K-AKT pathways (Aaronson and Horvath, 2002; Constantinescu *et al.*, 2008; Nefedova and Gabrilovich, 2007). The JAK-STAT pathway, which plays a role in facilitating cell proliferation and growth, has been related to head and neck carcinogenesis (Lai *et al.*, 2005; Lai and Johnson, 2010; Song and Grandis, 2000). STAT3 is overexpressed in both HNSCC cell lines and tumor tissue specimens, which

serves as an early event in patients with smoking-related HNSCC (Grandis *et al.*, 1998; Grandis *et al.*, 2000; Nagpal *et al.*, 2002). In addition, activated STAT3 is attributed to trigger Ras and EGFR signaling cascades (Arredondo *et al.*, 2006). Although STAT3 is the most significant STAT molecule in HNSCC, several studies suggest that active STAT5 also sustains tumor development and resistance to therapy-induced apoptosis in HNSCC (Koppikar *et al.*, 2008; Xi *et al.*, 2003).

1.2.6 Additional cancer-related genes and pathways

There are also some additional candidate genes and pathways involved in molecular mechanisms of HNSCC, such as the transforming growth factor- β (TGF- β) (Oshimori *et al.*, 2015), vascular endothelial growth factor (VEGF) (Vassilakopoulou *et al.*, 2015), matrix metalloproteinases (MMPs) (Rosenthal and Matrisian, 2006), Notch-p63 axis (Mountzios *et al.*, 2014), hepatocyte growth factor (HGF)/ (Met proto-oncogene) (Hartmann *et al.*, 2016) and Wnt signaling pathway (Shiah *et al.*, 2016). Moreover, HNSCCs reveal a great range of somatic mutations in genes implicated in antigen presentation and immune evasion, like *CD274*, *HLA-A*, *B2M*, *TGFBR2* and *TRAF3* (Hammerman *et al.*, 2015). The alterations in these or other genes may play a remarkable function in immune surveillance of HNSCCs.

1.3 Preclinical mouse model for tumor recurrence

As mentioned previously, 5-year survival rate of patients with HNSCC remains at approximately 50% due to a high rate of local recurrences and distant metastasis. Therefore, it is urgent to find better biomarkers that predict the subpopulation of patients at high risk for tumor recurrence and treatment failure and to unravel new targets for a more efficient and less toxic therapy. Already about 50 years ago the term

of “field cancerization” was proposed to interpret the great tendency of tumor relapse and treatment failure in HNSCC (Slaughter *et al.*, 1953). The tumor-adjacent mucosal epithelium contains genetic changes, which is term “field”. In retrospective studies, local recurrences and second primary tumor after surgical resection remain to appear in the surgical margins (Roesch-Ely *et al.*, 2007; Schaaij-Visser *et al.*, 2009; Tabor *et al.*, 2004). To better understand the cellular and molecular alterations between primary and local recurrent tumors, Behren et al (Behren *et al.*, 2010) developed a reliable and reproducible orthotopic floor-of-mouth squamous cell carcinoma murine model. Recurrent mouse tumors were collected after surgical resection of primary tumors. Global gene expression analysis was applied on matched specimens of primary and recurrent tumors derived from this mouse model and unraveled 49 differentially expressed candidate genes implying a crucial role during tumor relapse. One candidate gene encoded for Smr1, the murine homolog of human submaxillary gland androgen-regulated protein 3A gene (SMR3A), which belong to a gene family encoding the opiorphin-related pentapeptides.

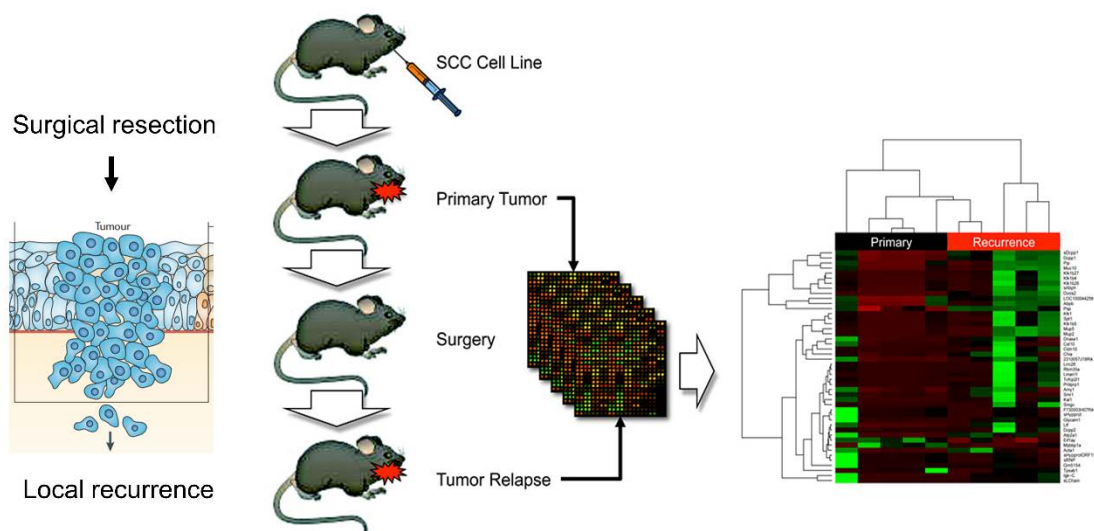


Figure 1-5: Preclinical murine model for tumor relapse after surgery.

Mice were injected with SCC-7 cells to generate primary tumors and after microsurgical removal of the primary tumors local recurrences developed a high frequency. Matched specimens of primary and recurrent tumors were analyzed by global gene expression profiling, which disclosed a list of differentially expressed genes, shown in the heat map. One of the candidate genes encoded Smr1, the mouse homolog of human SMR3A gene (Acuna Sanhueza *et al.*,

2012).

1.4 The opiorphin gene family

1.4.1 The pathophysiological function of opiorphin genes

In humans, there are three homologous genes of opiorphin, OPRPN (known as *ProL1* previously), SMR3A and SMR3B (Tong *et al.*, 2008). The opiorphin that corresponds to the mature pentapeptide product of the OPRPN precursor protein acts as efficient as morphine in a rat model of pain (Rougeot *et al.*, 2003). SMR3A and SMR3B are two closely interrelated genes, both of which are potentially post-translationally processed to the identical opiorphin homolog. Previous studies revealed that aberrant expression of all three members of the human opiorphin family genes plays a key role in the modulation of erectile physiology (Tong *et al.*, 2008). Furthermore, OPRPN-derived opiorphin have been demonstrated to act as a potent inhibitor of two cell membrane bound enkephalin-inactivating peptidases, namely neutral endopeptidase (NEP, also known as CD10) and aminopeptidase N (APN, also known as CD13) (Wisner *et al.*, 2006). CD10 and CD13 are widely distributed among a wide range of tissues and organs, where they fulfill distinct roles, for example, act as ectoenzymes to deactivate neuropeptides and regulate other signaling pathway mediating cell migration, proliferation and survival (Chen *et al.*, 2012; Maguer-Satta *et al.*, 2011; Mizerska-Dudka and Kandefer-Szerszen, 2015). Dysregulated expression of both protein has been shown in distinct human carcinomas, such as pancreas, gastric, prostate, breast, lung, and oral carcinomas (Erhuma *et al.*, 2007; Kawamura *et al.*, 2007; Piattelli *et al.*, 2006; Sorensen *et al.*, 2013).

1.4.2 Opiorphin genes in HNSCC

Our previous data revealed variable protein expression patterns for both CD10 and

CD13 in a cohort of patients with OPSCC. In addition, we also found strong SMR3A protein expression in 36% of all primary OPSCC by IHC staining of tissue microarrays (TMAs), which served as an unfavorable risk factor for survival of patients with OPSCC (Koffler *et al.*, 2013). Regulation of SMR3A expression was further addressed in HNSCC cell lines after fractionated IR in vitro. Interestingly, an enrichment of SMR3A-positive cells was observed in the fraction of vital tumor cells after fractionated IR. Furthermore, up-regulation of SMR3A expression after fractionated IR was dependent on estrogen receptor 2 (ESR2) signaling (Grunow *et al.*, 2017).

1.5 Aims of the study

So far, our group has addressed the correlation of SMR3A expression and clinical prognosis in HNSCC and provided experimental evidence supporting a model in which SMR3A serves as a surrogate marker for ESR2-dependent signaling in radioresistant tumor cells. The following work was performed to investigate:

- (1) the co-expression of ESR2 and SMR3A in tumor specimens of OPSCC and correlation with clinical feature;
- (2) the expression and clinical relevance of OPRPN, one homologous gene of opiorphin, in pathogenesis and treatment failure after radiotherapy;
- (3) the expression and regulation of ESR2 in established HNSCC cell lines under conditions of fractionated IR or targeted therapy (cetuximab).
- (4) the impact of drugs targeting the EGFR-MEK-MAPK pathway (e.g. Cetuximab and MEK1/2 inhibitor) on tumor cell survival and clonal expansion as well as expression of ESR2 and programmed death ligand 1 (PD-L1).

2. Materials

2.1 Equipment and consumables

Table 2-1: Equipment and consumables

Equipment and consumables	Providers
Autoclave	Ibs Technomara GmbH
Biochrom Anthos 2010 Microplate Reader	Biochrom GmbH
Black/White Camera XM10	Olympus GmbH
Blotting System Mini Trans-Blot Cell	Bio-Rad Laboratories, Inc
Brightfield Camera SC30	Olympus GmbH
Casy Cell Counter	Schärfe System GmbH
Cell Culture Inserts (Transparent PET Membrane, 0,4µm Pore Size)	Falcon Technologies BD
Cell Culture Plates (10cm-dishes, 96well-, 48well-, 24well-, 12well-, 6well-plates, 25cm ² -, 75cm ² -flasks)	SIGMA-Aldrich, Inc.
Cell Lifter Costar	Corning Incorporated
Centrifuge 5417R	Eppendorf AG
Centrifuge Tube (15ml, 50ml)	SIGMA-Aldrich, Inc.
Coverslips (12mmØ)	Menzel-Gläser GmbH
Coverslips (24x36 mm, 24x50mm)	Menzel-Gläser GmbH
Cryo Tube Vials (1,8ml)	Thermo Fisher Scientific Inc.
DAB substrate	Dako GmbH
DAKO PAP Pen	Dako GmbH
dd H ₂ O Milli-Q	Millipore, Merck KGaA
Disposable Weighing Pans	C. Roth GmbH
DMEM	SIGMA-Aldrich, Inc.
Eppendorf Research Pipettes	Eppendorf AG
Erlenmeyer Flasks	Brand GmbH
Extra-thick Blot Paper	Bio-Rad Laboratories, Inc
Fetal Bovine Serum (FBS)	SIGMA-Aldrich, Inc.
Filtertips (10µl-1000µl)	nerbePlus GmbH
Fluorescence Microscope BX-50F	Olympus GmbH
Fluorescence Microscope BZ-9000	Keyence, Germany
Forceps 37SA, 5SA	VOMM GmbH
Forceps, fine	Fine Science Tools GmbH
Freezer (-20°C) Liebherr Comfort	Liebherr Group
Freezer (-80°C) HERAfreeze	Heraeus
Freezing container	SIGMA-Aldrich, Inc.

Fridge (4°C) Liebherr Premium Funnel	Liebherr Group C. Roth GmbH
GFL 1083 Shaking Waterbath	GFL Gesellschaft für Labortechnik mbH
Glas Beakers	Fisher Scientific GmbH
Glas Bottles	Schott AG
Glas Containers for Histology	Schott AG
Glas Pipettes (2ml, 5ml, 10ml, 20ml)	Hirschmann Laborgeräte GmbH
Graduated Cylinder, Glas	Brand GmbH
Graduated Cylinder, Plastic	VITLAB GmbH
Heating Block BiothermBT-11	Cryologic Pty. Ltd.
Heraeus HERAsafe Safety Cabinet	Kendro Laboratory Products
Horizontal Gel Electrophoresis Chamber (Rotiphorese Chamber)	C. Roth GmbH
Ice-Machine AF20	Scotsman Ice Systems
ImageQuant LAS500	GE Healthcare Europe GmbH
Immobilon-P Transfer Membrane	Millipore, Merck KGaA
Incubator Unimax 1010	Heidolph Instruments GmbH
L-Glutamine	SIGMA-Aldrich, Inc.
MicroAmp Fast Optical 96-well Reaction Plate	Applied Biosystems, Life Technologies
MicroAmp Optical Adhesive Film	Applied Biosystems, Life Technologies
MicroPlate 96-well	Greiner Bio-One GmbH
Microscope Axiovert 25	Carl Zeiss AG
Microscope BX-50F	Olympus GmbH
Microscope IX51	Olympus GmbH
Microwave	Robert Bosch GmbH
MR200 Magnetic Stirrer	Heidolph Instruments GmbH
Nanodrop Spectrophotometer, ND-1000	PEQLAB Biotechnologie GMBH
neoLab-Rocking Shaker	neoLab GmbH
Neubauer Chamber	Brand GmbH
Nuclease-free Reaction Caps, Safe Lock	Eppendorf AG
Parafilm "M"	Brand GmbH
pH-Meter 761 Calimatic	Knick Elektronische Messgeräte GmbH
Pipetman Classic	Gilson Inc.
Pipettetips (RFL-300-C, RFL-222-C, RFL-1000-C)	Axygen Scientific
Plastic Beakers	Brand GmbH
Plastic Containers for Histology	Schott AG
Plastic Pipettes Costar Stripette (5ml, 10ml, 25ml)	Corning Incorporated
Power Supply Power Pac 300/300	Bio-Rad Laboratories, Inc

Precision Scales	Sartorius AG
Precision Scales Microbalance XS205	Mettler Toledo Intl. Inc
Pump Cell Culture	neoLab GmbH
Reaction Tubes (1,5 ml, 2 ml)	Eppendorf AG
Rotilabo Magnetic Stirrer	C. Roth GmbH
RotoShake Genie	Scientific Industries, Inc.
Ruler	Rotring GmbH
SDS-PAGE System Mini-PROTEAN Tetra	Bio-Rad Laboratories, Inc
Handcast Systems (10well, 1,0-1,5mm)	Heidolph Instruments GmbH
Shaker Polymax 1040	Labnet International Inc.
Spectrafuge Mini Centrifuge	Fine Science Tools GmbH
Spring Scissors, fine	C. Roth GmbH
Staining Chamber/Humid Chamber	Braun GmbH
Steam-Cooker Multi-Gourmet	Fujifilm Europe GmbH
Super RX (18x24 cm)	Menzel-Gläser GmbH
SuperFrost Microscope Slides	mediaware, Servoprax GmbH
TBC-Syringe (1ml)	Eppendorf AG
Thermomixer	SIGMA-Aldrich, Inc.
Trypsin	Heidolph, GER
Vortex Reax 2000	Bio-Rad Laboratories, Inc
Wet blotting transfer system	GE Healthcare Europe GmbH
Whatman Syringe Filters (0,2µm)	Precision X-Ray Inc.
XRAD320	

2.2 Chemicals

Table 2-2: Chemicals

Chemicals	Provider
Acetic Acid	Merck KGaA
Acrylamide/Bisacrylamide	C. Roth GmbH
Agarose SeaKem GTG	AppliChem GmbH
Albumin from Bovine Serum (BSA)	SIGMA-Aldrich, Inc.
Ammonium Persulfate (APS)	SIGMA-Aldrich, Inc.
beta-Mercaptoethanol	AppliChem GmbH
Boric Acid	SIGMA-Aldrich, Inc.
Bromphenol Blue	AppliChem GmbH
Calcium Chloride (CaCl ₂)	Merck KGaA
Crystal Violet	Merck KGaA
Dimethylformamide	AppliChem GmbH

Dimethylsulfoxide (DMSO)	SIGMA-Aldrich, Inc.
Disodium Phosphate (Na ₂ HPO ₄)	C. Roth GmbH
Dithiothreitol (DTT)	Merck KGaA
Ethanol p.a.	SIGMA-Aldrich, Inc.
Ethanol, denatured 99,7%	SIGMA-Aldrich, Inc.
Ethanolamine	Merck KGaA
Ethylenediaminetetraacetic Acid (EDTA)	AppliChem GmbH
Eukitt	O. Kindler GmbH
Glycerol	C. Roth GmbH
Glycine	GERBU Biotechnik GmbH
Haemalaun	C. Roth GmbH
Hoechst H33342	Biomol, Germany
Hydrochloric acid (HCl)	SIGMA-Aldrich, Inc.
Hydrogen peroxide (H ₂ O ₂)	AppliChem GmbH
Isopropanol	SIGMA-Aldrich, Inc.
Magnesium Chloride Hexahydrate (MgCl ₂ x 6H ₂ O)	Merck KGaA
Manganese (II) Chloride Dihydrate (MnCl ₂ x 2H ₂ O)	Merck KGaA
Methanol	SIGMA-Aldrich, Inc.
Milk Powder	C. Roth GmbH
Mowiol 4-88	C. Roth GmbH
N,N,N',N',Tetramethyl-ethylenediamine (TEMED)	C. Roth GmbH
Natrium Chloride (NaCl)	SIGMA-Aldrich, Inc.
Non-fat Milk powder	C. Roth GmbH
Nonidet P-40	Fluka Chemie AG
Paraformaldehyde (PFA)	C. Roth GmbH
Potassium Chloride (KCl)	C. Roth GmbH
Potassium Dihydrogen Phosphate (KH ₂ PO ₄)	C. Roth GmbH
Sodium Citrate	C. Roth GmbH
Sodium Deoxycholate	Merck KGaA
Sodium Dodecylsulfate (SDS) Pellets	C. Roth GmbH
Sodium Hydroxide (NaOH)	Merck KGaA
Sodium Tetraborate	SIGMA-Aldrich, Inc.
Tris/Base (Trizma Base)	SIGMA-Aldrich, Inc.
Tris/HCl	C. Roth GmbH
Triton X-100	AppliChem GmbH

Trypan Blue	SIGMA-Aldrich, Inc.
Tween 20	GERBU Biotechnik GmbH
Xylencyanol	Merck KGaA
Xylene	SIGMA-Aldrich, Inc.
Xylol	VWR.Germany

2.3 Molecular biological reagents

Table 2-3: Molecular biological reagents

Reagents	COMPANY
4-Hydroxytamoxifen	SIGMA-Aldrich, Inc.
cetuximab	Merck KGaA
DAB Kit	Vector Laboratories
Fulvestrant	SIGMA-Aldrich, Inc.
ImPRESS anti-goat	Vector Laboratories
MEK1/2 Inhibitor PD0325901	SIGMA-Aldrich, Inc.
Pierce BCA Protein Assay	Thermo Fisher Scientific Inc.
Senescence- β -Gal staining Kit	Cell signaling Technology, Germany
TSA Biotin-System	Perkin Elmer
Vectastain Elite-ABC-Peroxidase	Vector Laboratories
Western Lighting Plus-ECL	Perkin Elmer

2.4 Antibodies

Table 2-4: Primary antibodies

Primary antibody	Application dilution	and Species	Company and product NO.
anti-beta-Actin	WB (1:25000)	mouse	Abcam, ab49900
Anti-Estrogen receptor	IF (1:100), (1:1000) IHC (1:900)	WB rabbit	Abcam, 133467
Anti-ProL1	IF (1:200),	mouse	Abcam, ab169504
Anti-ProL1	IF (1:200), (1:300)	IHC Rabbit	Abcam, ab204562
Anti-SMR3A	IF (1:100)	Rabbit	Abcam, ab97942
Anti-pERK1/2	IF (1:250), (1:1000)	WB Rabbit	Cell signaling 9101
Anti-ERK1/2	WB (1:1000)	Rabbit	Cell signaling 4695

Anti-pAKT(Ser473)	WB (1:2000)	Rabbit	Cell signaling 4060
Anti-Histone H2A.X	WB (1:1000)	Rabbit	Cell signaling 9718
Anti-PD-L1	WB (1:1000)	Rabbit	Cell signaling 13684

Table 2-5: Secondary Antibodies

Secondary antibody	Application and dilution	Label	Company
Goat anti-rabbit	IHC (1:200)	biotinylated	Vector Laboratories
Goat anti-mouse	WB (1:10000)	HRP	Santa Cruz
Goat anti-rabbit	WB (1:10000)	HRP	Santa Cruz
Goat anti-rabbit	IF (1:200)	Alexa488	Sigma-Aldrich
Goat anti-mouse	IF (1:200)	Cy3	Sigma-Aldrich
Goat anti-rabbit	IF (1:200)	Cy3	Sigma-Aldrich

2.5 Buffers and solutions

Table 2-6: Buffers and solutions

4% PFA	500ml	1xPBS
	200µl	NaOH
	20g	Paraformaldehyde
Borate Buffer 0,1M pH 8,4	25mM	Sodium Tetraborate
	75mM	NaCl
	100mM	Boric Acid
Crystal violet staining solution	500mg	Crystal violet
	25ml	Methanol
	75ml	ddH ₂ O
Equilibration Buffer	20mM	Tris/HCl pH 7,4
	500mM	NaCl
Mowiol	6g	Glycerol
	2,4g	Mowiol 4-88
	6ml	H ₂ O
	12ml	0,2M Tris pH 8,5
PBST	0.05%	Tween-20
	1x	PBS
PBS pH 7,4 (10x)	20Mm	KH ₂ PO ₄
	27mM	KCl
	100mM	Na ₂ HPO ₄
	1,37M	NaCl
Pre-Load Buffer	1M	NaCl
	5mM	MgCl ₂
	5mM	MnCl ₂

	5mM	CaCl ₂
RIPA Buffer	50mM	Tris/HCl pH 7,4
	150mM	NaCl
	0,1%	SDS
	0,5%	Sodium Deoxycholate
	1%	Nonidet P-40
SDS Running Buffer (10x)	250mM	Tris Base
	2,5M	Glycine pH 8,3
	1%	SDS
Sodium Citrate Buffer (10x)	100mM	Sodium Citrate
	0,5%	Tween 20
TBS pH 7,4 (10x)	500mM	Tris HCl pH 7,4
	1,5M	NaCl
T-Buffer	0,2%	Tween 20
	1%	BSA
		in 1xTBS
TNT-Blocking Buffer (TNB)	1g	Blocking Reagent (TSA-Kit)
	200ml	1xTNT-Buffer
Transfer Buffer	25mM	Glycine
	0,15%	Ethanolamine
	25% (v/v)	Methanol
Tris HCl – NaCl – Tween Buffer (TNT) (10x)	1M	Tris-HCl pH 7,4
	1,5M	NaCl
	0,5%	Tween 20
Tris-Boric Acid-EDTA Buffer (TBE) (10x)	20mM	EDTA
	890mM	Tris Base
	890mM	Boric Acid
X-Buffer	0,5%	Triton X-100
		in 1xPBS

2.6 Cell lines

Table 2-7: Cell lines

NAME	Source	Type, Characteristics	Supplier
FaDu	Human, pharynx	SCC, adherent	ATCC
Cal27	Human, tongue	SCC, adherent	ATCC
Detroit562	Human, pharynx	SCC, adherent	CLS GmbH
SCC4	Human, tongue	SCC, adherent	ATCC

SCC9	Human, tongue	SCC, adherent	ATCC
SCC25	Human, tongue	SCC, adherent	ATCC

2.7 Softwares

Table 2-8: Softwares

NAME	COMPANY
ADAP	Biochrom GmbH
Adobe Acrobat Reader 9.0	Adobe San Jose
Adobe Photoshop CS5.1	Adobe San Jose
Cell Sens Dimension 1.5	Olympus
Clono Counter (Java based program)	
Endnote X7	Thomson Reuters (Scientific) Inc.
Hamamatsu NanoZoomer (NDP Viewer)	Hamamatsu Photonics
IBM SPSS Statistics 20	IBM Corporation
Image J (public domain, Java-based image processing program)	W. Rasband, National Institutes of Health, Maryland, USA
Microsoft Office 2016	Microsoft Corporation
Nikon NIS-Elements 3.20.02	Nikon
Nikon NIS-Elements Viewer 3.20.02	Nikon

3. Methods

3.1 Cell culture

3.1.1 Cultivation of cell lines and treatment

Human HNSCC cell lines FaDu, Cal27, SCC4, SCC9 and SCC25 were purchased from ATCC (<https://www.lgcstandards-atcc.org>), Detroit562 from CLS (Cell Lines Service, GmbH, Germany <http://clsgmbh.de/>). Cells were maintained in Dulbecco's Modified Eagle's Medium (DMEM) supplemented with 10% fetal bovine serum (Invitrogen, Germany), 2Mm L-glutamine and 50µg/ml penicillin-streptomycin in a humidified and sterile conditions with 6% CO₂ at 37°C. Mycoplasma tests were done routinely by PCR analysis using the PromoKine Mycoplasma PCR test kit. When culture reaching 80-90% confluency, the cells were passaged by adding 1ml 0.2% Trypsin in PBS/EDTA for 5 minutes at 37°C. After detaching of cells trypsin reaction was terminated by adding DMEM containing FBS. Trypsinized cells were transferred to a Falcon tube and centrifuged at 1200 rpm for 3 minutes. The cell pellet was resuspended in the appropriate amount of DMEM and calculated in a counting chamber. The viability of cells was detected with trypan blue. According to individual experiment, cells were seeded in new culture flasks or on culture plates or dishes. For cryopreservation, the cells were trypsinized, counted with the number of 1×10^6 and resuspended in 1.5 ml freezing medium (10% DMSO in FBS-supplemented DMEM). For long-term reserve cryotubes were stored in liquid nitrogen.

The cells were treated with several substances in the experiments. Details and concentrations were summarized as Table 3-1.

Table 3-1: Substances used for cell treatment.

Substance	Final concentrations	Treatment Time	Medium
4-Hydroxytamoxifen	1 μ M	Every 24hours	FBS free medium
Fulvestrant	10nM for IF and WB, 30nM for CFA	Every 48hours	normal medium
Cetuximab	5,10 μ g/ml for WB, 2.5, 5 μ g/ml for CFA	Every 48hours	normal medium
PD-0325901	0.1,1 μ M for WB, 0.1,0.3,1 μ M for CFA	Every 24hours	normal medium

3.1.2 Colony forming Assay

To investigate the clonal expansion of HNSCC cells upon fractionated irradiation, 100, 300 and 1000 cells were seeded per well in 6-well plates and irradiated on four consecutive days with a daily dose of 2 gray (Gy) using X-RAD 320 (Precision X-Ray, North Branford, CT USA) or kept untreated as controls. Half of the cells were administrated daily with 4-Hydroxytamoxifen (TAM, Sigma-Adrich, Germany), MEK1/2 inhibitor PD0325901 (Sigma-Adrich, Germany) or every second day with Fulvestrant (Sigma-Adrich, Germany) at the indicated concentrations. To assess the sensitivities of tumor cells upon cetuximab or PD-0325901, 1000 and 3000 cells were seeded per well in 6-well plates. Half of the cells were treated daily with PD0325901 or every second day with cetuximab at the indicated concentrations. After 10-14 days in culture, clones were coloured with crystal violet and total amount of colonies was quantified as described in (Niyazi *et al.*, 2007). The survival fraction was calculated using a freely available software Clono-counter according to (Franken *et al.*, 2006).

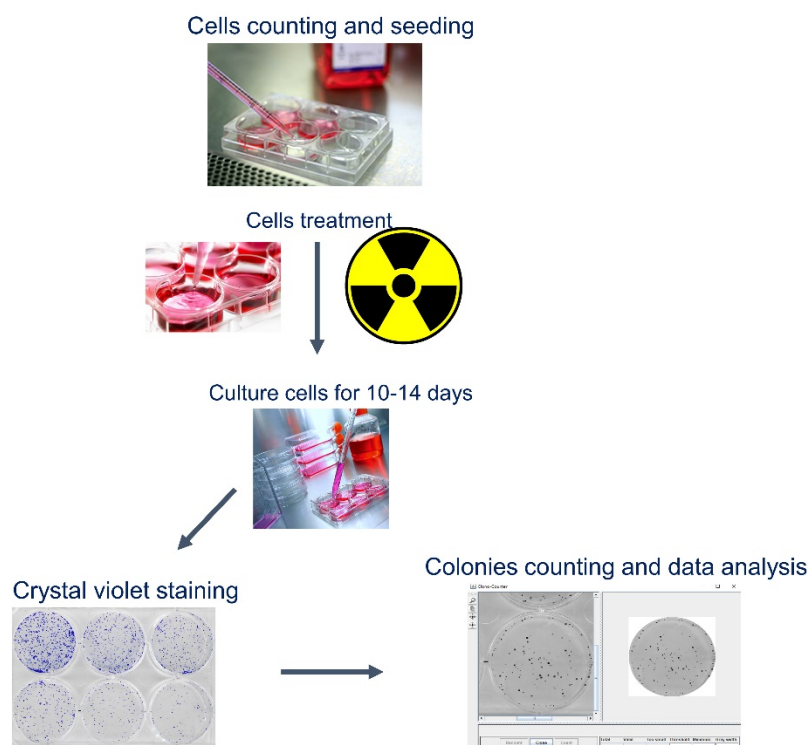


Figure 3-1: Schematic protocol of the colony forming Assay

Cells were seeded in six-well plates and treated with substances or IR as indicated time. After culture cells for 10-14 days, colonies were assessed by microscope. Staining with crystal violet was performed depending on the size of colonies. Number of colonies was counted by a freely available software Clono-counter.

3.1.3 Immunofluorescence (IF)

Cells were seeded on sterile coverslips in a 12-well plate and fixed with 4% paraformaldehyde for 15 mins at room temperature. After being wash with phosphate-buffered saline (PBS) three times. The cells were permeabilized with 0.5% Triton X-100 buffer in PBS for 30 mins, and after being wash again three times with PBS, blocked with 1% bovine serum albumin (BSA)/0.2% Tween 20 in 1x PBS for 30 mins at room temperature. The primary antibody diluted in T-buffer with indicated concentrations was incubated with cells for 1 hour at room temperature or overnight at 4°C. Following washing with PBS three times, the secondary antibody plus H33342 diluted in T buffer was added for 30 mins at room temperature in the dark. Finally, cells were again washed with PBS for 3 times and embedded on glass slides with Mowiol.

The glass slides were kept in the dark at 4°C for at least 12 hours before taking pictures.

3.1.4 Senescence-associated β -galactosidase (SA- β -gal) staining

Cells were seeded on 6 cm dishes and treated with PD-901 as an indicated protocol. Cells were fixed in fixation buffer (provided in kit) and SA- β -gal staining was performed using a kit (Cell Signaling Technology, Germany) following with the manufacturer's protocols strictly. Pictures were taken by Keyence microscopy and blue SA- β -gal positive cells ratios were quantified by ImageJ software.

3.2 Protein biochemistry methods

3.2.1 Protein extraction and determination of protein concentration

Cells were seeded on a 10cm culture dish and harvested in cold 1x PBS after indicated treatment. Pelleted cells were resuspended in ice-cold RIPA buffer with freshly added protease inhibitor and phosphatase inhibitor cocktail (1:100). The samples were incubated for 15mins on ice and centrifuged at 4°C for 10mins at 13,000 rpm (Centrifuge 5403, Eppendorf) to separate protein lysate from cell debris. The supernatant was collected and transferred to a new 1.5ml tube. An aliquot of 4 μ l was taken to determine the protein concentration.

Protein concentration of RIPA lysates was measured utilizing BCA protein assay kit (Fisher Scientific Inc), which is a detergent-compatible formulation based on colorimetric reaction of bicinchoninic acid (BCA) with reduced Cu^{+2} to Cu^{+1} for the quantitation of total protein at 562nm. This method can be used for quantitation of

protein concentration since the reaction is linear in a certain range. RIPA lysates were diluted 1:10 in ddH₂O and pipetted in triplicates into a 96-well plate. 200µl of BCA mixture reagent (reagent A : reagent B = 50:1) was transferred to each well. Parallely, a dilution series of Albumin (BSA) standards ranging from 0 to 2000µg/ml was prepared according to manufacturer's protocol and added to the plate as a standard curve. The reaction plate with slight shaking was incubated for 30mins at 37°C. The colorimetric value of each well was measured at 600nm with microplate reader (Biochrom Anthos Microplate Reader).

3.2.2 SDS polyacrylamide gel electrophoresis (SDS-PAGE)

The sodiumdodecylsulfate-polyacrylamide gel electrophoresis (SDS-PAGE) was performed for protein separation. Firstly, the separation gel (10-15% acrylamide/bisacrylamide, 375mM Tris-HCl pH 8.8, 0.1% SDS, 0.1% APS, 0.1% TEMED) was prepared, then the stacking gel (4% acrylamide/bisacrylamide, 125mM Tris-HCl pH 6.8, 0.1% SDS, 0.1% APS, 0.1% TEMED) was added. The concentration of the separation gel was dependent on the target proteins. Equal amounts of protein sample (20µg) were mixed with 4 x Laemmli buffer and incubated at 95°C for 5min, loaded onto the gel after cooling. A pre-stained protein marker (Fisher Scientific Inc) was loaded in one well in parallel. The gel electrophoresis was performed at 25-35Ma in 1x SDS running buffer.

3.2.3 Western bolt

Proteins separated by SDS-PAGE were transferred onto a polyvinylidene difluoride (PVDF)- membrane by wet blotting system from Bio-rad. The PVDF membrane was activated for 30seconds in methanol, washed for 2 mins in ddH₂O and then incubated in 1 x transfer buffer for 5mins. The blotting sandwich was prepared in following order:

anode plate, sponge, filter paper, PVDF-membrane, PAGE gel, filter paper, sponge, cathode plate. The sandwich was installed in a blotting chamber with ice for preventing overheating. The transfer was performed at 100V for 1h in 1x transfer buffer. After transfer, the membrane was blocked in 5% milk or 5% BSA in PBS/0.5% Tween (PBST) for 1h at room temperature on a shaker. The membrane was incubated with the diluted primary antibody with a indicated concentration () overnight at 4°C. Before and after incubated with the secondary antibody-HRP in blocking buffer for 1 h, the membrane was washed three times for 10mins in PBST on a shaker. The membrane was incubated for 1min with the enhanced chemiluminescence (ECL) solution. The signal was measured by ImageQuant LAS500 system with the appropriate time.

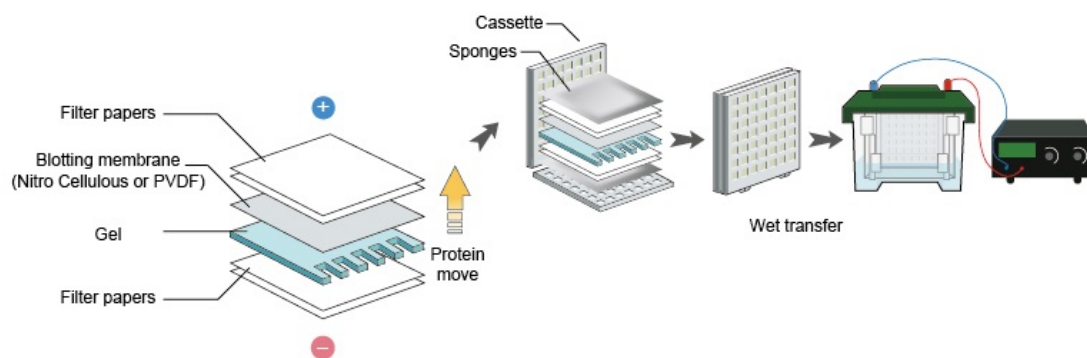


Figure 3-2: Schematic diagram of wet electro-transfer technique.
(modified from *creative-diagnostics.com*).

3.3 Immunohistochemistry(IHC) with TSA

Immunohistochemistry(IHC) is a standard method for the test of specific proteins on tissue sections with antibodies. The tissue sections on slides were deparaffinized in xylene for 10mins and then rehydrated in a decreasing concentration of ethanol series (100%, 100%,90%, 70%) for 3mins each. Endogenous peroxidase was blocked with 3% H_2O_2 and 70% ethanol for 10min and heat-mediated antigen retrieval was performed in 10mM citrate buffer (pH6.0) for 30mins in a steam cooker. Then cooled

down for room temperature and washed shortly in ddH₂O for 1min, in 1x PBS for 5min. During the time the tissue sections were encircled with a hydrophobic PAP pen. The slides were washed for five minutes in 1x TNT buffer before blocked for 30 minutes in TNB buffer in a humid chamber to prevent from drying off. Then the tumor tissues were incubated with the primary antibody diluted in 1x TNB buffer for overnight at 4°C in a humid chamber. After removal of primary antibody the slides were washed 3 times with 1x TNT buffer for 5 mins. Afterwards, they were incubated for 30 minutes with secondary antibody (diluted 1:200 in TNB buffer) in a humid chamber at room temperature. Next, three times washing were repeated. For signal amplification the slides were incubated in a humid chamber with streptavidin-HRP (diluted 1:100 in TNB) for 30 minutes at room temperature, washed three times in 1 x TNT buffer and incubated with biotin-labelled tyramide (diluted 1:200 in amplification diluent from PerkinElmer TSA kit) 10 minutes exactly at room temperature. The slides were washed repeatedly and incubated with streptavidin-HRP to enhance the signal for additional 30 minutes again. Another washing in 1 x TNT was repeated. Next, the signal was developed using the DAB detection kit following the manufacturer's manual and applied until a change in color was visible. Finally, the slides were washed with ddH₂O briefly and counterstained using haematoxylin solution, washed for 10 minutes under running tap water subsequently. The tissue sections were dehydrated with increasing concentrations of ethanol series (70%, 96%, 100%, 100%) and xylene. The slides were embedded using Eukitt and observed using light microscopy.

3.4 Tissue microarray (TMA)

3.4.1 TMA production

A tissue microarray (TMA) is a slide with circular tissue sections that cover samples from up to 200 patients. TMAs are created by punching cylindrical samples of tumor

tissue and arranging these parallel to each other in paraffin. These paraffin blocks were cut with a microtome into 2- μ m-thick sections. Paraffin-embedded tissue samples were provided by the tissue bank of the National Center for Tumor Disease (NCT) in collaboration with Dr.Flechtenmacher (Institute of Pathology, University Hospital Heidelberg) after approval by the local institutional review board (ethic vote 206/2005). For all patients, clinic-pathological and follow-up data were available from the Department of Otolaryngology, Head and Neck Surgery at the University Hospital Heidelberg.

The retrospective study cohort included patients with OPSCC who were treated at the University Hospital Heidelberg between 1990 and 2008. The tumor samples include primary tumors as well as recurrence, metastasis and secondary carcinomas. For oropharyngeal cohort three TMAs (TMA 18, 19 and 20) were combined. Overall, they include 176 patients represented by 586 samples of primary tumors, recurrence, metastasis and secondary carcinomas and an additional 29 samples of healthy mucosa.

3.4.2 TMA scoring

TMAs were scanned utilizing the Nanozoomer HT Scan system (Hamamatsu Photonics, Japan) following accomplishment of IHC as clarified in 3.3. At least three experienced raters scored scanned TMAs slides by using NDP Viewer software. The semi-quantitative analysis was performed based on two independent categories: first, the relative number of stained tumor cells (score A ranging from 1 to 4: score 1 = no positive cells, score 2 = less than 33 %, score 3 = between 34 and 66 %, and score 4 = more than 66 % positive cells), and second, the staining intensity (score B ranging from 1 to 4: score 1 = no staining, score 2 = weak staining, score 3 = moderate staining, and score 4 = strong staining). Only primary tumors were included for the data analysis. Subsequently, the median score A and B were multiplied resulting in the final

expression score ranging from 1 to 16, which represented informative values for tumor specimens of patients. Accordingly, patients were arranged in different groups with various staining patterns.

3.4.3 Statistical analysis

Statistical analysis was performed by using IBM SPSS22 Software. Person and Spearman's correlation analysis between score A and B were done before they were multiplied. The scores were correlated to patient's data and clinical pathological factors. Differences of clinical pathological parameters between the groups were determined by χ^2 test (chi squared test) or Fisher's exact test.

Disease-specific survival (DSS) was calculated as the time from the date of primary tumor diagnosis to the date of OPSCC-related death within the follow-up interval (events). Survival time of patients who were alive or were dead due to OPSCC-unrelated causes were censored. Progression-free survival (PFS) was calculated from the date of primary tumor diagnosis to the date of the first local recurrence, lymph node or distant metastasis, second primary carcinoma or date of OPSCC-related death within the follow-up period (events), or to the date of OPSCC-unrelated death or without progression (censored). The method of Kaplan–Meier was used to estimate survival distributions and differences between groups were determined by log-rank tests. To adjust for possible con-founders, multivariate cox proportional hazard models were utilized.

All experiments were performed in triplicate or duplicate independently. A representative figure is depicted for western blot. Statistical analysis of data was performed with Excel2016, IBM SPSS 22 and Graphpad Online QuickCalcs. Error bars represent standard error of mean (SEM). Student's *t* test was used for comparisons

between groups. A p-value of 0.05 and below was considered as statistically significant (marked by*, ** or *** as p-value <0.05, <0.005, <0.0005, respectively).

4. Results

4.1 Co-expression of ESR2 and SMR3A in HNSCC and correlation with clinical features (Published)

Our previous data provided an experimental evidence that a subpopulation of radiotherapy resistant malignant cells reveal co-expression of estrogen receptor 2 (ESR2) and SMR3A after fractionated irradiation (IR) (Grunow *et al.*, 2017). To investigate the clinical relevance of our *in vitro* results, we evaluated ESR2 expression by IHC staining on TMAs containing tumor specimens of OPSCC patients, which were treated with either definitive or post-surgical radiotherapy with or without adjuvant chemotherapy. Evaluable staining specimens were obtained from 109 OPSCC patients (Figure 4-1A). Positive staining for ESR2 (ESR2^{pos}) in tumor cells was detected in 65.1% of tumors and a high staining pattern correlated significantly with an elevated SMR3A immunoreactivity score as compared to specimens with undetectable ESR2 staining (Figure 4-1B). Subsequently, ESR2 expression pattern and clinic-pathological features were compared, it was not observed any statistically significant correlation between ESR2^{neg} and ESR2^{pos} subgroups except for age, T status and smoking. ESR2^{pos} staining pattern was related significantly to older age, smaller tumor size and never or former smoking (Table 4-1). Next, Kaplan-Meier analysis and log rank testing were performed to reveal an unfavorable clinical outcome in ESR2^{neg} as compared to ESR2^{pos} tumors (Figure 4-1C-D). Nevertheless, patients with ESR2^{pos} tumors had a significantly worse PFS and DSS in the presence of SMR3A^{high} expression, similar to the ESR2^{neg} subgroup, whereas the pattern of ESR2^{pos}SMR3A^{low} displayed the most favorable clinical prognosis (Figure 4-1C-D). Multivariable analysis by Cox proportional hazard regression models was performed to confirm that a subgroup of ESR2^{pos}SMR3A^{low} had a favorable PFS and DSS as compared to either

ESR2^{pos}SMR3A^{high} or all other staining patterns (Supplements).

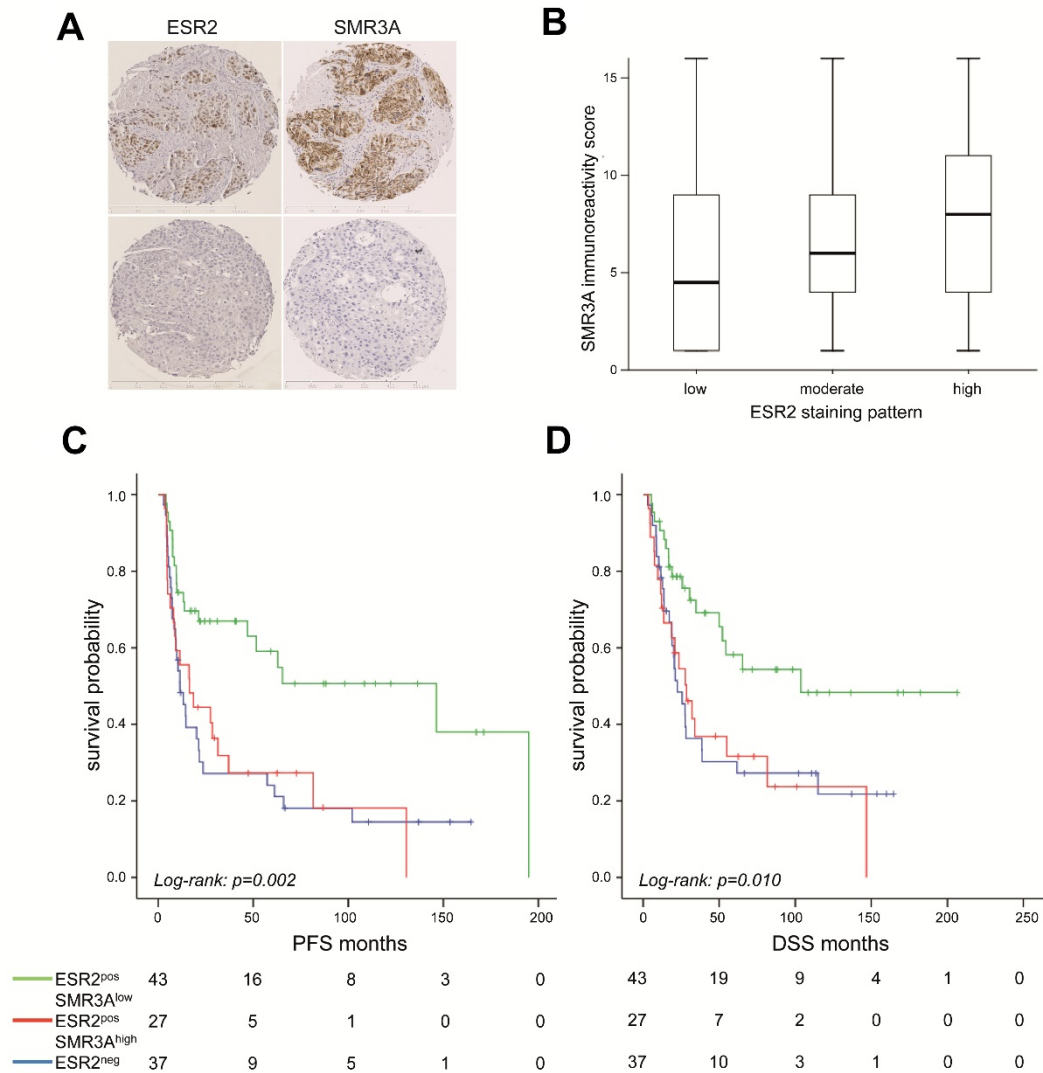


Figure 4-1: SMR3A and ESR2 expression in HNSCC patients.

(A) Representative pictures of immunohistochemical staining (brown signal) of serial tumor sections with anti-ESR2 (left row) or anti-SMR3A antibodies (right row). Haematoxyline counterstaining (blue staining) demonstrates the tissue architecture. Scale bars = 500 μ m. (B) Boxplot depicts the SMR3A immunoreactivity score as mean value and 5th/95th percentile for individual tumors with low, moderate or high ESR2 staining pattern ($p=0.044$). (C-D) Kaplan-Meier graphs show differences in DSS and PFS between subgroups without detectable ESR2 staining (ESR2^{neg}, blue line) and ESR2-positive tumors with low (green line) or high SMR3A expression (red line). Published in (Grunow *et al.*, 2017).

Table 4-1: Correlation of ESR2 expression with histopathological and clinical characteristics.

Features	Category	ESR2 ^{neg}		ESR2 ^{pos}		p value ³
		N	%	N	%	
Age [years]	< 57.5	25	65.8	30	42.3	0.019
	≥ 57.5	13	34.2	41	57.7	
Gender	Male	33	86.8	50	71.4	0.055
	Female	5	13.2	21	29.6	
T status	T1-T2	10	26.3	33	46.5	0.040
	T3-T4	28	73.7	38	53.5	
N status	N0	4	10.5	8	11.3	0.906
	N+	34	89.5	63	88.7	
M status	M0	35	92.1	66	95.7	0.445
	M+	3	7.9	3	4.3	
Pathological grading	G1-2	17	54.8	35	57.4	0.816
	G3	14	45.2	26	42.6	
Clinical staging	I-III	8	21.1	21	29.6	0.337
	IV	30	78.9	50	70.4	
Alcohol	no/former	5	13.2	14	19.7	0.390
	current	33	86.8	57	80.3	
Tobacco	no/former	5	13.2	22	31.0	0.040
	current	33	86.8	49	69.0	
HPV	non-related ¹	31	81.6	50	74.6	0.415
	related ²	7	18.4	17	25.4	
Therapy	adjuvant RT & RCT	22	57.9	49	69.0	0.246
	definitive RT & RCT	16	42.1	22	31.0	
	all RT	28	73.7	44	62.0	0.218
	all RCT	10	26.3	27	38.0	

RT, radiotherapy, RCT, radiochemotherapy, ¹ viral DNA-negative or DNA-positive but transcript-negative; ² viral DNA- and transcript-positive according to Holzinger et al (Holzinger et al., 2012); ³ Chi-square test. (published in (Grunow et al., 2017))

4.2 Co-expression of OPRPN and SMR3A in HNSCC cell lines and response to fractionated irradiation

Experimental data of our research group demonstrated that SMR3A is expressed in HNSCC cell lines at low levels, but the relative amount of SMR3A-positive cells increase after fractionated irradiation (Grunow et al., 2017). To investigate whether OPRPN is co-expressed with SMR3A in HNSCC cell lines, a co-immunofluorescence staining (co-IF) was performed in FaDu and Cal27 cells. Similar to SMR3A, basal OPRPN protein expression was low and detected only in a sub-fraction of both cell lines (Figure 4-2B). However, upon fractionated IR prominent OPRPN expression was found in the majority of cells and was co-expressed with SMR3A (Figure 4-2B)

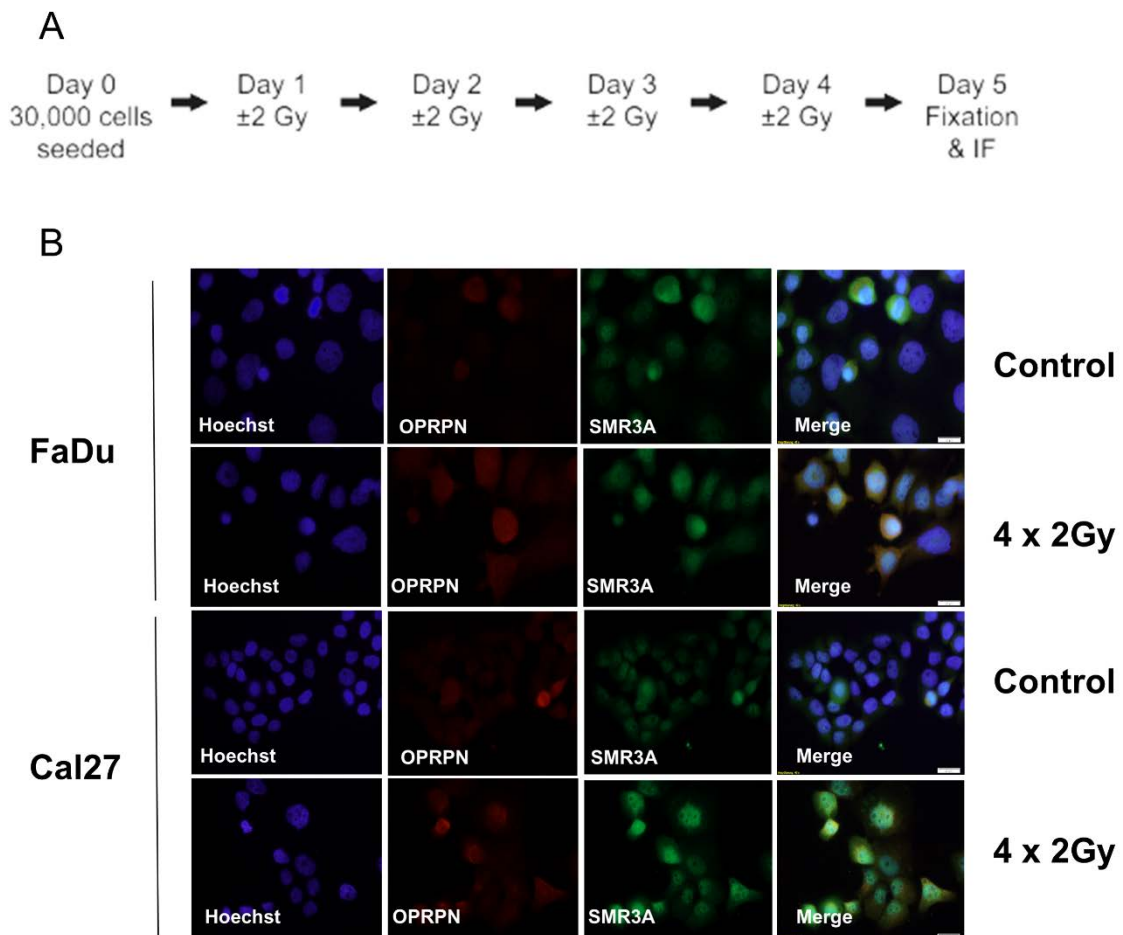


Figure 4-2: Co-expression of OPRPN and SMR3A in HNSCC cell lines in response to fractionated irradiation.

(A) Schematic representation of the treatment protocol for fractionated irradiation (4x2Gy); (B) Representative pictures of the co-immunofluorescence staining confirms induced OPRPN (red signal) and SMR3A (green signal) expression upon fractionated irradiation. Cell nuclei were stained by Hoechst33324 (blue staining), white bar= 20µm.

4.3 Expression of OPRPN in primary OPSCC and correlation with clinic-pathological features

To determine whether aberrant OPRPN expression is relevant for the pathogenesis and/or the malignant progression of OPSCC, tissue microarrays with tissue samples of normal mucosa and OPSCC were stained by immunohistochemistry. A weak staining of OPRPN was observed in basal and supra-basal keratinocytes of normal mucosa, which

was utilized as reference (Figure 4-3A, B). A heterogeneous staining pattern of OPRPN protein was observed in primary OPSCC varying from low to high expression (Figure 4-3C-F).

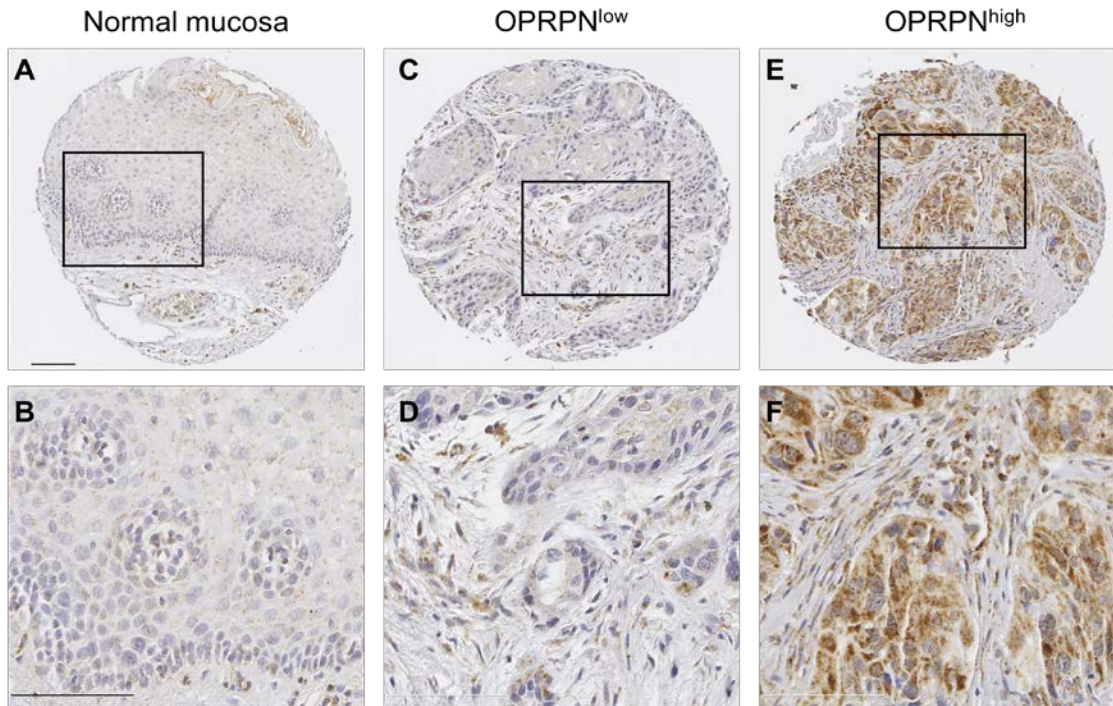


Figure 4-3: OPRPN protein expression in normal mucosa and primary tumors of OPSCC patients.

Representative pictures for OPRPN expression (signal in brown) in normal mucosa (A and B) and primary OPSCC with low (C and D) or high OPRPN protein levels (E and F) as determined by IHC staining of TMAs. Counterstaining of cell nuclei was performed with haematoxylin (signal in blue) to demonstrate tissue architecture. Scale bars equal 100 μ m.

Relative number of positive tumor cells and staining intensity were estimated by three observers independently. Both scores revealed a significant correlation (Spearman correlation of 0.825 and a Pearson correlation of 0.846) and were multiplied to obtain a final OPRPN expression score for further analysis. According to the final score, patients were arranged into two categories: patients with low protein expression of OPRPN (OPRPN^{low}) and those with high protein expression of OPRPN (OPRPN^{high}). Overall, 39.3% (55/140) of all patients were arranged as OPRPN^{low} and 60.7% (85/140) of those as OPRPN^{high}.

Subsequently, OPRPN expression pattern and clinic-pathological features were compared, including age, gender, TNM status (*AJCC Cancer Staging Manual 7th ed*), pathological grade, HPV status, smoking and alcohol consumption. However, these parameters were not significantly correlated with OPRPN protein levels (Table 4-2). These data are in line with previous findings that SMR3A has no correlation with clinic-pathological features in OPSCC (Koffler *et al.*, 2013). Accordingly, the regulation of opiorphin gene family is independent of initial events during neoplastic transformation and malignant progression of OPSCC.

Table 4-2: Correlation analysis for OPRPN expression and clinic-pathological features in the OPSCC patients Cohort

Clinic-pathological features		OPRPN ^{low}	OPRPN ^{high}	p-value
Age(years)	< 58	31	38	0.178
	≥58	24	47	
Gender	Male	39	63	0.677
	Female	16	22	
Tumor size	T1/T2	25	36	0.763
	T3/T4	30	48	
	missing ¹		1	
Lymph node	N0	11	15	0.751
	N+	44	69	
	missing ¹		1	
Metastasis	M0	49	80	0.431 ²
	M+	4	3	
	missing ¹	2	2	
Clinical stage	I/II/III	17	25	0.885
	IV	38	59	
	missing ¹		1	
Pathological Grading	G1/G2	29	38	0.457
	G3	19	33	
	missing ¹	7	14	
Tobacco	Never/former	12	23	0.484
	Current	43	62	
Alcohol	Never/former	11	16	0.863
	Current	44	69	
HPV status	HPV- ³	42	70	0.387
	HPV+ ⁴	13	15	

¹ missing data, no information available; ² Fisher's exact test; ³viral DNA+RNA- or DNA-; ⁴viral DNA+RNA+ according to (Holzinger et al., 2012)

4.4 Correlation of OPRPN and SMR3A expression with disease-specific and progression-free survival

Next, the prognostic value of OPRPN expression for disease-specific survival (DSS) and progression-free survival (PFS) of OPSCC patients was analyzed by Kaplan-Meier plots and log rank testing, but no statistically significant difference was observed (Figure 4-4). As final immunoreactivity scores of OPRPN and SMR3A had a moderate but significant correlation (Spearman correlation of 0.380 and a Pearson correlation of 0.385) and a strong staining pattern of SMR3A was correlated significantly with a higher OPRPN immunoreactivity score ($P < 0.05$), a combinatorial subgroup analysis was performed. However, patients with a SMR3A^{high}OPRPN^{high} staining pattern in the tumor had a similar clinical outcome as compare to other subgroups (Figure 4-5).

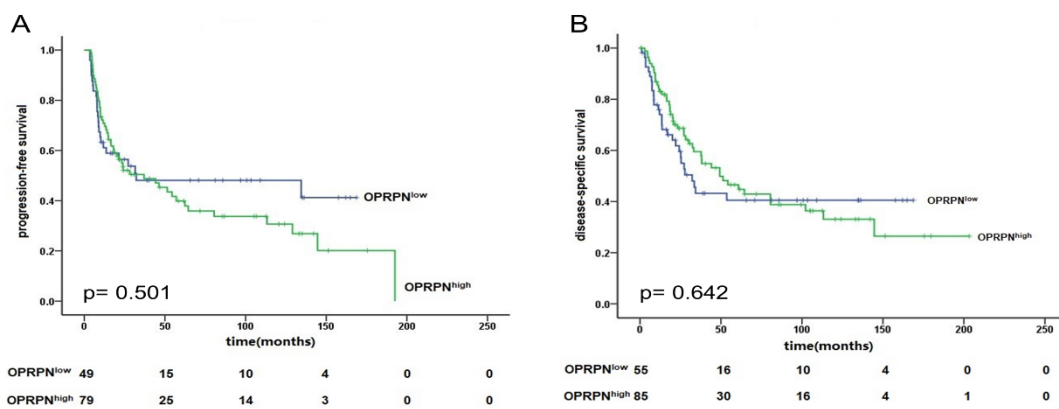


Figure 4-4: Progression-free survival and disease-specific survival in the cohort of OPSCC patients depending on OPRPN expression

OPSCC patients were arranged into two categories: patients with low protein expression of OPRPN (OPRPN^{low}, final score < 9; blue curves) and those with high protein expression of OPRPN (SMR3A^{high}OPRPN^{high}, final score ≥ 9 ; green curves). Progression-free survival (A) and disease-specific survival (B) were evaluated by Kaplan-Meier analysis and log-rank test. Total number of patients at risk were listed at indicated time points.

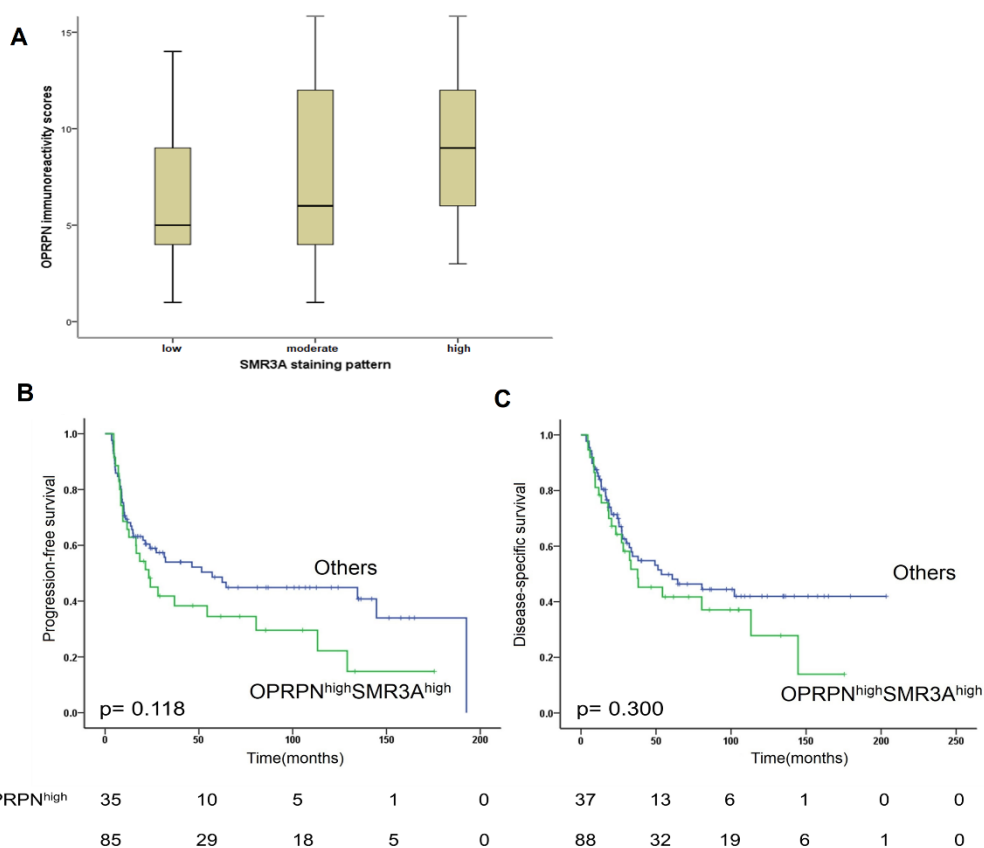


Figure 4-5: Combinatorial analysis of progression-free survival and disease-specific survival in the cohort of OPSCC patients depending on OPRPN and SMR3A expression

(A). Boxplot depicts the OPRPN immunoreactivity score as mean value and 5%-95% for individual tumors with low, moderate or high SMR3A staining pattern. OPSCC patients were arranged into two categories: patients with high protein expression of OPRPN and SMR3A (OPRPN^{high}SMR3A^{high}; green curves) and those all other combinations (others, blue curves). Progression-free survival (B) and disease-specific survival (C) were evaluated by Kaplan-Meier analysis and log-rank test. Total number of patients at risk were listed at indicated time points.

Next, a combinatorial analysis has been performed in subgroup of OPSCC patients, which were treated with either definitive or post-surgical radiotherapy with or without chemotherapy. Concerning PFS and DSS, SMR3A^{high}OPRPN^{high} staining pattern tumor revealed an unfavorable clinical outcome as compare to other subgroups (Figure 4-6).

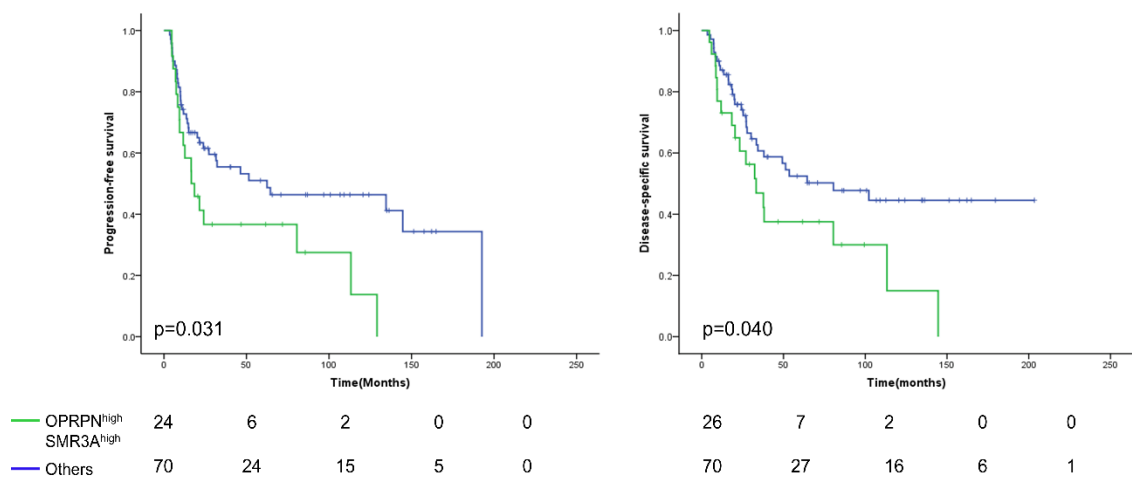


Figure 4-6: Combinatorial analysis of progression-free survival and disease-specific survival in the subgroup of OPSCC patients with radiotherapy depending on OPRPN and SMR3A expression

OPSCC patients with radiotherapy were arranged into two categories: patients with high protein expression of OPRPN and SMR3A (OPRPN^{high}SMR3A^{high}; green curves) and those all other combinations (others, blue curves). Progression-free survival (A) and disease-specific survival (B) were evaluated by Kaplan-Meier analysis and log-rank test. Total number of patients at risk were listed at indicated time points.

4.5 Inhibition of ESR2 signaling sensitizes HNSCC cell lines to irradiation

Previous findings demonstrated that neither androgen receptor (AR) nor estrogen receptor 1 (ESR1) expression are expressed in FaDu or Cal27 cell lines under normal growth conditions. In contrast, estrogen receptor 2 (ESR2) was detected in both cell lines and was strongly up-regulated upon fractionated IR, suggesting a causal role in the response to irradiation (Grunow *et al.*, 2017). To investigate whether inhibition of ESR2 alters the sensitivity of HNSCC cell lines upon radiotherapy, FaDu and Cal27 cells were treated for 24h or 48h with 10nM fulvestrant, which is a selective ESR degrader (Lai and Crews, 2017). ESR2 protein levels were determined by immunofluorescence staining. Fulvestrant treatment revealed reduced ESR2 protein levels in FaDu but not Cal27 cells as compared to DMSO-treated controls (Figure 4-7A).

In addition, no impact of fulvestrant on the relative survival fraction of FaDu cells and a slight increase of the relative survival fraction of Cal27 cells after fulvestrant treatment was found. Fulvestrant treatment significantly reduced the relative survival fraction of FaDu cells in combination with fractionated IR, suggesting a causal role of ESR2 in radioresistance (Figure 4-7B). However, no significant difference was observed for Cal27 cells. To further confirm the impact of ESR2 in radioresistance, both cell lines were treated with 4-Hydroxytamoxifen (4-OH-TAM), which resulted in a reduced relative survival fraction with or without fractionated IR in FaDu and Cal27 cell lines (Figure 4-7 C). 4-OH-TAM belongs to a family of drugs, which are known as selective estrogen receptor modulators (SERMS) and function as either antagonists or agonists depending on the target tissue. In line with the less efficient reduction of ESR2 by fulvestrant, Cal27 cells exhibited a significant decrease in the relative survival fraction only with treatment of 4-OH-TAM but not fulvestrant (Figure 4-7 B, C).

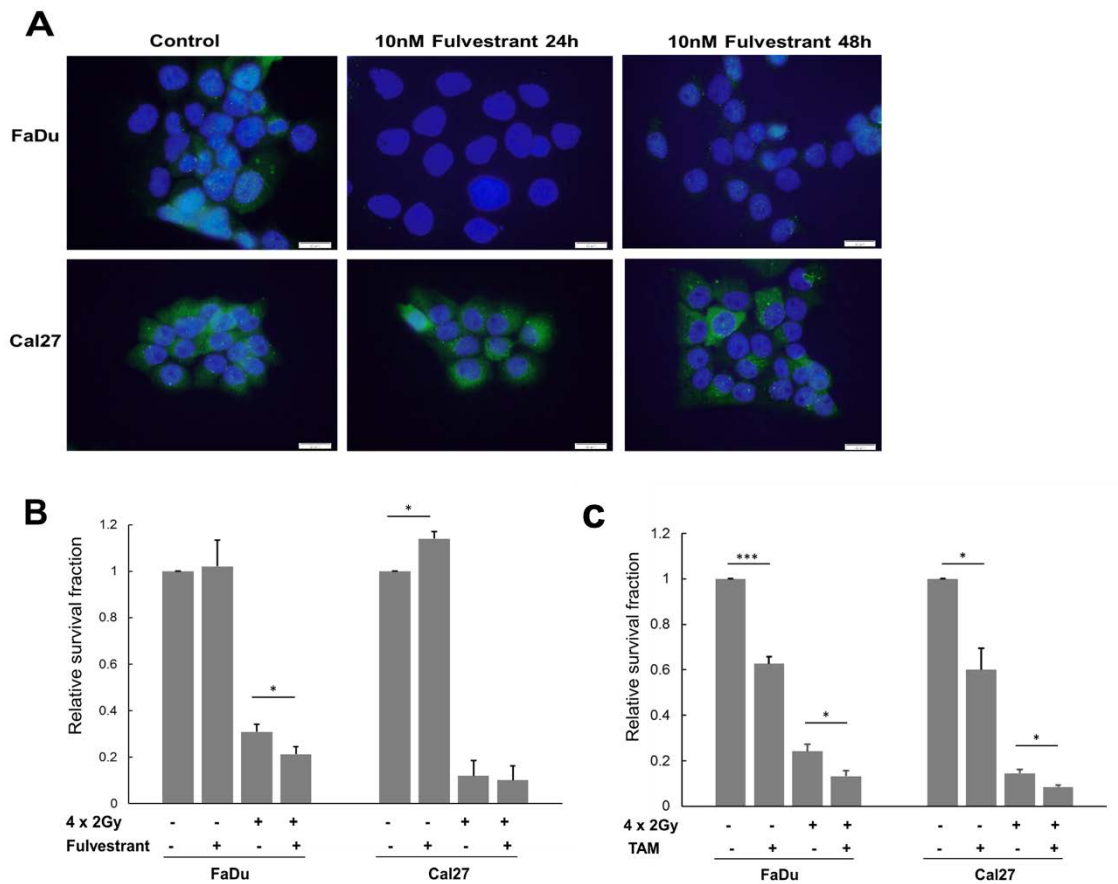


Figure 4-7: Impact of fulvestrant or TAM treatment on FaDu and Cal27 with fractionated IR.

(A) Representative pictures of immunofluorescence staining for ESR2 protein levels of control (DMSO) and 10 nM fulvestrant-treated FaDu and Cal27 cells. Graphs represent the relative survival fraction of FaDu and Cal27 cells after fractionated IR (4 x 2Gy) and either 30 nM fulvestrant (B) or 1 μM TAM (C) administration, respectively. Control groups are set to one and bars represent mean values ± standard error of the mean (SEM) of at least three independent experiments. * $p \leq 0.05$, *** $p \leq 0.0005$. (B and C were published in (Grunow et al., 2017))

4.6 Regulation of ESR2 and pERK1/2 in FaDu cells upon fractionated-IR and MEK1/2 inhibitor treatment

An increasing body of experimental evidence supports that irradiation-induced phosphorylation of ERK1/2 (pERK1/2) serves as a mechanism of radioresistance in HNSCC (Affolter *et al.*, 2016; Drigotas *et al.*, 2013; Gupta *et al.*, 2001). To investigate

the impact of the clinically tested MEK1/2 inhibitor PD-0325901 (PD-901) on ERK1/2 phosphorylation and ESR2 protein levels in HNSCC cell lines, FaDu cells were treated with 0.1 μ M PD-901 with or without fractionated-IR (4x2Gy) (Figure 4-8 A). Increase in pERK and ESR2 after fractionated IR was determined by IF staining (Figure 4-8 B) and confirmed for pERK by western blot analysis (Figure 4-8 C). As expected, inhibition of basal and IR-induced pERK levels was observed after PD-901 treatment. Elevated ESR2 levels after PD-901 treatment were found without IR but not with IR. In addition, neither basal nor IR-induced pERK levels were affected by fulvestrant treatment. Although both pERK and ESR2 are induced upon fractionated IR and seem to play significant roles in radioresistance, these data do not support a direct functional cross-talk between ERK signaling and regulation of ESR2 in irradiated FaDu cells.

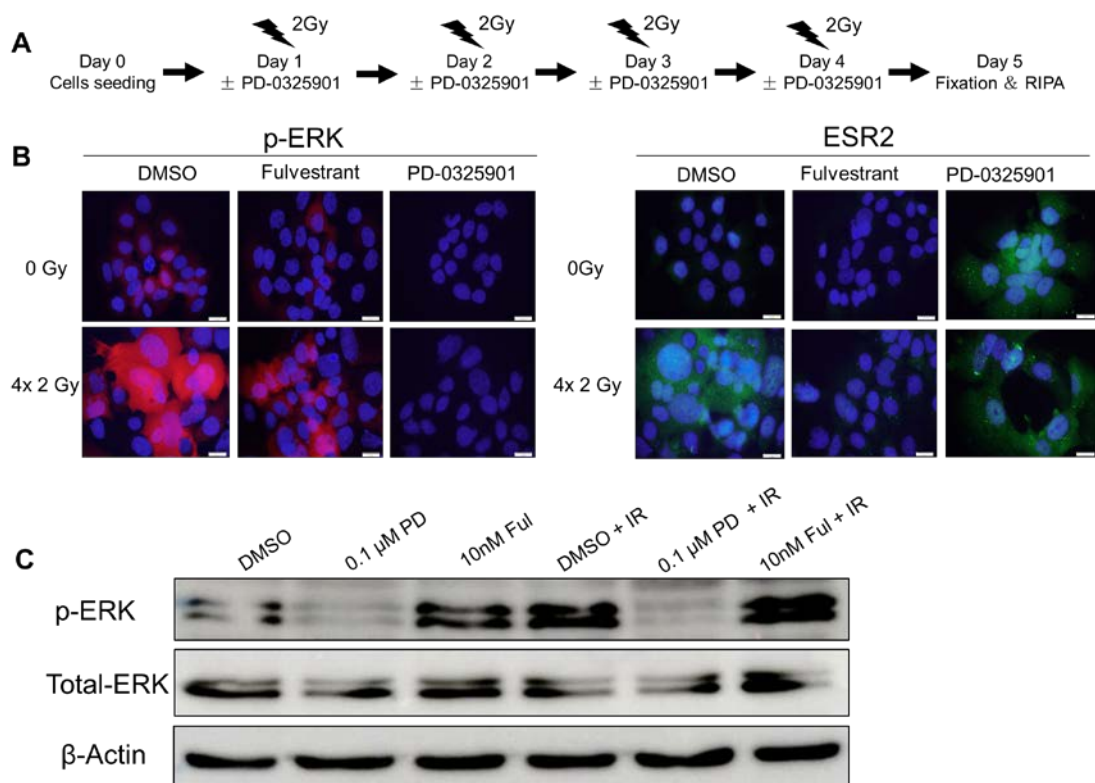


Figure 4-8: Effect of fractionated-IR and MEK1/2 inhibitor treatment on ESR2 and phospho-ERK1/2 protein levels in FaDu cells.

(A) Schematic summary treatment protocol with the 0.1 μ M PD-0325901 (PD) or 10nM Fulvestrant and fractionated IR (4 x 2Gy). ESR2 and pERK1/2 protein levels in FaDu cells after treatment was determined by immunofluorescence staining (B; red signal for pERK and green

signal for ESR2) and Western blot analysis with whole cell lysate (C). Cell nuclei were counterstained with Hoechst H33342 (blue signal). Scale bars = 20µm.

4.7 Impact of MEK1/2 inhibitor on the radiosensitivity of FaDu and Cal27 cells

Previous data demonstrated that fractionated-IR stimulated pERK as a potential mechanism of increased radioresistance. The elevation of pERK was almost completely restrained after treatment of FaDu cell with a MEK1/2 inhibitor. To investigate whether MEK inhibitor treatment alters the radiosensitivity of FaDu and Cal27, CFAs were performed using FaDu and Cal27 cells after treatment with 0.1 µM, 0.3µM PD-901 with or without fractionated-IR (4x2Gy). In the absence of fractionated IR, a concentration dependent reduction in the survival fraction for both cell lines was observed. Moreover, FaDu cells were more sensitive to PD-901 treatment than Cal27 cells. Administration of PD-901 sensitized FaDu and Cal27 cells to fractionated IR in a concentration dependent manner (Figure 4-9).

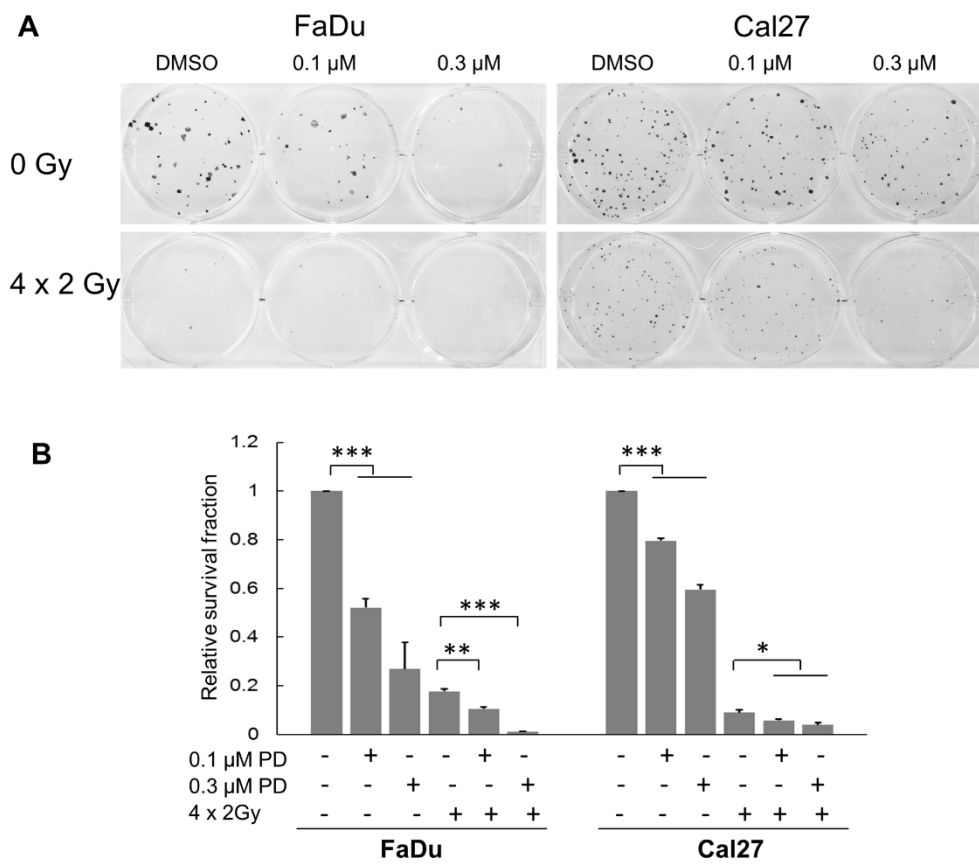


Figure 4-9: PD-901 treatment sensitizes HNSCC cell lines to fractionated IR.

(A) Representative staining of control (DMSO) or PD-901 treated FaDu and Cal27 cells with or without fractionated IR (4x 2 Gy). (B) Graphs indicate the relative survival fraction of FaDu and Cal27 cells after treatment with given concentrations of PD-901 with or without fractionated IR (4 x 2Gy). DMSO-treated control cells are normalized to one and bars depict mean values + SEM of three independent experiments. * $P \leq 0.05$, ** $P \leq 0.005$, *** $P \leq 0.0005$.

4.8 Sensitivity of HNSCC cell lines to MEK1/2 inhibitor treatment

To address whether PD-901 has a similar impact on survival and expansion of other HNSCC cell lines, CFAs using 0.1 μ M and 1 μ M PD-901 were performed in Detroit562, SCC4, SCC9 and SCC25. These experiments confirmed a concentration dependent reduction in the survival fraction for all cell lines, which was significant at a dose of 1 μ M PD-901. However, it is worth noting that at lower PD-901 concentration (0.1 μ M) no significant difference was found for Cal27 and Detroit562 cells, indicating a higher level

of resistance. (Figure 4-10 A, B).

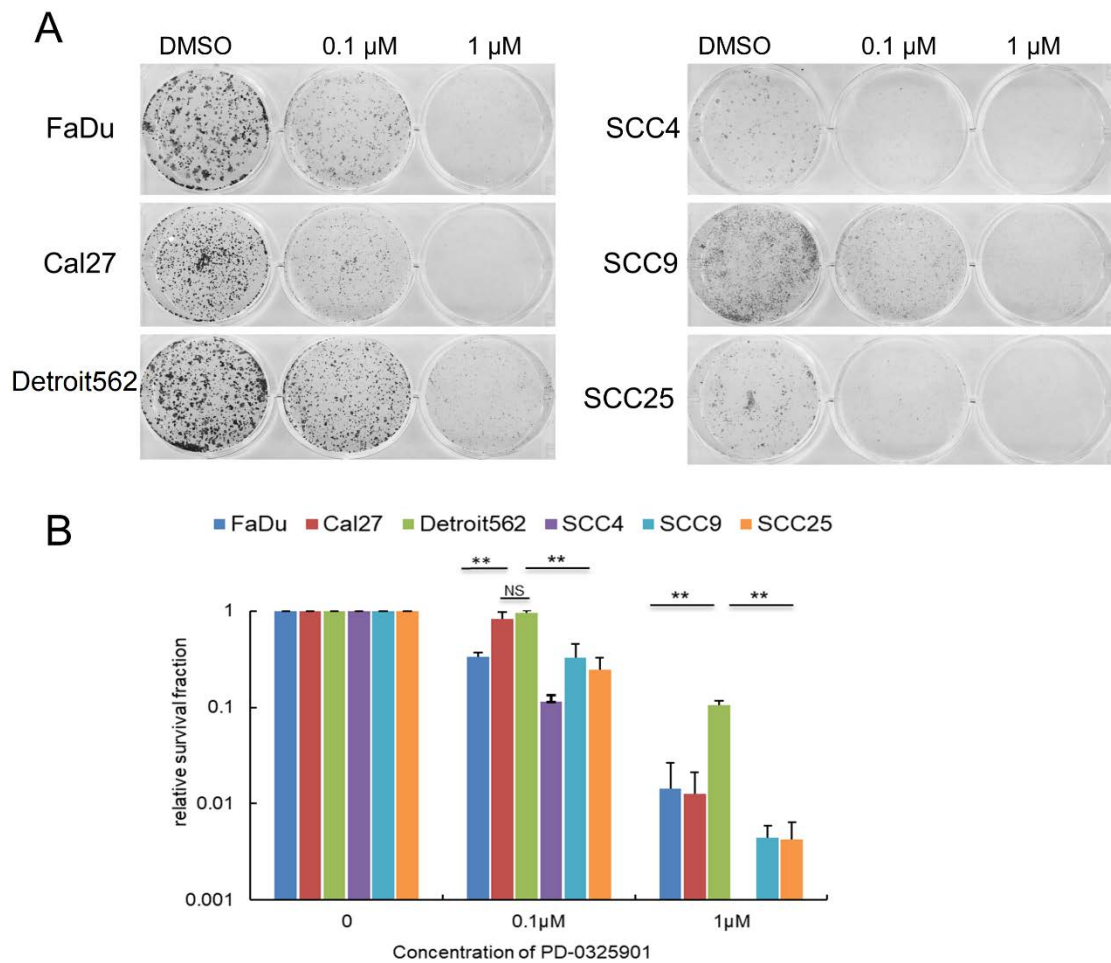


Figure 4-10: Sensitivity of HNSCC cell lines to the treatment with the MEK1/2 inhibitor PD-901.

(A) Representative staining of a CFA with control (DMSO) or PD-901 treated HNSCC cell lines. (B) Graphs represent the relative survival fraction of HNSCC cell lines after treatment with indicated concentrations of PD-901. DMSO-treated control cells are normalized to one and bars depict mean values + SEM of three independent experiments. * $P \leq 0.05$, ** $P \leq 0.005$.

4.9 Regulation of ESR2 in FaDu and Cal27 cells after cetuximab treatment

The epidermal growth factor receptor (EGFR)-targeted IgG1 monoclonal antibody, cetuximab, has revealed clinical benefits in the therapy of HNSCC. Cetuximab

represents FDA-approved and European Medicines Agency-approved targeted therapy in HNSCC and is employed with no correlation with EGFR status (Bourhis *et al.*, 2010). To monitor the impact of cetuximab on ESR2 expression in HNSCC cell lines, FaDu and Cal27 cells were treated with either 5 or 10 $\mu\text{g/ml}$ cetuximab respectively, as a single dose (Figure 4-11A) or three times every second day (Figure 4-12A). ESR2 protein levels were determined by Western blot analysis or IF staining. While a single dose treatment had no major impact on ESR2 protein levels in both cell lines as compared to controls (Figure 4-11B), a dose-dependent increase of ESR2 was detected in FaDu but not in Cal27 cells after repeated treatment with cetuximab. (Figure 4-12B, C).

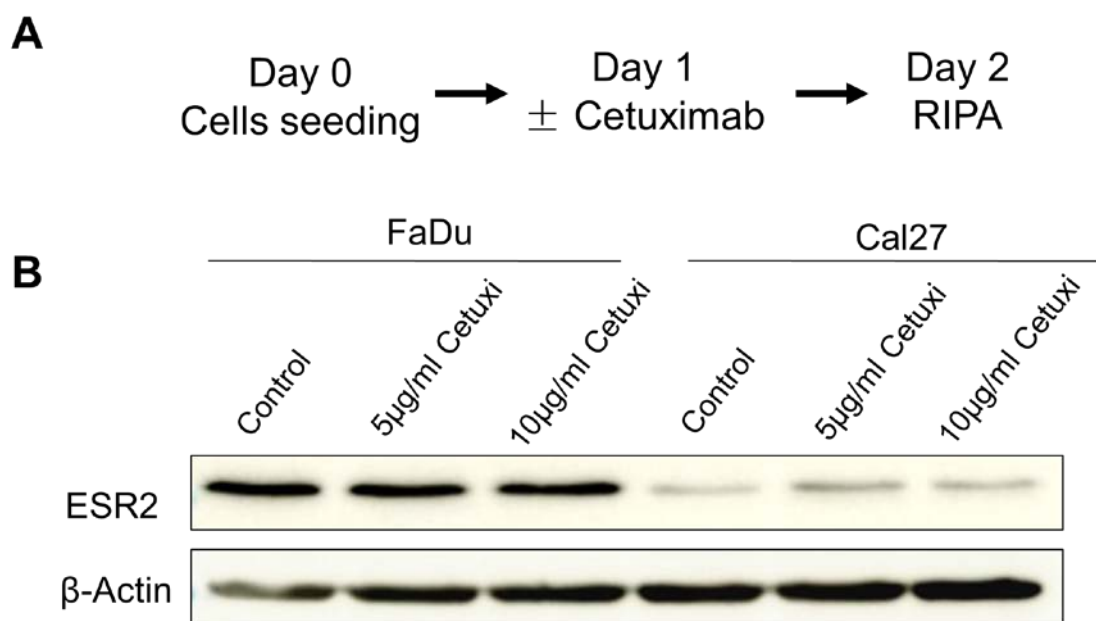


Figure 4-11: Regulation of ESR2 by cetuximab in single dose treatment.

(A) Schematic summary of the single dose cetuximab treatment protocol. (B) Expression of ESR2 in FaDu and Cal27 cells after cetuximab single dose treatment was demonstrated by Western blot analysis with whole cell lysate. Detection of β -actin served as a control for quantity and quality of protein lysates.

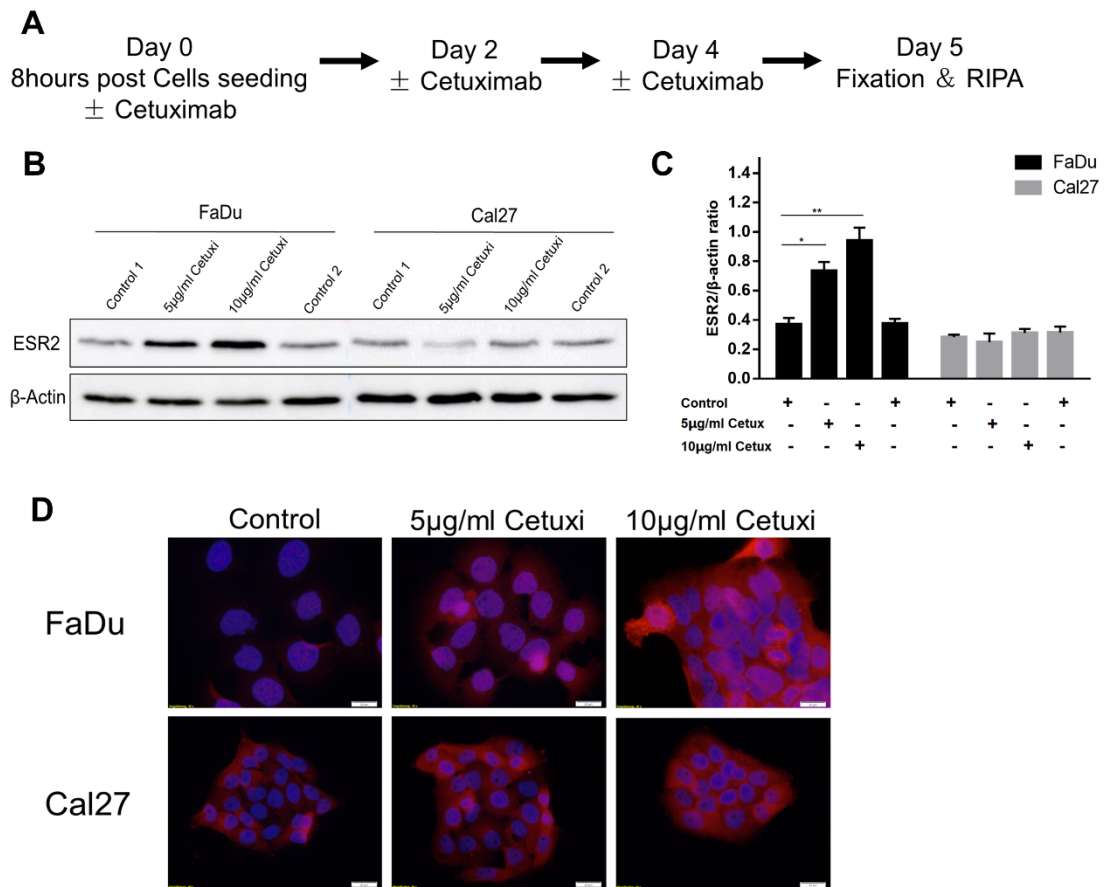


Figure 4-12: Regulation of ESR2 by cetuximab in three times-repeated treatment. (A) Schematic summary of the repeated cetuximab treatment protocol. (B) Expression of ESR2 in FaDu and Cal27 cells after repeated cetuximab treatment was demonstrated by Western blot analysis with whole cell lysates. (C) Signals were quantified by image J and bars in the graph show the ratio of ESR2 and β -actin. Data represent mean \pm SEM of two independent experiments measured in triplicates, * $P \leq 0.05$, ** $P \leq 0.005$. (D) Representative pictures of an immunofluorescence staining for ESR2 (red signal) in FaDu and Cal27 cells after treatment with indicated concentrations of Cetuximab. Cell nuclei were counterstained with Hoechst H33342 (blue signal). Scale bars = 20 μ m.

4.10 Sensitivity of HNSCC cell lines to cetuximab

Multiple clinical studies have confirmed a survival advantage for patients with locally advanced HNSCC, who were treated with Cetuximab in combination with radiotherapy as compared with irradiation alone considering PFS and DSS (Brockstein, 2011). Nevertheless, the response and sensitivity of individual patient to cetuximab varies

significantly. To address whether cetuximab has similar impact on HNSCC cell lines, CFAs were performed to evaluate the susceptibilities of several HNSCC cell lines to cetuximab. Our data revealed that SCC25 is more sensitive to cetuximab as compared to all other cell lines tested (Figure 4-13 A, B).

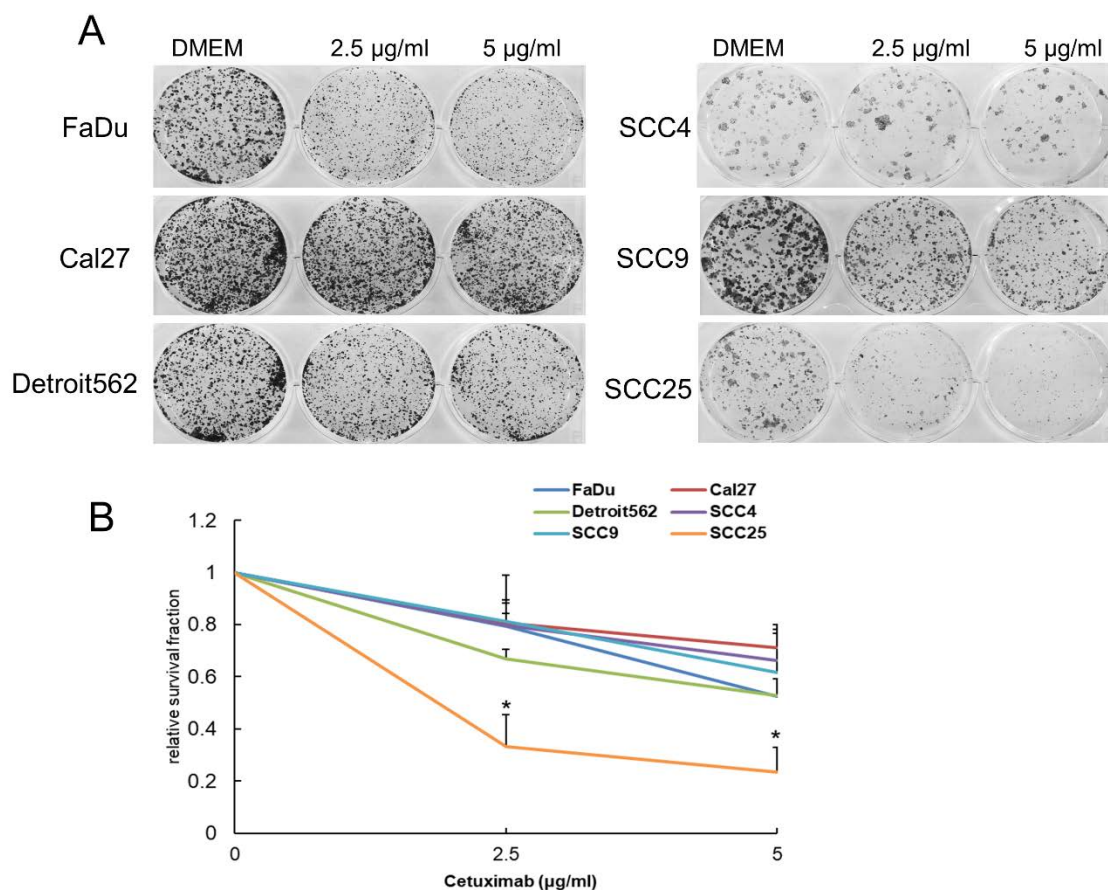


Figure 4-13: Sensitivity of HNSCC cell lines to cetuximab.

(A) Representative staining of a CFA with control (DMEM) or cetuximab treated HNSCC cell lines. (B) Graphs represent the relative survival fraction of HNSCC cell lines after treatment with indicated concentrations of cetuximab. DMEM-treated control cells are normalized to one and bars represent mean values + SEM of three independent experiments. * $P \leq 0.05$.

4.11 Regulation of pERK1/2 and PD-L1 by cetuximab treatment.

Programmed death-1(PD-1) is an immune checkpoint receptor expressed in tumor infiltrating lymphocytes (TIL), which restricts activated T lymphocytes function (Hamid and Carvajal, 2013). Its cognate ligand, programmed death ligand-1 (PD-L1) is expressed on tumor cells, including HNSCC (Chen and Han, 2015; Hammerman *et al.*, 2015). The MAPK/ERK pathway is one of the downstream signaling pathways stimulated by EGFR. To assess the impact of cetuximab on pERK1/2 and PD-L1 protein levels of HNSCC cell lines in single (Figure 4-14 A) and repeated treatment (Figure 4-15 A), whole protein lysate of several HNSCC cell lines were analyzed by Western blot. Data showed various regulatory effects on pERK/PD-L1 by cetuximab treatment in different cell lines. As expected, single cetuximab treatment reduced pERK levels in Cal27, Detroit562, SCC4, SCC9, and SCC25 cells as compared to controls. Moreover, Detroit562 and SCC9 exhibited a concentration dependent reduction of pERK levels. It is worth noting that SCC25, which was most sensitive to cetuximab, had the most effective reduction of pERK expression. By contrast, FaDu cells showed elevated pERK levels in response to cetuximab. There was no significant alteration of PD-L1 expression in Cal27, Detroit562 and SCC25 after single dose of cetuximab treatment. In addition, no obvious correlation between basal pERK and PD-L1 levels was found, but PD-L1 levels were decreased in FaDu, SCC4 and SCC9 cells after cetuximab treatment (Figure 4-14 B). In summary, these data demonstrate a heterogeneous response of short-term cetuximab treatment on PD-L1 levels, which is independent of ERK phosphorylation.

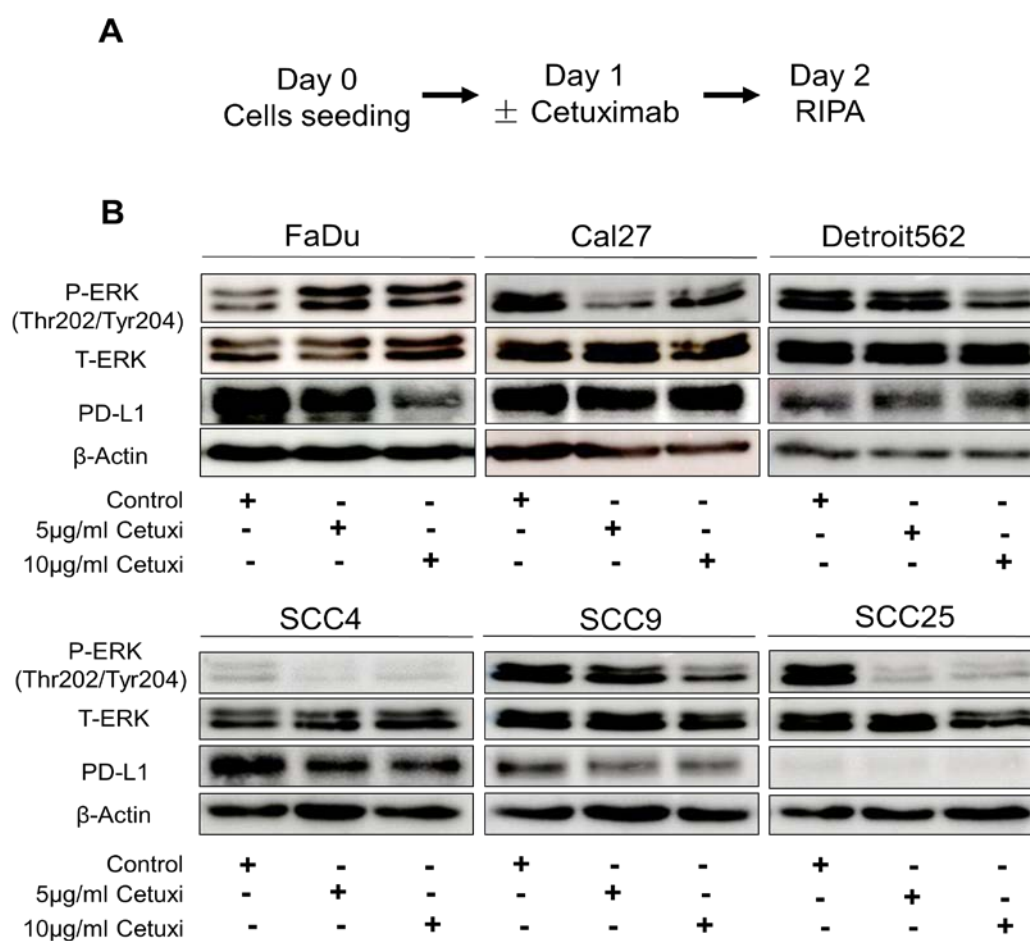


Figure 4-14: Regulation of pERK1/2 and PD-L1 by cetuximab after a single dose treatment.

(A) Schematic summary of the short-term cetuximab treatment protocol. (B) Expression of pERK, total-ERK and PD-L1 in HNSCC cell lines after short-term cetuximab treatment was demonstrated by Western blot analysis with whole cell lysates. Detection of β -actin served as a control for quantity and quality of protein lysates.

In terms of repeated cetuximab treatment, a similar trend with minor differences in ERK phosphorylation was observed for FaDu and SCC9. In contrast to short-term treatment, repeated cetuximab treatment of Detroit562 revealed elevated of pERK levels. There was no prominent alteration of pERK in Cal27, SCC4 and SCC25 after repeated cetuximab treatment, which all showed a reduced pERK levels after short-term treatment. Collectively, these data demonstrated that most HNSCC cell lines adapt to prolonged cetuximab treatment by means of ERK phosphorylation. In contrast, similar

trends for cetuximab dependent regulation of PD-L1 expression were found for FaDu, SCC4 and SCC9 cells, in part even more pronounced after repeated treatment. Down-regulation was observed in Detroit562 cells only after prolonged cetuximab treatment. It is worth noting that an elevated expression of PD-L1 was only detected for Cal27 after prolonged cetuximab treatment. Consistent with data after short-term treatment, a low expression of PD-L1 was found in SCC25 cells, which was not altered by cetuximab treatment (Figure 4-15B). Thus, data from repeated treatment experiments confirmed a heterogeneous response on PD-L1 expression, which is independent of ERK phosphorylation.

Together, these data indicate that the majority of HNSCC cell lines adapt to prolonged cetuximab treatment and regain baseline pERK levels. Moreover, up-regulation of PD-L1 was observed in Cal27 cells after long-term treatment, which is the most resistant cell line to cetuximab. These results provide a first proof-of-concept that up-regulation of PD-L1 might be a potential mechanism of resistance to cetuximab treatment in HNSCC.

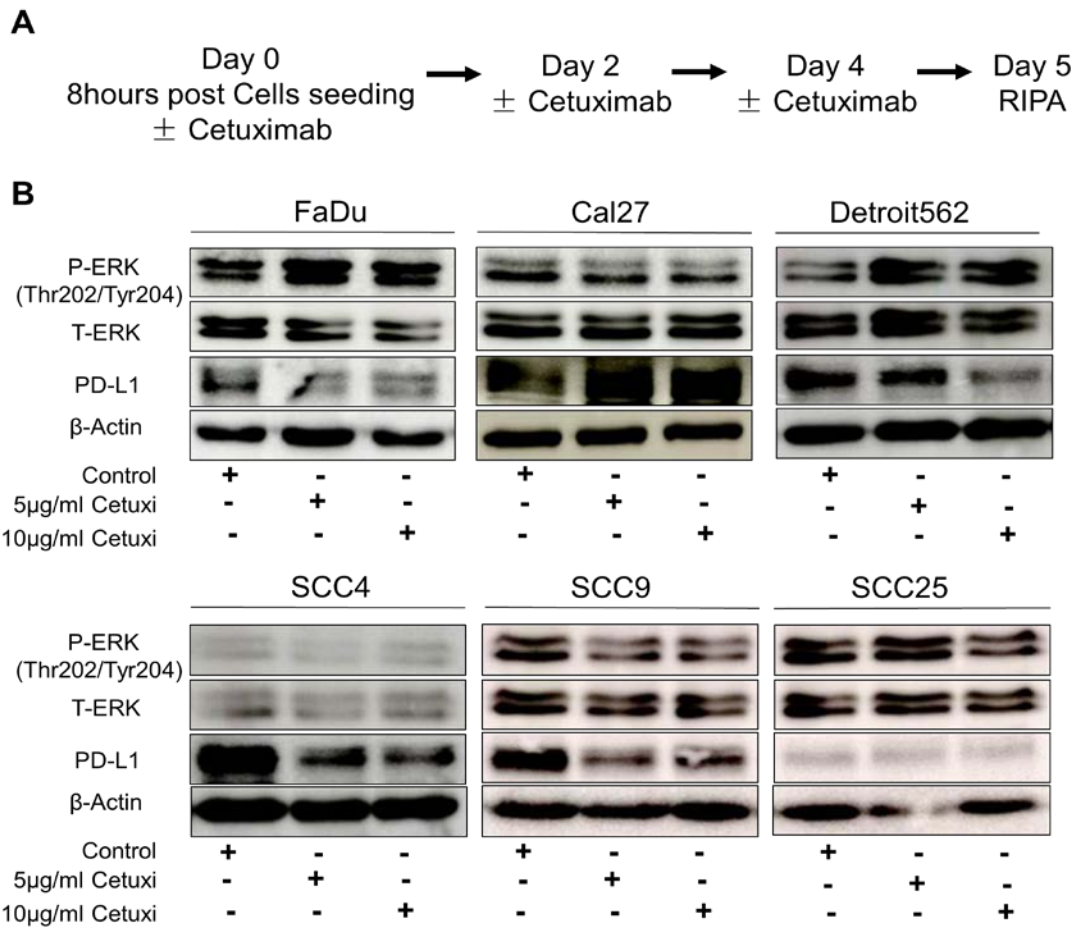


Figure 4-15: Regulation of P-ERK1/2 and PD-L1 by cetuximab in three times-repeated treatment.

(A) Schematic summary of the cetuxi long-term treatment protocol. (B) Expression of pERK, total-ERK and PD-L1 in HNSCC cell lines after long-term cetuximab treatment was demonstrated by Western blot analysis with whole cell lysates. Detection of β -actin served as a control for quantity and quality of protein lysates.

4.12 Impact of MEK1/2 inhibitor treatment and fractionated IR on PD-L1 expression in FaDu cells

Previous results demonstrated that administration of the MEK1/2 inhibitor PD-901 sensitized FaDu and Cal27 cells to fractionated IR. To address the question, whether PD-901 and fractionated-IR have any impact on PD-L1 expression, whole protein lysate of FaDu cells after 0.1 μ M PD-901 treatment with or without fractionated IR (4x2Gy)

were analyzed by Western blot. Both PD-901 treatment and fractionated IR revealed an up-regulation of PD-L1 in FaDu cells. However, it is worth noting that induction of PD-L1 protein levels was higher upon PD-901 treatment as compared to fractionated IR, and combined treatment did not further induce PDL1 expression (Figure 4-16).

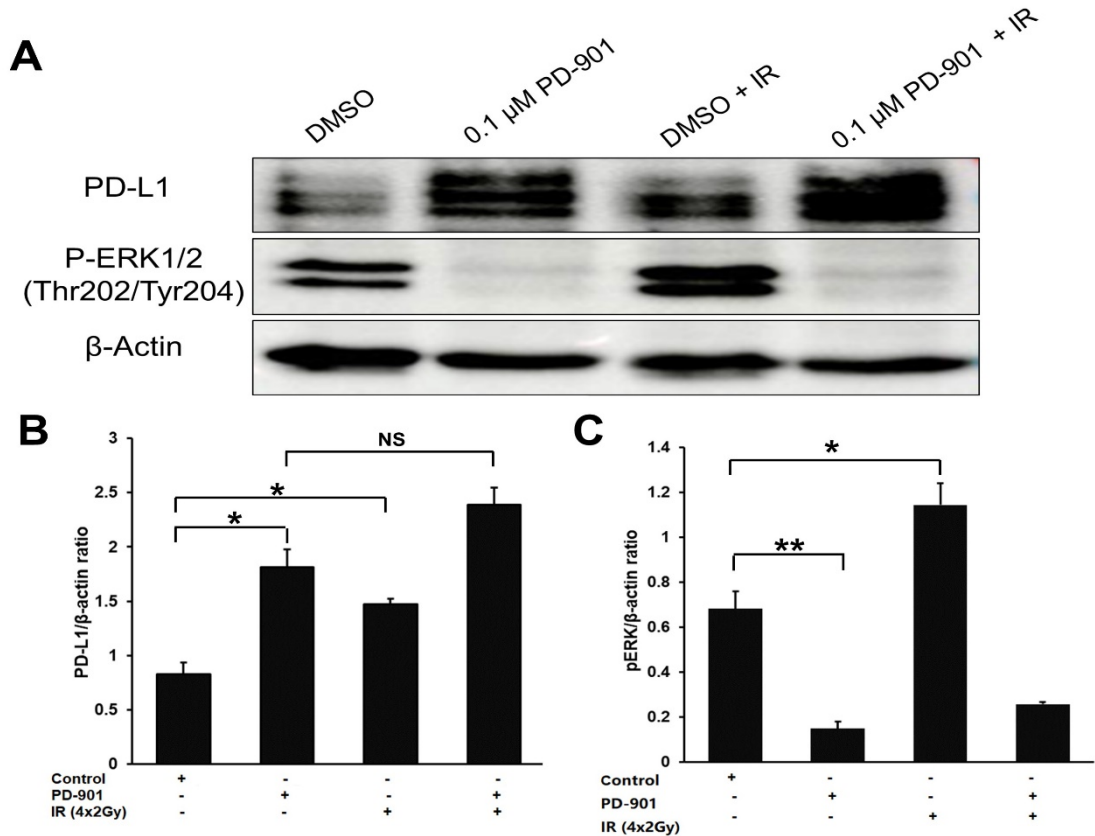


Figure 4-16: Impact of MEK1/2 inhibitor and fractionated IR on PD-L1 expression in FaDu cells.

(A) PD-L1 and pERK1/2 expression in whole cell lysates of FaDu cells after 0.1 μM PD-901 treatment, fractionated-IR (4 x 2Gy) or combined treatment was determined by Western blot analysis. Detection of pERK1/2 protein levels served as a control for MEK1/2 inhibitor efficacy and detection of β-Actin served as a control for quantity and quality of protein lysates. (B, C) Signals were quantified by image J and bars in graphs show the ratio of the target proteins and β-actin. Data represent mean ± SEM of two independent experiments measured in triplicates, *P < 0.05, **P < 0.005.

4.13 Regulation of p-ERK1/2 and PD-L1 by MEK1/2 inhibitor treatment.

As no remarkable induction of PD-L1 by fractionated IR was detected in FaDu cells, further experiments were conducted with PD-901 without fractionated IR. To determine whether a similar trend of PD-L1 regulation is evident in other HNSCC cell lines, the effect of PD-901 on p-ERK1/2 and PD-L1 were assessed by Western blot analysis. Again, after single treatment, pERK1/2 levels were suppressed at a dose of 0.1 and 1 μ M PD-901 in all cell lines (Figure 4-17 A). Notably, only SCC25 cells showed a dose-dependent response to PD-901 concerning ERK1/2 phosphorylation. However, PD-L1 expression was not altered by PD-901 treatment in the majority of cell lines, only SCC4 cells exhibited a down-regulation of PD-L1 in response to short-term PD-901 treatment (Figure 4-17 B).

In terms of repeated treatment (Figure 4-18 A), a potent inhibition of ERK phosphorylation was observed in all HNSCC cell lines after treatment with 0.1 μ M of PD-901. Consistent with the short-term treatment data, PD-L1 expression was not altered by PD-901 in Detroit562, SCC9 and SCC25, but elevated PD-L1 expression was found in FaDu cells. Moreover, SCC4 cells displayed a reduced expression of PD-L1 but a lower extent of variation as compared to findings of short-term treatment. A down-regulated expression of PD-L1 as compared to controls was also detected for Cal27 cells (Figure 4-18 B).

Taken together, these data confirmed that PD-L1 regulation in HNSCC cell lines is largely independent of MEK-ERK signaling. Only in SCC4 cells, loss of ERK phosphorylation by the MEK1/2 inhibitor is accompanied by reduced PD-L1 protein levels.

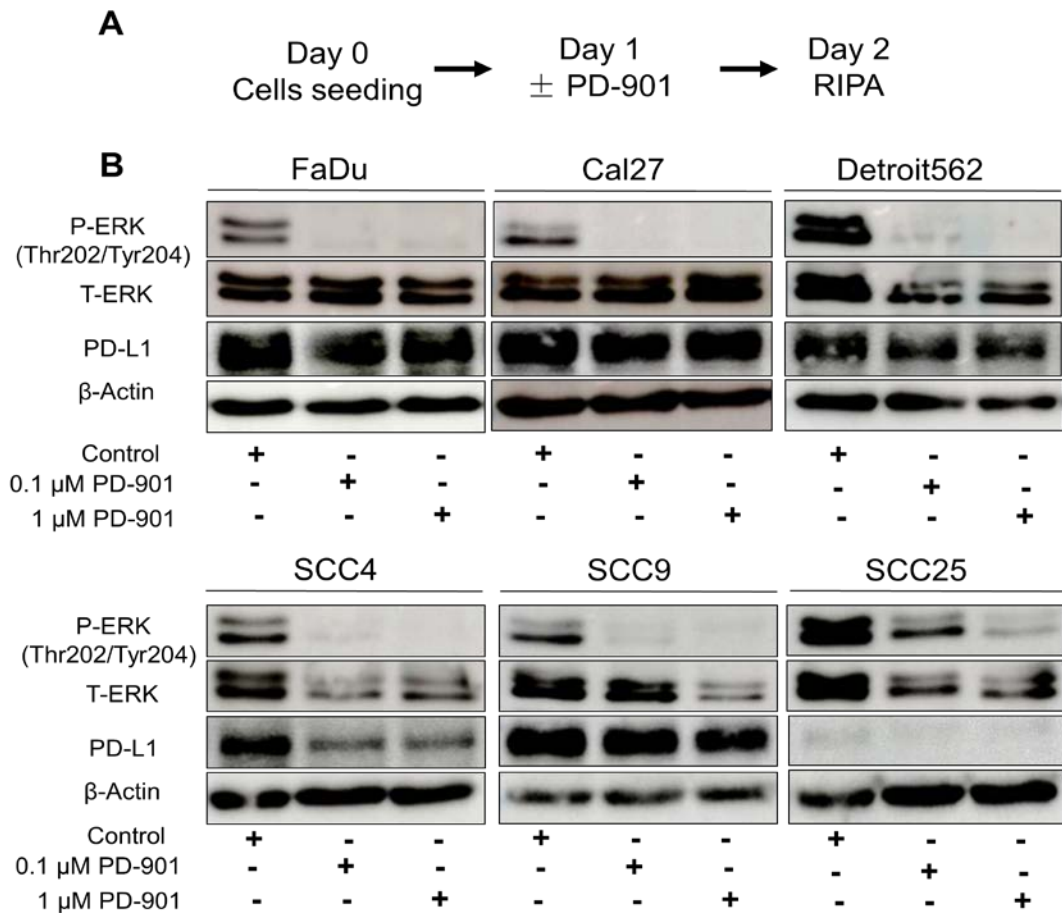


Figure 4-17: Regulation of P-ERK1/2 and PD-L1 by PD-901 in single dose treatment.

(A) Schematic summary of the short-term PD-901 treatment protocol. (B) Expression of pERK, total-ERK and PD-L1 in HNSCC cell lines after short-term PD-901 treatment was demonstrated by Western blot analysis with whole cell lysates. Detection of β -actin served as a control for quantity and quality of protein lysates.

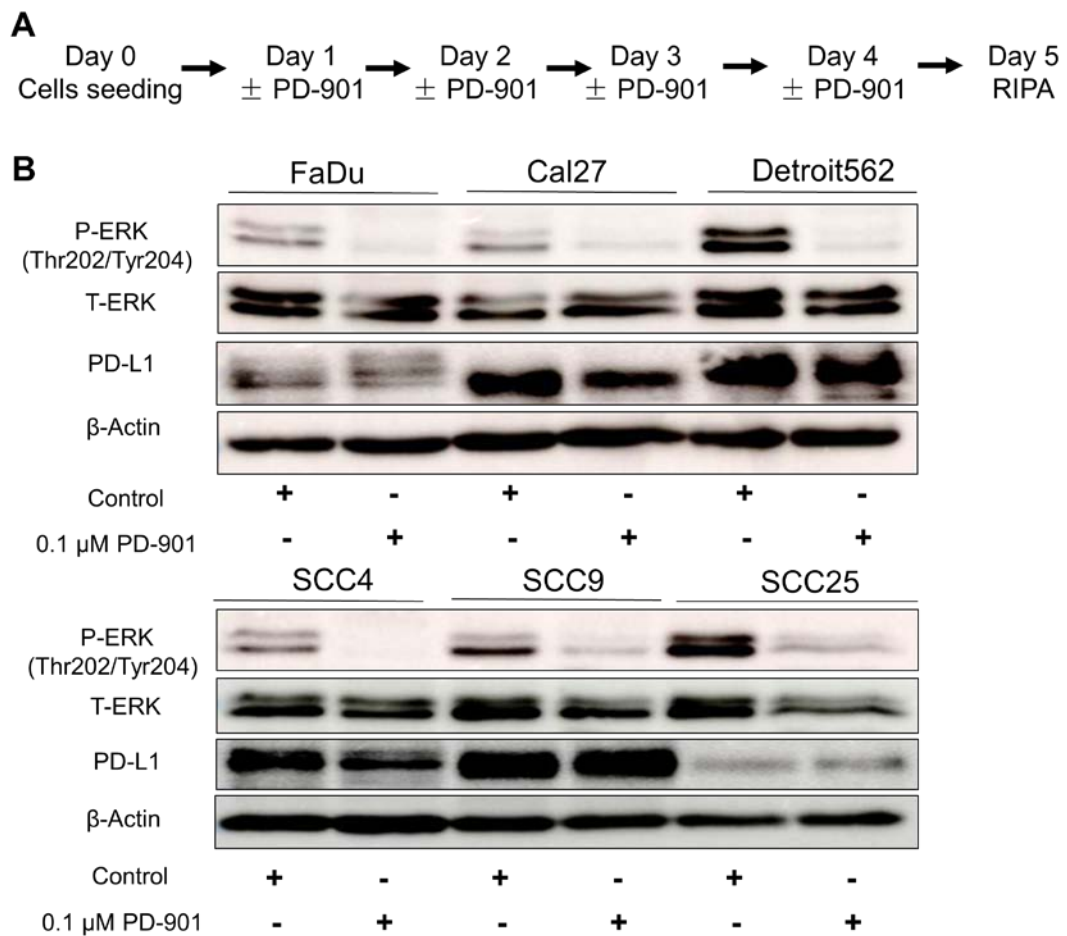


Figure 4-18: Regulation of P-ERK1/2 and PD-L1 by PD-901 in three times-repeated treatment.

(A) Schematic summary of the long-term PD-901 treatment protocol. (B) Expression of pERK, total-ERK and PD-L1 in HNSCC cell lines after long-term treatment 0.1μM PD-901 was demonstrated by Western blot analysis with whole cell lysates. Detection of β-actin served as a control for quantity and quality of protein lysates.

4.14 Effects of MEK1/2 inhibitor on Akt and Histone H2AX phosphorylation in HNSCC cell lines

Recent findings have established PI3K (Phosphoinositide 3-kinase) and MEK signaling cascades as drivers of carcinogenesis and potential target for pharmacological intervention in a wide range of human cancers, including HNSCC

(Cancer Genome Atlas, 2015). However, treatment with MEK inhibitors often result in elevated AKT phosphorylation, reducing the efficacy of MEK inhibitors as single agents (Faber *et al.*, 2009; Hoeflich *et al.*, 2009; Yoon *et al.*, 2009). To investigate whether the MEK1/2 inhibitor PD-901 affects PI3K signaling in HNSCC cell lines, AKT phosphorylation (p-AKT) was determined in whole cell lysate of HNSCC cell lines after repeated treatment with 0.1 μ M PD-901. As shown in (Figure 4-19), AKT phosphorylation was not affected by PD-901 in all cell lines tested. Next, the effects of PD-901 on DNA damage marker, phosphorylation of Histone H2A.X were also investigated. In most HNSCC cell lines, PD-901 treatment did not alter levels of pH2A.X except for SCC25 cells, which showed a marked up-regulation of pH2A.X expression.

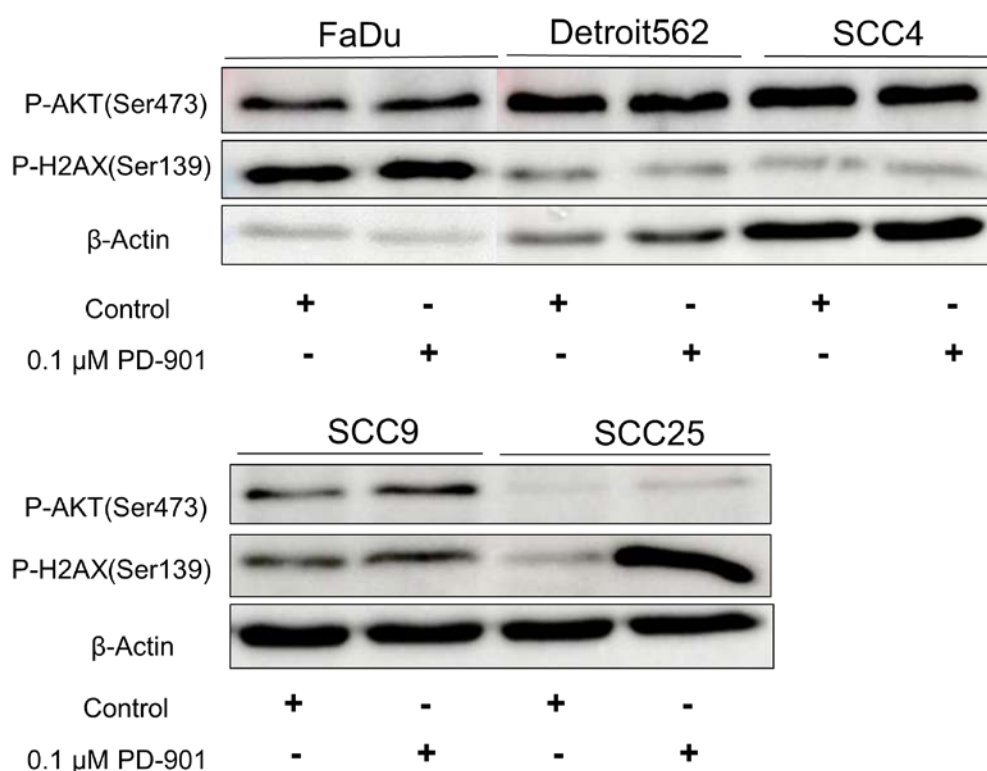


Figure 4-19: Effects of MEK1/2 inhibitor on AKT and Histone H2AX phosphorylation in HNSCC cell lines.

AKT and Histone H2AX phosphorylation of in HNSCC cell lines after long-term treatment with 0.1 μ M PD-901 was determined by Western blot analysis. Detection of β -Actin served as a control for quantity and quality of protein lysates.

4.15 MEK1/2 inhibitor induced cellular senescence in HNSCC cell lines

Cellular senescence is a process in which cultured cells stop dividing and undergo a form of irreversible growth arrest. An increasing body of studies have established a crucial role of cellular senescence in cancer prevention (Nardella *et al.*, 2011). To address whether MEK1/2 inhibitor induce cellular senescence in HNSCC cell lines, cells were treated several times with PD-901 at a concentration of 1 μ M and assayed for β -galactosidase (β -gal) activity. Microscopic inspection revealed a flattened cellular morphology in most HNSCC cell line after PD-901 treatment, which is characteristic feature of senescent cells (Figure 4-20 A, B). In addition, prominent β -gal staining was detected in FaDu, Cal27, SCC4 and SCC9 cells. Interestingly, no increase in β -gal activity was observed in Detroit562 and SCC25 cells (Figure 4-20 C). Furthermore, Detroit562, which is a resistant cell line to MEK1/2 inhibitor, revealed no β -gal activity with or without PD-901 treatment. Thus, these data suggest that inhibition of MEK1/2 activity induce senescence in sensitive but not in resistant HNSCC cell lines.

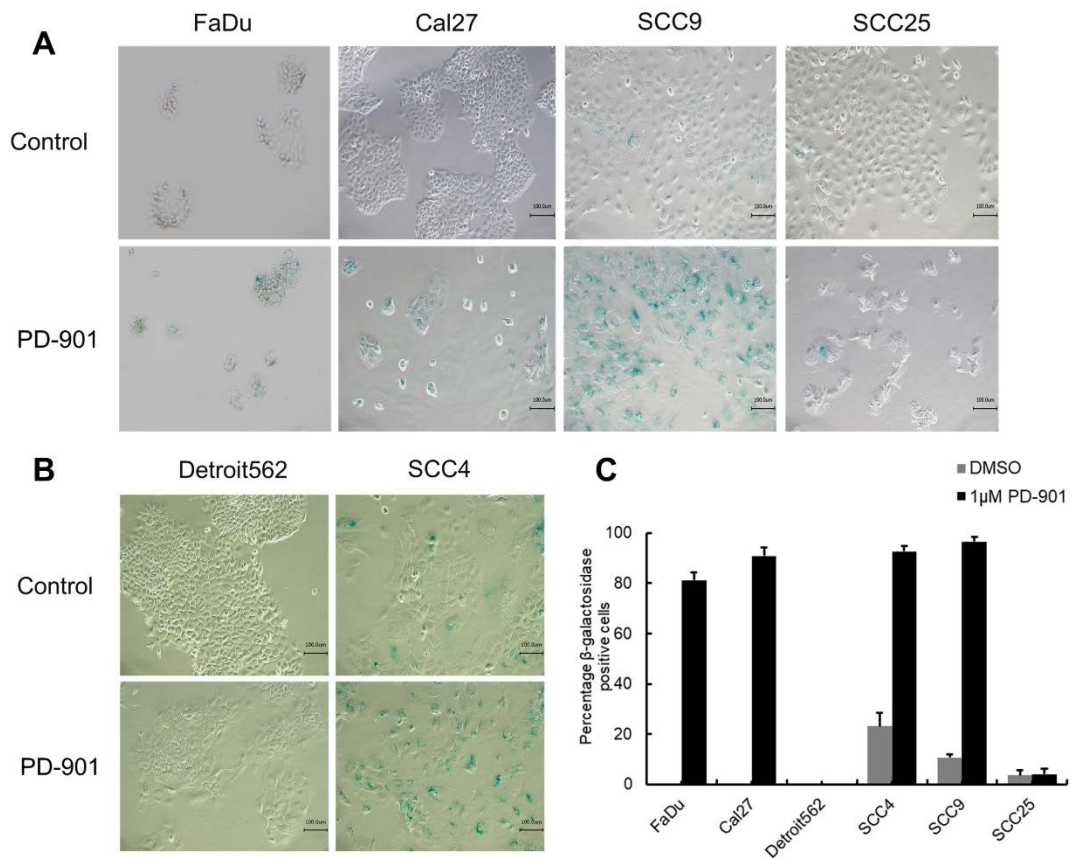


Figure 4-20: Long-term treatment of PD-901 induced cellular senescence in HNSCC cell lines.

HNSCC cell lines were treated after long term with 1 μ M PD-901 and stained for β -galactosidase. Blue cells were stained with senescence-associated β -galactosidase. Representative images (scale bar=100 μ m) for FaDu, Cal27, SCC9 and SCC25 shown in (A), for Detroit562 and SCC4 shown in (B), with quantitation analysis in (C).

5. Discussion

5.1 Opiorphins serve as a surrogate marker for radioresistance.

The therapeutic strategy of loco-regionally advanced HNSCC has developed gradually from surgery to radiotherapy (Gregoire *et al.*, 2015). Approximately 75% of patients with HNSCC will benefit from radiotherapy as part of a primary therapeutic scheme or as adjuvant therapy after surgery (Barton *et al.*, 2014). Although significant improvements have been achieved in novel techniques and new protocols of radiotherapy for the treatment of HNSCC, intrinsic and acquired radioresistance remain crucial barriers for curative therapy of HNSCC. Unraveling molecular mechanism of radioresistance and identifying new biomarkers for HNSCC patients at high risk for treatment failure is urgently needed.

Previous data identified the mouse homolog of human SMR3A gene, *Smr1*, to be differentially expressed in primary and recurrent tumors of an orthotopic mouse xenograft model for oral cancer (Acuna Sanhueza *et al.*, 2012). In addition, elevated SMR3A protein expression has been detected in 36% of patients with OPSCC and serves as a prognostic risk factor for unfavorable PFS and OS (Koffler *et al.*, 2013). It is worth noting that an increased transcript levels of *Muc10*, which is the mouse homolog of the human *OPRPN* gene, another member of the opiorphin gene family, was found in recurrent tumors after surgery as compared to matched primary tumors. It indicates a general principle of regulation and function of opiorphin family members in the progression of tumor recurrence and treatment failure (Acuna Sanhueza *et al.*, 2012). So far, the opiorphin family members have been studied in a variety of physiological and pathological conditions, such as erectile dysfunction (ED), colonic motility and nociception, pain and mood disorders, hypoxic response, etc. (Fu *et al.*, 2014; Javelot *et al.*, 2010; Tian *et al.*, 2009; Tong *et al.*, 2008).

Studies on erectile physiology revealed a crucial role for SMR3A and OPRPN in ED suggesting that all members of the opiorphin family can act as markers for organic ED in human patients. These findings provided compelling evidence that opiorphins are key players in male sexual function and their downstream pathways might represent novel pharmacological targets (Davies *et al.*, 2007; Messaoudi *et al.*, 2004; Tong *et al.*, 2008; Tong *et al.*, 2007). It was also reported that the pentapeptide opiorphin reveals potent analgesic function in chemical and mechanical pain models as an inhibitor of pain perception. In addition, the pain-suppressive efficacy is equal to morphine in the behavioral rat model, suggesting opiorphin might act as a potential initiator to develop novel candidate drug for pain control (Wisner *et al.*, 2006). Opiorphin has been identified as a potent inhibitor of two enkephalin-degrading enzymes, namely neutral endopeptidase (NEP; also known as CD10) and aminopeptidase N (NEP; also known as CD13). Many previous studies demonstrated that CD10 and CD13 function as ectoenzymes to inactivate neuropeptides and regulate signaling pathways involving in tumor progression and invasion (Carl-McGrath *et al.*, 2006; Fujita *et al.*, 2007; Kawamura *et al.*, 2007; Kuniyasu *et al.*, 2010; Luo *et al.*, 2009; Sorensen *et al.*, 2013). Moreover, a positive regulation of opiorphin family members by hormone signaling have been reported in several studies (Chua *et al.*, 2009; Senorale-Pose *et al.*, 1998).

Likewise, our findings suggested that ESR2 signaling regulates SMR3A expression and plays an important role in resistance to radiotherapy. Furthermore, the results in a new cell culture model of fractionated irradiation provided compelling experimental evidence for the existence and expansion of a subpopulation of radioresistant tumor cells, which were characterized by ESR2, SMR3A and OPRPN expression. Notwithstanding, a statistically significant correlation was not observed between OPRPN expression pattern and clinical outcome of patients with OPSCC. Combined expression of ESR2 and OPRPN or SMR3A was associated with unfavorable clinical prognosis post definitive or adjuvant radiotherapy, suggesting that opiorphin-related genes serve as a

surrogate marker for HNSCC cells with intrinsic radioresistance.

5.2 Distinct functions of ESR subtypes in cancer

Estrogen exerts its functions in target tissues mainly via two members of the nuclear receptor superfamily: ESR1 (also known as ER α) and ESR2 (also known as ER β) (Heldring *et al.*, 2007). Both receptors possess four functional domains, harboring a DNA-binding domain (DBD), a ligand-binding domain (LBD) and two transcriptional activation functions (AF-1 and AF-2). These domains share a proportional homology between ESR1 and ESR2 (Figure 5-1) (Roman-Blas *et al.*, 2009). Both receptors mediate their effects as transcription factors in the nucleus when they are bound to their specific ligands (Osborne *et al.*, 2001). They can also interact and modulate the activity of each other, and participate in membrane and cytoplasmic signaling cascades (Bjornstrom and Sjoberg, 2005). In the present study, a prominent ESR2 but not ESR1 expression was found in HNSCC cell lines and tumor tissues. An active ESR2 signaling as a common event in HNSCC predicts treatment resistance and has a prognostic value for patient survival. However, we did not observe significant difference between ESR2 staining pattern and gender, in line with the findings that ESR expression and function in HNSCC cell lines is independent of the gender of patients from whom the cell lines were derived (Egloff *et al.*, 2009). These data suggest that ESR2 likely plays a significant role in HNSCC of both males and females. The synthesis of estrogen through the action of aromatase in extra gonadal has been identified as the major source of estrogen for men and post-menopausal women. Aromatase has been shown to be expressed in various tumors and play a significant role in the growth of malignancies, including HNSCC (Cheng *et al.*, 2006). It is worth noting that larger tumor size and tobacco consumption is significantly correlation with negative ESR2 staining, which is consistent with our survival data that OPSCC without detectable ESR2 reveal a poor prognosis. These results also suggest that ESR2 displays dual roles in tumor

growth and radioresistance. Loss of ESR2 could contribute to growth of tumor cells during neoplastic transformation and malignant development, while ESR2-positive tumor cells reveal radioresistance and survive after radiotherapy.

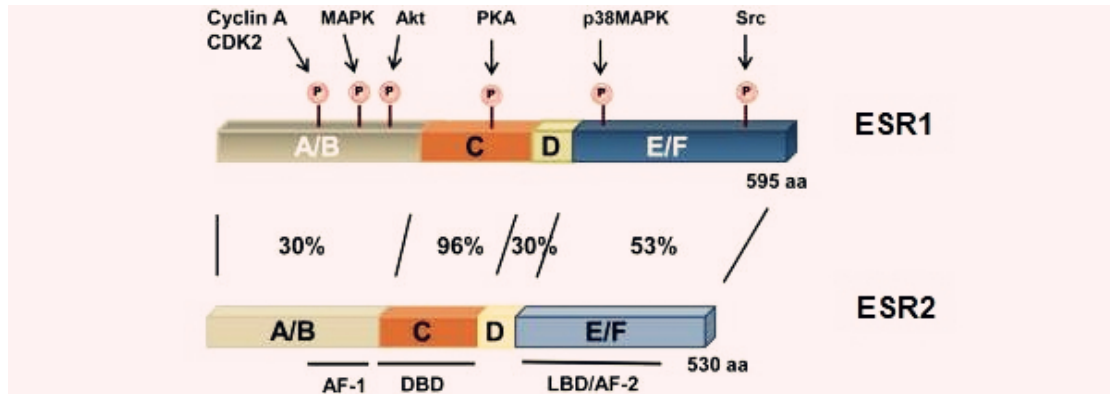


Figure 5-1. Structural composition of ESR1 and ESR2

(modified from (Roman-Blas *et al.*, 2009)).

Studies of the proportion of ESR-positive HNSCC vary considerably. Either ESR subtype has been detected in only 2.7% of HNSCC tumors by ESR assay and in 50.7% of HNSCC tumors by immunohistochemistry (Lukits *et al.*, 2007; Schuller *et al.*, 1984). Several reports show that HNSCC tumors and cell lines display no expression of ESR1 or the proportion was less than 10% of HNSCC tumors or cell lines (Ferguson *et al.*, 1987; Hagedorn and Nerlich, 2002). A study indicated that ESR expression was observed more frequently in laryngeal tumor than other head and neck tumors. However, another study reported that both ESR1 and ESR2 were detected in the majority of HNSCC tumors independent anatomical tumor sites (Egloff *et al.*, 2009). In line with our findings, a study in oral squamous cell carcinoma reported high levels of ESR2 expression, but ESR1 expression was neither observed in primary tumor tissues nor several cultured cell lines, supporting a specific regulation and function of ESR2 in HNSCC (Ishida *et al.*, 2007). The differences between our study and other reports could be due to the various antibodies and the distinct techniques, including immunohistochemistry (IHC) and ligand-binding assay. Currently, most laboratories determine the ESR status by IHC on formalin-fixed paraffin-embedded tissue

specimens (Harvey *et al.*, 1999). Interestingly, it has been reported that ESR2 plays a role in smoking-related susceptibility of male and female patients with lung cancer (Kiyohara and Ohno, 2010). Risks related to tobacco are higher for women than men in HNSCC. ESR-mediated events are likely responsible for the higher smoking-related hazards for women than men owing to higher circulating levels of estrogen. However, amount of estrogen in men are sufficient to exert biological effects because aromatase expression can be detected in normal oral keratinocytes and oral SCC, which can catalyze the conversion of androgen to estrogen (Cheng *et al.*, 2006). These findings indicate that ESR also plays a significant role in pathogenesis of male patients with HNSCC.

So far, few studies have evaluated the contribution of ESR on the clinical outcome of HNSCC patients. In 2009, Egloff and coworkers investigated the expression levels of ESR1 and ESR2 in HNSCC by immunohistochemistry, revealing that patients with high ESR1 nuclear staining tend to have shorter progression-free survival as compared to patients with low levels (Egloff *et al.*, 2009). The relationship between ESR levels and clinical outcome has been studied in more detail for other cancer entities. In breast cancer, ESR1 protein levels are associated with low tumor grade and negative lymph node metastasis. ESR1-positive tumor cells tend to be less invasive and reveal a better prognosis (Platet *et al.*, 2004). The expression of ESR2 isotypes has been determined in 442 invasive breast cancers. This study revealed that ESR2, in particular the isotype ESR2-1 is associated with better survival in triple-negative breast cancers and sensitive to tamoxifen treatment. Moreover, nuclear accumulation of ESR2-2 was negatively associated with metastasis and vascular invasion. In contrast, a cytoplasmic ESR2-2 expression pattern was correlated with more unfavorable prognosis and resistance to chemotherapy (Honma *et al.*, 2008). In a study of non-small cell lung carcinoma (NSCLC), ESR1 overexpression was associated with shorter overall survival and was correlated with EGFR mutations, serving as an independent factor for unfavorable

prognosis (Stabile *et al.*, 2011). An elevated nuclear ESR2 level correlated with better survival in men only (Schwartz *et al.*, 2005; Skov *et al.*, 2008), also predicting a favorable outcome for lung adenocarcinoma after EGFR tyrosine kinase inhibitor treatment (Nose *et al.*, 2011). These data suggest that ESR subtypes and subcellular localization may act as important determinants of involvement in various tumors. Accordingly, it will be a major challenge for the future to assess the subcellular localizations of ESR2 in a larger cohort of HNSCC patients.

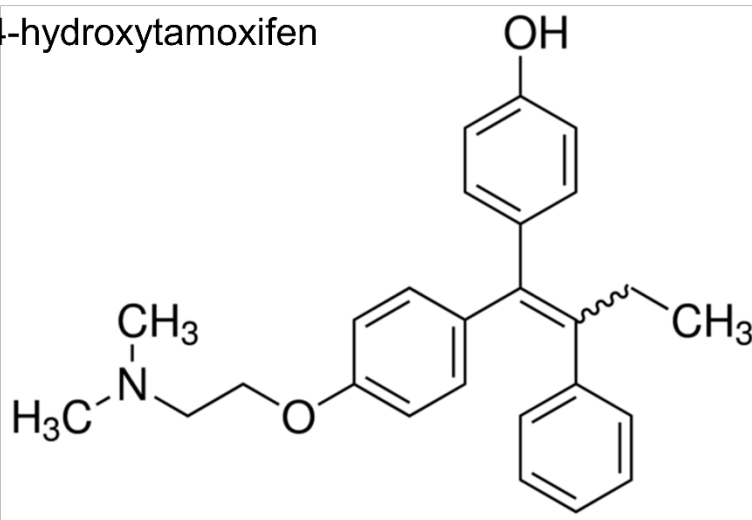
5.3 Targeting the ESR signaling for cancer therapy

To the best of our knowledge, there are no reports evaluating the inhibition of ESR signaling in combination with radiotherapy for HNSCC patients. Presented results revealed that two well-established anti-estrogen drugs, 4-Hydroxytamoxifen (4-OH-TAM) and fulvestrant (Figure 5-2), can sensitize HNSCC cell lines to fractionated irradiation in a colony-forming assay (CFA). These findings suggest that combination of anti-estrogen drugs and irradiation has a synergic effect on restraint proliferation in HNSCC cells, which might reveal implications for combination therapy in subpopulations of HNSCC patients.

Anti-estrogen therapy exerts effects by competing with estrogens for binding to the ESR, most widely used for the management of ESR-related breast cancer. In 1971, a new anti-estrogen tamoxifen was reported firstly in treatment for patients with breast cancer (Cole *et al.*, 1971). Until now tamoxifen is the most frequently prescribed anti-estrogen, revealing a significant clinical benefit for breast patients. Tamoxifen is a triphenylethylene and several derivatives have been produced, including toremifene (chloro-tamoxifen), 3-hydroxytamoxifen (droloxifene) and 4-hydroxytamoxifen (4-OH-TAM). 4-OH-TAM, which was used in this study, is a potent metabolite of TAM. This anti-estrogen drug reveals the equal pharmacologic activity as TAM, but

possesses a higher binding affinity for ESRs (Jordan *et al.*, 1977). The anti-estrogen TAM is an effective cytostatic drug which is employed in combination of fractionated IR for the therapy of ESR positive breast cancer (Anonymous, 1988; Anonymous, 1992; Stewart, 1992). Wazer and colleagues (Wazer *et al.*, 1989) observed that growth-inhibitory doses of TAM reduce the radiosensitivity of MCF-7 breast cancer cells *in vitro*. Furthermore, an assay *in vivo* assessed the efficacy of treatment by irradiation and concurrent tamoxifen, indicating that combined irradiation and tamoxifen display significant suppression in tumor volumes and tumor growth (Kantorowitz *et al.*, 1993). It has been clarified that the tumor-suppression effect of tamoxifen on breast carcinoma cells is owing to the expression of cyclin-dependent kinase inhibitors, particularly P21^{WAF1/CIP}, which is regulated by wild type P53 (Ichikawa *et al.*, 2008). Another report demonstrated that anti-estrogen might alter radiosensitivity independent of the ESR status, suggesting that hormone therapy function through estrogen receptors but also independent mechanisms (Paulsen *et al.*, 1996).

A. 4-hydroxytamoxifen



B. Fulvestrant

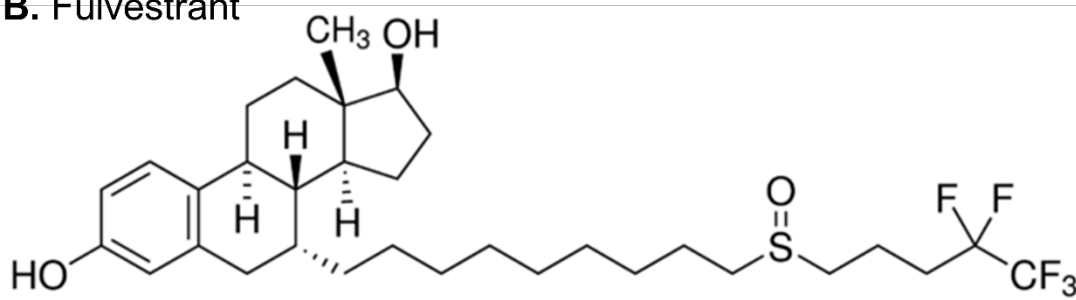


Figure 5-2. Structure of 4-hydroxytamoxifen (A) and fulvestrant (B).

Fulvestrant, one of the more promising new anti-estrogen drugs, is the first new type of ESR antagonists that down-regulates ESR function as a 'pure' antagonist with no partial agonist properties as have been described for tamoxifen (Wakeling *et al.*, 1991). Fulvestrant competitively prevents binding of estradiol to ESRs. The binding of Fulvestrant and ESR prevents receptor dimerisation and energy-dependent nuclear shuttling (Dauvois *et al.*, 1993; Fawell *et al.*, 1990). ESR protein degradation is aggravated due to the unstable fulvestrant-ESR complex. Therefore, fulvestrant binds and accelerates degradation of ESR proteins, resulting in a block of estrogen signaling via ESR degradation (Figure 5-3) (Osborne *et al.*, 1995; Osborne *et al.*, 2004; Wakeling, 2000; Wardley, 2002). This pure antagonist has been approved for treatment of hormone receptor positive metastatic breast cancer or locally advanced inoperable tumors in postmenopausal women (Lee *et al.*, 2017). Our results revealed that

fulvestrant can eliminate the ESR2 expression in FaDu cells but to a lesser extent in Cal27 cells, which might explain a more prominent increased radiosensitivity in FaDu cells. Furthermore, fulvestrant alone has no negative impact on colony growth of both cell lines, even a slight increase in Cal27 cells. It might be due to a higher sensitivity of Cal27 to irradiation, resulting in unimproved radiosensitivity by fulvestrant. In breast cancer, a study reported that fulvestrant can sensitize ESR-positive tumor cells to radiotherapy (Wang *et al.*, 2013). In view of these data and our results, endocrine therapy can enhance radiosensitivity by inhibition of tumor cell proliferation and growth, paving the way for future clinical trials in which administration of anti-estrogen therapy in combination with radiotherapy will be assessed for HNSCC patients.

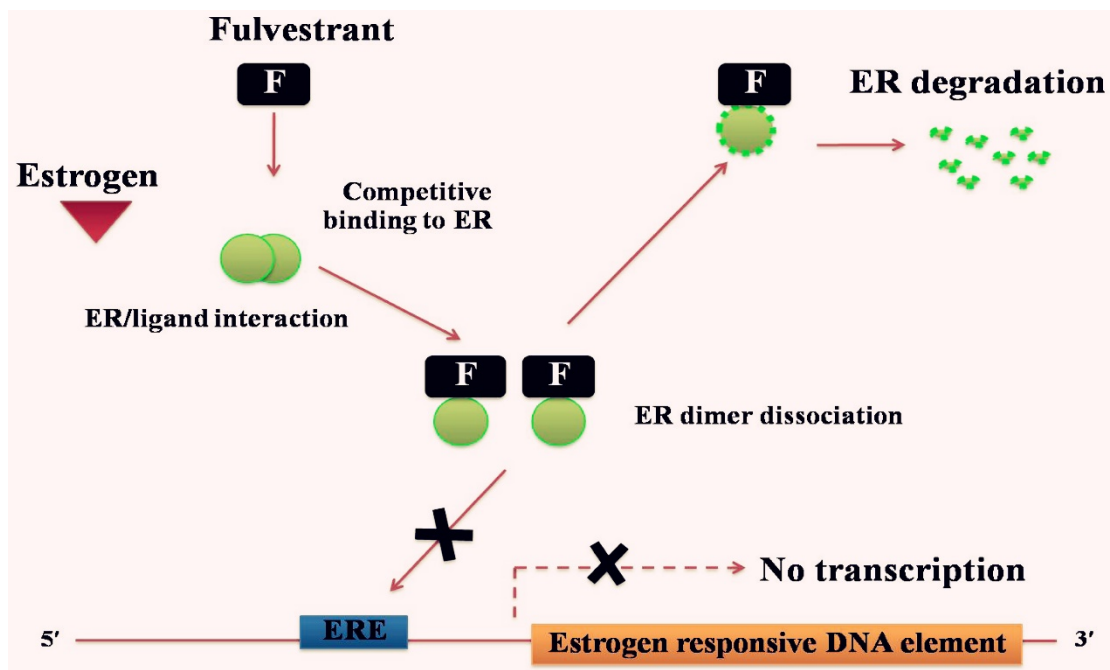


Figure 5-3. Mechanism of the steroidal ER α antagonist, fulvestrant, at the level of transcriptional regulation.

(ERE= estrogen response element; F= fulvestrant). Figure was modified from (Ratanaphan, 2012).

5.4 Interaction of ESR with EGFR signaling

Activities of the ESR2 could be explained by genomic or non-genomic signaling pathways. Non-genomic signaling pathways depend on second messengers such as

cyclic adenosine monophosphate (cAMP) and calcium, or the activation of PI3K and MAPK (Siegfried *et al.*, 2009). In lung cancer, the steroid receptor coactivator (SRC) protein and the osteopontin (OPN) contribute to the cross-talk between the ESR and the EGFR (Figure 5-4) (Hsu *et al.*, 2017). Hence, ESRs share common intracellular non-genomic signaling pathways with EGFR, suggesting that activation of ESR signaling might induce resistance to EGFR-targeted therapy (Hsu *et al.*, 2017). A crucial role of tyrosine kinase receptors of the EGFR/HER family has been well established in growth and invasion HNSCC cells. Moreover, a functional crosstalk between ESR and EGFR signaling has been reported for HNSCC, in which estrogen and EGF stimulate MAPK signaling. In addition, the combination of fulvestrant and gefitinib, an EGFR tyrosine kinase inhibitor, maximally inhibits cell invasion (Egloff *et al.*, 2009). A concentration-dependent induction of ESR2 was detected in FaDu cells after long-term treatment with cetuximab. Blocking ERK signaling, one of downstream pathways following EGFR activation, might activate ESR2 signaling in FaDu cell under normal growth condition. Taken together, these data provide experimental evidence that ESR2 interacts with the EGFR signaling pathway as alternate signaling mechanisms.

It is worth noting that dual targeting of ESR and EGFR signaling has already been proposed for the treatment of lung cancer. The combined treatment inhibited cell proliferation and suppressed tumor growth more effectively than individual treatment *in vitro* and *in vivo* (Marquez-Garban *et al.*, 2007; Osborne *et al.*, 2005; Siegfried *et al.*, 2012; Stabile *et al.*, 2005). Furthermore, in NSCLC cell lines, the EGFR protein level was reduced in response to estrogen and induced in response to fulvestrant. Conversely, the ESR2 expression was down-regulated in response to EGF and up-regulated in response to gefitinib, suggesting an inverse regulation of ESR and EGFR signaling. (Stabile *et al.*, 2005). Nose *et al.* (Nose *et al.*, 2009) demonstrated a strong association between nuclear expression of ESR2 and EGFR mutations in lung adenocarcinoma, indicating that the favorable prognosis of nuclear ESR2 expression is

influenced by EGFR mutations. These studies have supported a rationale for combined targeting of ESR and EGFR pathways. A pilot clinical study of combined therapy with an EGFR inhibitor and fulvestrant in NSCLC revealed enhanced anti-tumor effects (Traynor *et al.*, 2009). Several phase II clinical trials are currently in progress to evaluate hormone therapy effects on advanced NSCLC, and in combination with an EGFR tyrosine kinase inhibitor (ClinicalTrials.gov).

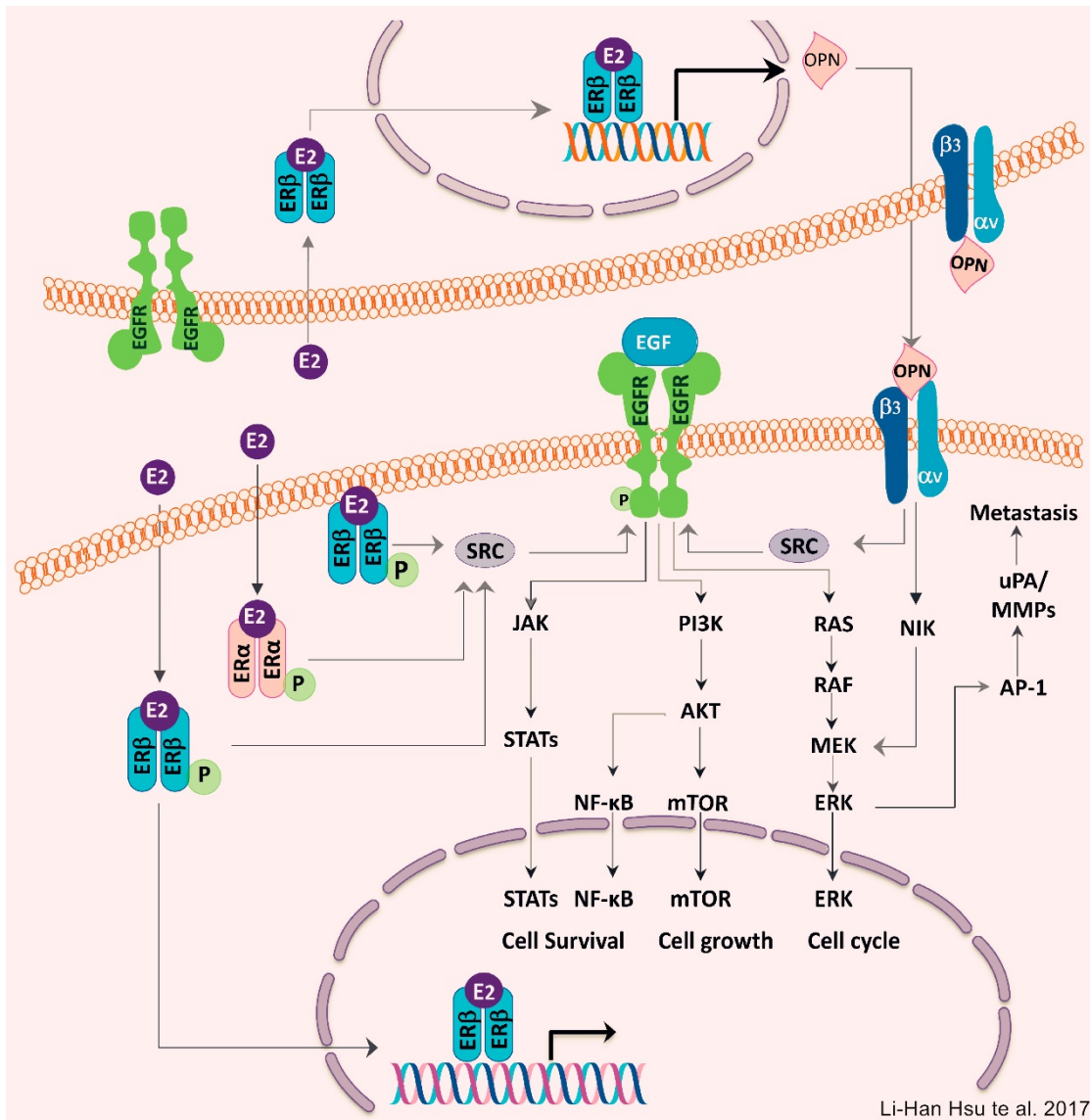


Figure 5-4. Schematic model for mechanisms on how the estrogen receptor (ESR) interacts with the epidermal growth factor receptor (EGFR) to influence the cellular signaling even and cells growth in the lung cancer.

Estrogen activates the steroid receptor coactivator (SRC) protein, which in turn, triggers the EGFR signaling pathway. Furthermore, estrogen increases the osteopontin (OPN) level and facilitates the lung carcinoma cell migration via the MEK/ERK signaling pathway. Whereupon, the SRC and OPN contribute to the cross-talk between the ESR and the EGFR.

5.5 Effects of EGFR-MAPK pathway on PD-L1 expression in HNSCC

A growing body of more specific drugs targeting key regulators of oncogenic signaling cascades or immune checkpoints have been or will be approved in the near future for the treatment of HNSCC patients in combination with radiotherapy. Hence, further insights into the anti-tumor effects of targeted therapies along with radiotherapy are urgently needed. To address this issue several cell culture models were established to investigate the impact of drugs targeting the EGFR-MEK-MAPK pathway (e.g. Cetuximab and MEK1/2 inhibitor) on tumor cell survival and clonal expansion as well as expression of the immune checkpoint inhibitor PD-L1. It is well known that tumors have developed distinct mechanisms to alleviate T-cells antitumor responses and escape the immune elimination, including stimulation of inhibitory immune checkpoint receptors (Sharma and Allison, 2015). Current immune-based therapies of HNSCC are focused on targeting T-cell inhibitory receptors, like antagonists of the cytotoxic T lymphocyte-associated antigen 4 (CTLA4) or programmed cell death protein (PD1)-PD1 ligand 1 (PD-L1) pathways, known as immune checkpoint inhibitors (Ferris, 2015; Whiteside, 2017). PD-L1 is the main ligand of PD1, which counteracts T-cell induced immune response and signaling. PD-L1 can be expressed on the surface of many solid tumor cells including HNSCC (Lee *et al.*, 2016). Sofia Lyford-Pike *et al.* (Lyford-Pike *et al.*, 2013) have provided evidence that the PD-1/PD-L1 pathway offers an immune-privileged site for HPV infection and serves as an adaptive resistance mechanism of tumors against host. Moreover, PD-L1 expression has been identified as a significant biomarker for patients with HPV-negative HNSCC at high risk of treatment failure, which appears to be related to Axl/PI3 kinase signaling (Skinner *et al.*, 2017). Multiple factors have been demonstrated to affect PD-L1 expression including epithelial-mesenchymal transition (EMT), viruses, and sub-lethal damage induced by cytotoxic chemotherapy via MAPK or JAK-STAT pathway signaling (Atefi *et al.*, 2014;

Jiang *et al.*, 2013; Ritprajak and Azuma, 2015; Yang *et al.*, 2013).

In the present study, the impact of single or repeated treatment with cetuximab on ERK1/2 phosphorylation and PD-L1 protein levels was investigated in HNSCC cell lines. The data indicate a heterogeneous and context-specific response of cetuximab on PD-L1 expression after short or long-term treatment, which was independent of ERK phosphorylation. The majority of HNSCC cell lines under long-term treatment exhibited regain of ERK phosphorylation as compared to the short-term treatment. Up-regulation of PD-L1 was observed in Cal27 cells with long-term treatment, which was the most resistant cell line to cetuximab treatment. These results provide a proof-of-concept that up-regulation of ERK phosphorylation and PD-L1 expression might be a potential mechanism of resistance to cetuximab treatment in HNSCC, suggesting potential benefits of combining cetuximab with immunotherapy. In line with the presented results, PD-L1 expression is believed to be associated with EMT features, immune escape and treatment resistance, predicting an unfavorable clinical outcome (Kakavand *et al.*, 2017; Ock *et al.*, 2016; Yan *et al.*, 2016)

Cetuximab therapy has been reported to impact expression of checkpoint receptors on circulating and tumor-infiltrating lymphocytes (TILs). Cetuximab-activated natural killer (NK) cells selectively excluded intratumoral regulatory T cells (Treg) and maintained effector T cells (Jie *et al.*, 2015). Targeting PD-1/PD-L1 axis may stimulate cytolytic function of NK cells, cetuximab induced antibody dependent cellular cytotoxicity (ADCC), suggesting combined treatment of Durvalumab, an anti-PD-L1 monoclonal antibody, with cetuximab might provide enhanced benefit for HNSCC patients (Bonomo *et al.*, 2017). Furthermore, an elevation of PD-L1 positive peripheral blood T-cells after EGFR inhibitor treatment has been significantly associated with the clinical prognosis in NSCLC, providing the implication that up-regulation of PD-L1 might be one of the mechanisms of acquired resistance to EGFR inhibitors (Meniawy *et al.*, 2016).

The effects of a specific drug targeting ERK signaling, one of the EGFR downstream pathways, on radioresistance were further addressed in HNSCC cell lines. Up-regulation of ERK phosphorylation was observed in FaDu cells after fractionated IR, which is in line with a previous study (Affolter *et al.*, 2016). PD-0325901 (PD-901) is a second-generation small molecular inhibitor that restrains the activation of ERK by inhibition of MEK1/2. Presented CFA data have revealed that PD-901 improves the radiosensitivity of HNSCC cell lines, providing potential clinical benefit from combination treatment of MEK1/2 inhibitor and radiotherapy. Up-regulation of PD-L1 protein expression was observed in FaDu cells after treatment with PD-901 with or without fractionated IR. It is worth noting that induction of PD-L1 protein level was higher upon PD-901 treatment as compared to fractionated IR, and combined treatment did not further induce PD-L1 expression in FaDu cells. To gain further insight into the impact of MEK inhibitor on ERK1/2 phosphorylation and PD-L1 expression in HNSCC cell lines, their levels were examined after single or repeated administration by western blot analysis. The presented data confirmed that PD-L1 regulation in HNSCC cell lines *in vitro* is mainly independent of MEK-ERK signaling.

The effect of targeted therapy on expression and signaling of immune checkpoint inhibitor and the potential combination treatment with immune-based drugs have been reported in several studies (Brauner *et al.*, 2016; Comin-Anduix *et al.*, 2010; Wilmott *et al.*, 2012). In line with our findings, PD-L1 expression was analyzed in a larger panel of melanoma cell lines with or without treatment of MAPK inhibitors, showing no straight-forward cell-intrinsic regulation of PD-L1 expression by MAPK signaling (Atefi *et al.*, 2014). However, PD-L1 expression was found to be regulated by MAPK signaling in a study of lymphomas (Yamamoto *et al.*, 2009). In a murine carcinoma model, trametinib, a MEK inhibitor, synergized in combination with targeting PD1, PD-L1, and CTLA-4 antibody to increase antitumor efficacy (Liu *et al.*, 2015). The inconsistency in

the discovery of these studies with our findings may attribute to the diversity in signaling context of HNSCC and other tumors. Interestingly, another recent study demonstrates that inhibition of the HER2/EGFR signaling pathway reduced PD-L1 expression and cytokines release in HER2-amplified cancer cells. Moreover, the PI3K but not MEK pathway was involved in reduction of PD-L1 expression in these cell lines, indicating that the regulation of PD-L1 expression by the EGFR/HER2 pathway may be dependent on the PI3K-AKT-mTOR signaling pathway (Koung Jin Suh, 2017).

5.6 Conclusion and perspective

In summary, obtained results from a new cell culture model of fractionated irradiation provided compelling experimental evidence for the existence and expansion of a subpopulation of radioresistant tumor cells, which were characterized by ESR2 and opiorphin gene (SMR3A, OPRPN) expression. Notwithstanding, a statistically significant correlation was not observed between OPRPN expression pattern and clinical outcome of patients with OPSCC. Combined expression of ESR2 and OPRPN or SMR3A was associated with unfavorable clinical prognosis post definitive or adjuvant radiotherapy, suggesting that opiorphin-related genes serve as a surrogate marker for HNSCC cells with intrinsic radioresistance. Moreover, treatment with 4-hydroxytamoxifen or Fulvestrant, two well-established antagonists of estrogen receptor signaling, increases the sensitivity of HNSCC cell lines upon fractionated irradiation *in vitro*, paving the way for future clinical trials in which administration of anti-estrogen therapy in combination with radiotherapy will be assessed for HNSCC patients.

In addition, several cell culture models have been established to investigate the impact of drugs targeting the EGFR-MEK-MAPK pathway (Cetuximab and MEK1/2 inhibitor) on tumor cell survival and clonal expansion as well as expression of ESR2 and PD-L1. A concentration-dependent induction of ESR2 was detected in FaDu cells after

long-term treatment with cetuximab. Blocking ERK signaling, one of the downstream pathways of EGFR activation, can activate ESR2 signaling in FaDu cell under normal growth condition. These data provide experimental evidence that ESR2 interacts with the EGFR signaling pathway as alternate signaling mechanisms. The presented data indicated that impact of cetuximab on PD-L1 after short or long-term inhibition is heterogeneous but independent of ERK phosphorylation. The majority of HNSCC cell lines with long-term treatment regain phosphorylation of ERK1/2 as compared to short-term treatment, and up-regulation of PD-L1 was observed in the most resistant cell line with long-term treatment. These novel results provide a proof-of-concept that up-regulation of ERK phosphorylation and PD-L1 levels might be a potential mechanism of resistance to cetuximab treatment in HNSCC, suggesting potential benefits of combining cetuximab with immunotherapies. Furthermore, the experimental data not only reveal that PD-901, a MEK1/2 inhibitor, increases radiosensitivity of HNSCC cell lines, providing potential clinical benefit from combination treatment of MEK inhibitor and radiotherapy but also confirmed that PD-L1 regulation in HNSCC cell lines is mainly independent of MEK-ERK signaling. Taken together, these novel findings suggest a complex and context-dependent regulation of ESR2 as well as PD-L1 upon inhibition of the EGFR-MEK-MAPK signaling cascade, and might provide potential molecular targets for HNSCC treatment in the future.

Several issues should be addressed in future studies: 1). generation and analysis of HNSCC cell clones with a stable silencing of ESR2 expression using shRNA or CRISPR/Cas9 technology. With this cell culture models, ESR-dependent signaling and gene regulatory networks could be identified by global gene expression analysis. 2). expression and regulation of ESR2 in mouse tumor models, including HNSCC patient derived xenografts *in vivo*. 3). Functional characterization of other signaling pathways (e.g. PI3K, JAK-STAT, NFkB) involved in cell-intrinsic and extrinsic pathways of targeted-EGFR or PD-L1 regulation *in vitro* and *in vivo*.

6. Summary

Head and neck squamous cell carcinoma (HNSCC) is one of most common human malignancies worldwide with high tumor-related morbidity and mortality. Unraveling molecular mechanism of treatment resistance and identifying new biomarkers for HNSCC patients at high risk for treatment failure is urgently needed. Previous data have provided an experimental evidence that a subpopulation of radiotherapy resistant tumor cells reveals co-expression of estrogen receptor 2 (ESR2) and submaxillary gland androgen regulated protein 3A (SMR3A) after fractionated irradiation (IR). In first part of the present study, ESR2 expression was assessed by immunohistochemistry (IHC) staining on tissue microarrays (TMAs) containing tumor specimens of OPSCC patients, which were treated with either definitive or post-surgical radiotherapy with or without adjuvant chemotherapy. Statistical analysis revealed that a subgroup of patients with positive ESR-2 and high SMR3A had an unfavorable clinical outcome as compared to those with low SMR3A expression. Furthermore, a new cell culture model of fractionated irradiation provided compelling experimental evidence for the existence and expansion of a subpopulation of radioresistant tumor cells, which were characterized by ESR2, opiorphin genes (SMR3A, OPRPN) expression. Nevertheless, the protein expression of OPRPN, another member of the opiorphin gene family, and clinical outcome of patients with OPSCC were not significantly correlated. Combined expression of ESR2 and OPRPN or SMR3A was associated with an unfavorable clinical prognosis post definitive or adjuvant radiotherapy, suggesting that opiorphin-related genes serve as surrogate markers for HNSCC cells with intrinsic radioresistance. Treatment with 4-hydroxytamoxifen or fulvestrant, two well-established antagonists of estrogen receptor signaling, increased the sensitivity of HNSCC cell lines upon fractionated irradiation *in vitro*. These data provide a strong evidence in which evaluation of ESR2 and opiorphin gene co-expression in primary tumor samples supports the identification of HNSCC patients with a higher risk for treatment failure

after radiotherapy, who might benefit from an adjuvant treatment with antagonists of estrogen receptor signaling.

In this study, several cell culture models have been established to address the impact of drugs targeting the EGFR-MEK-MAPK pathway (cetuximab and MEK1/2 inhibitor) on tumor cell survival and clonal expansion as well as expression of ESR2 and programmed death-ligand 1 (PD-L1). A concentration-dependent induction of ESR2 was detected in FaDu cells after long-term treatment with cetuximab. Blocking ERK signaling, one of the downstream pathways of EGFR activation, can activate ESR2 signaling in FaDu cell under normal growth condition. These data provide the evidence that ESR2 interacts with the EGFR signaling pathway as alternate signaling mechanisms. The impact of cetuximab on PD-L1 after short or long-term inhibition has been clarified, which tends to be heterogenous but independent of ERK phosphorylation. The majority of HNSCC cell lines with long-term treatment regain expression of ERK phosphorylation as compared to short-term, and up-regulation of PD-L1 was observed in the most resistant cell line with long-term treatment. These results provide a proof-of-concept that up-regulation of PD-L1 might be a potential mechanism of resistance to cetuximab treatment in HNSCC, suggesting potential benefits of combining cetuximab with immunotherapy. Moreover, the experimental data not only reveal that PD-901, a MEK1/2 inhibitor, increases the radiosensitivity of HNSCC cell lines, providing potential clinical benefit from combination treatment of MEK1/2 inhibitor and radiotherapy but also confirmed that PD-L1 regulation in HNSCC cell lines is mainly independent of MEK-ERK signaling. Taken together, these novel findings suggest a complex and context-dependent regulation of ESR2 as well as PD-L1 upon inhibition of the EGFR-MEK-MAPK signaling cascade, may provide potential molecular targets for HNSCC treatment in the future.

7. Bibliography

- Aaronson, D. S. and Horvath, C. M. (2002). A road map for those who don't know JAK-STAT. *Science* 296, 1653-1655, doi: 10.1126/science.1071545.
- Acuna Sanhueza, G. A., Faller, L., George, B., Koffler, J., Misetic, V., Flechtenmacher, C., Dyckhoff, G., Plinkert, P. P., Angel, P., Simon, C. and Hess, J. (2012). Opposing function of MYBBP1A in proliferation and migration of head and neck squamous cell carcinoma cells. *BMC Cancer* 12, 72, doi: 10.1186/1471-2407-12-72.
- Affolter, A., Muller, M. F., Sommer, K., Stenzinger, A., Zaoui, K., Lorenz, K., Wolf, T., Sharma, S., Wolf, J., Perner, S., Weber, K. J., Freier, K., Plinkert, P. K., Hess, J. and Weichert, W. (2016). Targeting irradiation-induced mitogen-activated protein kinase activation in vitro and in an ex vivo model for human head and neck cancer. *Head Neck* 38 *Suppl* 1, E2049-2061, doi: 10.1002/hed.24376.
- Affolter, A., Samosny, G., Heimes, A. S., Schneider, J., Weichert, W., Stenzinger, A., Sommer, K., Jensen, A., Mayer, A., Brenner, W., Mann, W. J. and Brieger, J. (2017). Multikinase inhibitors sorafenib and sunitinib as radiosensitizers in head and neck cancer cell lines. *Head Neck* 39, 623-632, doi: 10.1002/hed.24557.
- Agrawal, N., Frederick, M. J., Pickering, C. R., Bettegowda, C., Chang, K., Li, R. J., Fakhry, C., Xie, T. X., Zhang, J., Wang, J., Zhang, N., El-Naggar, A. K., Jasser, S. A., Weinstein, J. N., Trevino, L., Drummond, J. A., Muzny, D. M., Wu, Y., Wood, L. D., Hruban, R. H., Westra, W. H., Koch, W. M., Califano, J. A., Gibbs, R. A., Sidransky, D., Vogelstein, B., Velculescu, V. E., Papadopoulos, N., Wheeler, D. A., Kinzler, K. W. and Myers, J. N. (2011). Exome sequencing of head and neck squamous cell carcinoma reveals inactivating mutations in NOTCH1. *Science* 333, 1154-1157, doi: 10.1126/science.1206923.
- Alter, B. P., Joenje, H., Oostra, A. B. and Pals, G. (2005). Fanconi anemia: adult head and neck cancer and hematopoietic mosaicism. *Arch Otolaryngol Head Neck Surg* 131, 635-639, doi: 10.1001/archotol.131.7.635.
- Anonymous (1988). Controlled trial of tamoxifen as a single adjuvant agent in the management of early breast cancer. 'Nolvadex' Adjuvant Trial Organisation. *Br J Cancer* 57, 608-611.
- Anonymous (1992). The effect of adjuvant tamoxifen: the latest results from the Cancer Research Campaign Adjuvant Breast Trial. *Cancer Research Campaign Breast*

Cancer Trials Group. *Eur J Cancer* 28A, 904-907.

Argiris, A., Karamouzis, M. V., Raben, D. and Ferris, R. L. (2008). Head and neck cancer. *Lancet* 371, 1695-1709, doi: 10.1016/S0140-6736(08)60728-X.

Arredondo, J., Chernyavsky, A. I., Jolkovsky, D. L., Pinkerton, K. E. and Grando, S. A. (2006). Receptor-mediated tobacco toxicity: cooperation of the Ras/Raf-1/MEK1/ERK and JAK-2/STAT-3 pathways downstream of alpha7 nicotinic receptor in oral keratinocytes. *FASEB J* 20, 2093-2101, doi: 10.1096/fj.06-6191com.

Atefi, M., Avramis, E., Lassen, A., Wong, D. J., Robert, L., Foulad, D., Cerniglia, M., Titz, B., Chodon, T., Graeber, T. G., Comin-Anduix, B. and Ribas, A. (2014). Effects of MAPK and PI3K pathways on PD-L1 expression in melanoma. *Clin Cancer Res* 20, 3446-3457, doi: 10.1158/1078-0432.CCR-13-2797.

Barton, M. B., Jacob, S., Shafiq, J., Wong, K., Thompson, S. R., Hanna, T. P. and Delaney, G. P. (2014). Estimating the demand for radiotherapy from the evidence: a review of changes from 2003 to 2012. *Radiother Oncol* 112, 140-144, doi: 10.1016/j.radonc.2014.03.024.

Bauman, J. E., Michel, L. S. and Chung, C. H. (2012). New promising molecular targets in head and neck squamous cell carcinoma. *Curr Opin Oncol* 24, 235-242, doi: 10.1097/CCO.0b013e3283517920.

Behren, A., Kamenisch, Y., Muehlen, S., Flechtenmacher, C., Haberkorn, U., Hilber, H., Myers, J. N., Bergmann, Z., Plinkert, P. K. and Simon, C. (2010). Development of an oral cancer recurrence mouse model after surgical resection. *Int J Oncol* 36, 849-855.

Bernstein, J. M., Bernstein, C. R., West, C. M. and Homer, J. J. (2013). Molecular and cellular processes underlying the hallmarks of head and neck cancer. *Eur Arch Otorhinolaryngol* 270, 2585-2593, doi: 10.1007/s00405-012-2323-x.

Bjornstrom, L. and Sjoberg, M. (2005). Mechanisms of estrogen receptor signaling: convergence of genomic and nongenomic actions on target genes. *Mol Endocrinol* 19, 833-842, doi: 10.1210/me.2004-0486.

Bonomo, P., Desideri, I., Loi, M., Mangoni, M., Sottili, M., Greto, D., Scotti, V., Meattini, I. and Livi, L. (2017). Anti-PD-L1 durvalumab combined with cetuximab and radiotherapy in locally advanced squamous cell carcinoma of the head and neck: A phase II study. *Journal of Clinical Oncology* 35, TPS6094-TPS6094, doi:

10.1200/JCO.2017.35.15_suppl.TPS6094.

Bose, P., Brockton, N. T. and Dort, J. C. (2013). Head and neck cancer: from anatomy to biology. *Int J Cancer* 133, 2013-2023, doi: 10.1002/ijc.28112.

Bossi, P. and Alfieri, S. (2016). Investigational drugs for head and neck cancer. *Expert Opin Investig Drugs* 25, 797-810, doi: 10.1080/13543784.2016.1175435.

Bourhis, J., Lefebvre, J. L. and Vermorken, J. B. (2010). Cetuximab in the management of locoregionally advanced head and neck cancer: expanding the treatment options? *Eur J Cancer* 46, 1979-1989, doi: 10.1016/j.ejca.2010.05.015.

Brauner, E., Gunda, V., Vanden Borre, P., Zurakowski, D., Kim, Y. S., Dennett, K. V., Amin, S., Freeman, G. J. and Parangi, S. (2016). Combining BRAF inhibitor and anti PD-L1 antibody dramatically improves tumor regression and anti tumor immunity in an immunocompetent murine model of anaplastic thyroid cancer. *Oncotarget* 7, 17194-17211, doi: 10.18632/oncotarget.7839.

Brennan, J. A., Boyle, J. O., Koch, W. M., Goodman, S. N., Hruban, R. H., Eby, Y. J., Couch, M. J., Forastiere, A. A. and Sidransky, D. (1995). Association between cigarette smoking and mutation of the p53 gene in squamous-cell carcinoma of the head and neck. *N Engl J Med* 332, 712-717, doi: 10.1056/NEJM199503163321104.

Brockstein, B. E. (2011). Management of recurrent head and neck cancer: recent progress and future directions. *Drugs* 71, 1551-1559, doi: 10.2165/11592540-000000000-00000.

Burtneß, B., Bauman, J. E. and Galloway, T. (2013). Novel targets in HPV-negative head and neck cancer: overcoming resistance to EGFR inhibition. *Lancet Oncol* 14, e302-309, doi: 10.1016/S1470-2045(13)70085-8.

Cancer Genome Atlas, N. (2015). Comprehensive genomic characterization of head and neck squamous cell carcinomas. *Nature* 517, 576-582, doi: 10.1038/nature14129.

Carl-McGrath, S., Lendeckel, U., Ebert, M. and Rocken, C. (2006). Ectopeptidases in tumour biology: a review. *Histol Histopathol* 21, 1339-1353, doi: 10.14670/HH-21.1339.

Carroll, P. E., Okuda, M., Horn, H. F., Biddinger, P., Stambrook, P. J., Gleich, L. L., Li, Y. Q., Tarapore, P. and Fukasawa, K. (1999). Centrosome hyperamplification in

human cancer: chromosome instability induced by p53 mutation and/or Mdm2 overexpression. *Oncogene* 18, 1935-1944, doi: 10.1038/sj.onc.1202515.

Chen, L. and Han, X. (2015). Anti-PD-1/PD-L1 therapy of human cancer: past, present, and future. *J Clin Invest* 125, 3384-3391, doi: 10.1172/JCI80011.

Chen, L., Lin, Y. L., Peng, G. and Li, F. (2012). Structural basis for multifunctional roles of mammalian aminopeptidase N. *Proc Natl Acad Sci U S A* 109, 17966-17971, doi: 10.1073/pnas.1210123109.

Chen, Y. J., Chang, J. T., Liao, C. T., Wang, H. M., Yen, T. C., Chiu, C. C., Lu, Y. C., Li, H. F. and Cheng, A. J. (2008). Head and neck cancer in the betel quid chewing area: recent advances in molecular carcinogenesis. *Cancer Sci* 99, 1507-1514, doi: 10.1111/j.1349-7006.2008.00863.x.

Cheng, Y. S., Mues, G., Wood, D. and Ding, J. (2006). Aromatase expression in normal human oral keratinocytes and oral squamous cell carcinoma. *Arch Oral Biol* 51, 612-620, doi: 10.1016/j.archoralbio.2006.01.002.

Choong, N. W. and Cohen, E. E. (2006). Epidermal growth factor receptor directed therapy in head and neck cancer. *Crit Rev Oncol Hematol* 57, 25-43, doi: 10.1016/j.critrevonc.2005.06.002.

Chua, R. G., Calenda, G., Zhang, X., Siragusa, J., Tong, Y., Tar, M., Aydin, M., DiSanto, M. E., Melman, A. and Davies, K. P. (2009). Testosterone regulates erectile function and Vcsa1 expression in the corpora of rats. *Mol Cell Endocrinol* 303, 67-73, doi: 10.1016/j.mce.2009.02.001.

ClinicalTrials.gov. U.S. National Institutes of Health. Available online: <http://www.clinicaltrial.gov/> (

Cole, M. P., Jones, C. T. and Todd, I. D. (1971). A new anti-oestrogenic agent in late breast cancer. An early clinical appraisal of ICI46474. *Br J Cancer* 25, 270-275.

Comin-Anduix, B., Chodon, T., Sazegar, H., Matsunaga, D., Mock, S., Jalil, J., Escuin-Ordinas, H., Chmielowski, B., Koya, R. C. and Ribas, A. (2010). The oncogenic BRAF kinase inhibitor PLX4032/RG7204 does not affect the viability or function of human lymphocytes across a wide range of concentrations. *Clin Cancer Res* 16, 6040-6048, doi: 10.1158/1078-0432.CCR-10-1911.

Constantinescu, S. N., Girardot, M. and Pecquet, C. (2008). Mining for JAK-STAT mutations in cancer. *Trends Biochem Sci* 33, 122-131, doi:

10.1016/j.tibs.2007.12.002.

- Dauvois, S., White, R. and Parker, M. G. (1993). The antiestrogen ICI 182780 disrupts estrogen receptor nucleocytoplasmic shuttling. *J Cell Sci* 106 (Pt 4), 1377-1388.
- Davies, K. P., Tar, M., Rougeot, C. and Melman, A. (2007). Sialorphin (the mature peptide product of Vcsa1) relaxes corporal smooth muscle tissue and increases erectile function in the ageing rat. *BJU Int* 99, 431-435, doi: 10.1111/j.1464-410X.2006.06577.x.
- de Villiers, E. M., Fauquet, C., Broker, T. R., Bernard, H. U. and zur Hausen, H. (2004). Classification of papillomaviruses. *Virology* 324, 17-27, doi: 10.1016/j.virol.2004.03.033.
- Denaro, N., Lo Nigro, C., Natoli, G., Russi, E. G., Adamo, V. and Merlano, M. C. (2011). The Role of p53 and MDM2 in Head and Neck Cancer. *ISRN Otolaryngol* 2011, 931813, doi: 10.5402/2011/931813.
- Deschler, D. G., Richmon, J. D., Khariwala, S. S., Ferris, R. L. and Wang, M. B. (2014). The "new" head and neck cancer patient-young, nonsmoker, nondrinker, and HPV positive: evaluation. *Otolaryngol Head Neck Surg* 151, 375-380, doi: 10.1177/0194599814538605.
- Deshpande, A. M. and Wong, D. T. (2008). Molecular mechanisms of head and neck cancer. *Expert Rev Anticancer Ther* 8, 799-809, doi: 10.1586/14737140.8.5.799.
- Dominguez, G., Silva, J., Garcia, J. M., Silva, J. M., Rodriguez, R., Munoz, C., Chacon, I., Sanchez, R., Carballido, J., Colas, A., Espana, P. and Bonilla, F. (2003). Prevalence of aberrant methylation of p14ARF over p16INK4a in some human primary tumors. *Mutat Res* 530, 9-17.
- Drigotas, M., Affolter, A., Mann, W. J. and Brieger, J. (2013). Reactive oxygen species activation of MAPK pathway results in VEGF upregulation as an undesired irradiation response. *J Oral Pathol Med* 42, 612-619, doi: 10.1111/jop.12056.
- Egloff, A. M., Rothstein, M. E., Seethala, R., Siegfried, J. M., Grandis, J. R. and Stabile, L. P. (2009). Cross-talk between estrogen receptor and epidermal growth factor receptor in head and neck squamous cell carcinoma. *Clin Cancer Res* 15, 6529-6540, doi: 10.1158/1078-0432.CCR-09-0862.

- Erhuma, M., Kobel, M., Mustafa, T., Wulfanger, J., Dralle, H., Hoang-Vu, C., Langner, J., Seliger, B. and Kehlen, A. (2007). Expression of neutral endopeptidase (NEP/CD10) on pancreatic tumor cell lines, pancreatitis and pancreatic tumor tissues. *Int J Cancer* 120, 2393-2400, doi: 10.1002/ijc.22252.
- Faber, A. C., Li, D., Song, Y., Liang, M. C., Yeap, B. Y., Bronson, R. T., Lifshits, E., Chen, Z., Maira, S. M., Garcia-Echeverria, C., Wong, K. K. and Engelman, J. A. (2009). Differential induction of apoptosis in HER2 and EGFR addicted cancers following PI3K inhibition. *Proc Natl Acad Sci U S A* 106, 19503-19508, doi: 10.1073/pnas.0905056106.
- Fawell, S. E., White, R., Hoare, S., Sydenham, M., Page, M. and Parker, M. G. (1990). Inhibition of estrogen receptor-DNA binding by the "pure" antiestrogen ICI 164,384 appears to be mediated by impaired receptor dimerization. *Proc Natl Acad Sci U S A* 87, 6883-6887.
- Ferguson, B. J., Hudson, W. R. and McCarty, K. S., Jr. (1987). Sex steroid receptor distribution in the human larynx and laryngeal carcinoma. *Arch Otolaryngol Head Neck Surg* 113, 1311-1315.
- Ferlay, J., Shin, H. R., Bray, F., Forman, D., Mathers, C. and Parkin, D. M. (2010). Estimates of worldwide burden of cancer in 2008: GLOBOCAN 2008. *Int J Cancer* 127, 2893-2917, doi: 10.1002/ijc.25516.
- Ferris, R. L. (2015). Immunology and Immunotherapy of Head and Neck Cancer. *J Clin Oncol* 33, 3293-3304, doi: 10.1200/JCO.2015.61.1509.
- Franken, N. A., Rodermond, H. M., Stap, J., Haveman, J. and van Bree, C. (2006). Clonogenic assay of cells in vitro. *Nat Protoc* 1, 2315-2319, doi: 10.1038/nprot.2006.339.
- Fu, S., Tar, M. T., Melman, A. and Davies, K. P. (2014). Opiorphin is a master regulator of the hypoxic response in corporal smooth muscle cells. *FASEB J* 28, 3633-3644, doi: 10.1096/fj.13-248708.
- Fujita, S., Yamamoto, S., Akasu, T., Moriya, Y., Taniguchi, H. and Shimoda, T. (2007). Quantification of CD10 mRNA in colorectal cancer and relationship between mRNA expression and liver metastasis. *Anticancer Res* 27, 3307-3311.
- Gatta, G., Botta, L., Sanchez, M. J., Anderson, L. A., Pierannunzio, D., Licitra, L. and Group, E. W. (2015). Prognoses and improvement for head and neck cancers diagnosed in Europe in early 2000s: The EURO CARE-5 population-based study.

Eur J Cancer 51, 2130-2143, doi: 10.1016/j.ejca.2015.07.043.

Gillison, M. L., D'Souza, G., Westra, W., Sugar, E., Xiao, W., Begum, S. and Viscidi, R. (2008). Distinct risk factor profiles for human papillomavirus type 16-positive and human papillomavirus type 16-negative head and neck cancers. *J Natl Cancer Inst* 100, 407-420, doi: 10.1093/jnci/djn025.

Gotwals, P., Cameron, S., Cipolletta, D., Cremasco, V., Crystal, A., Hewes, B., Mueller, B., Quaratino, S., Sabatos-Peyton, C., Petruzzelli, L., Engelman, J. A. and Dranoff, G. (2017). Prospects for combining targeted and conventional cancer therapy with immunotherapy. *Nat Rev Cancer* 17, 286-301, doi: 10.1038/nrc.2017.17.

Grandis, J. R., Drenning, S. D., Chakraborty, A., Zhou, M. Y., Zeng, Q., Pitt, A. S. and Tweardy, D. J. (1998). Requirement of Stat3 but not Stat1 activation for epidermal growth factor receptor-mediated cell growth *In vitro*. *J Clin Invest* 102, 1385-1392, doi: 10.1172/JCI3785.

Grandis, J. R., Drenning, S. D., Zeng, Q., Watkins, S. C., Melhem, M. F., Endo, S., Johnson, D. E., Huang, L., He, Y. and Kim, J. D. (2000). Constitutive activation of Stat3 signaling abrogates apoptosis in squamous cell carcinogenesis *in vivo*. *Proc Natl Acad Sci U S A* 97, 4227-4232.

Grandis, J. R. and Tweardy, D. J. (1993). Elevated levels of transforming growth factor alpha and epidermal growth factor receptor messenger RNA are early markers of carcinogenesis in head and neck cancer. *Cancer Res* 53, 3579-3584.

Gregoire, V., Langendijk, J. A. and Nuyts, S. (2015). Advances in Radiotherapy for Head and Neck Cancer. *J Clin Oncol* 33, 3277-3284, doi: 10.1200/JCO.2015.61.2994.

Grunow, J., Rong, C., Hischmann, J., Zaoui, K., Flechtenmacher, C., Weber, K. J., Plinkert, P. and Hess, J. (2017). Regulation of submaxillary gland androgen-regulated protein 3A via estrogen receptor 2 in radioresistant head and neck squamous cell carcinoma cells. *J Exp Clin Cancer Res* 36, 25, doi: 10.1186/s13046-017-0496-2.

Gupta, A. K., Bakanauskas, V. J., Cerniglia, G. J., Cheng, Y., Bernhard, E. J., Muschel, R. J. and McKenna, W. G. (2001). The Ras radiation resistance pathway. *Cancer Res* 61, 4278-4282.

Hagedorn, H. G. and Nerlich, A. G. (2002). Analysis of sex-hormone-receptor

expression in laryngeal carcinoma. *Eur Arch Otorhinolaryngol* 259, 205-210.

Hama, T., Yuza, Y., Saito, Y., J. O. u., Kondo, S., Okabe, M., Yamada, H., Kato, T., Moriyama, H., Kurihara, S. and Urashima, M. (2009). Prognostic significance of epidermal growth factor receptor phosphorylation and mutation in head and neck squamous cell carcinoma. *Oncologist* 14, 900-908, doi: 10.1634/theoncologist.2009-0058.

Hamid, O. and Carvajal, R. D. (2013). Anti-programmed death-1 and anti-programmed death-ligand 1 antibodies in cancer therapy. *Expert Opin Biol Ther* 13, 847-861, doi: 10.1517/14712598.2013.770836.

Hammerman, P. S., Hayes, D. N. and Grandis, J. R. (2015). Therapeutic insights from genomic studies of head and neck squamous cell carcinomas. *Cancer Discov* 5, 239-244, doi: 10.1158/2159-8290.CD-14-1205.

Hanahan, D. and Weinberg, R. A. (2011). Hallmarks of cancer: the next generation. *Cell* 144, 646-674, doi: 10.1016/j.cell.2011.02.013.

Hartmann, S., Bhola, N. E. and Grandis, J. R. (2016). HGF/Met Signaling in Head and Neck Cancer: Impact on the Tumor Microenvironment. *Clin Cancer Res* 22, 4005-4013, doi: 10.1158/1078-0432.CCR-16-0951.

Harvey, J. M., Clark, G. M., Osborne, C. K. and Allred, D. C. (1999). Estrogen Receptor Status by Immunohistochemistry Is Superior to the Ligand-Binding Assay for Predicting Response to Adjuvant Endocrine Therapy in Breast Cancer. *Journal of Clinical Oncology* 17, 1474-1474, doi: 10.1200/jco.1999.17.5.1474.

Heldring, N., Pike, A., Andersson, S., Matthews, J., Cheng, G., Hartman, J., Tujague, M., Strom, A., Treuter, E., Warner, M. and Gustafsson, J. A. (2007). Estrogen receptors: how do they signal and what are their targets. *Physiol Rev* 87, 905-931, doi: 10.1152/physrev.00026.2006.

Hoeflich, K. P., O'Brien, C., Boyd, Z., Cavet, G., Guerrero, S., Jung, K., Januario, T., Savage, H., Punnoose, E., Truong, T., Zhou, W., Berry, L., Murray, L., Amler, L., Belvin, M., Friedman, L. S. and Lackner, M. R. (2009). In vivo antitumor activity of MEK and phosphatidylinositol 3-kinase inhibitors in basal-like breast cancer models. *Clin Cancer Res* 15, 4649-4664, doi: 10.1158/1078-0432.CCR-09-0317.

Holzinger, D., Flechtenmacher, C., Henfling, N., Kaden, I., Grabe, N., Lahrmann, B., Schmitt, M., Hess, J., Pawlita, M. and Bosch, F. X. (2013). Identification of

oropharyngeal squamous cell carcinomas with active HPV16 involvement by immunohistochemical analysis of the retinoblastoma protein pathway. *Int J Cancer* 133, 1389-1399, doi: 10.1002/ijc.28142.

Holzinger, D., Schmitt, M., Dyckhoff, G., Benner, A., Pawlita, M. and Bosch, F. X. (2012). Viral RNA patterns and high viral load reliably define oropharynx carcinomas with active HPV16 involvement. *Cancer Res* 72, 4993-5003, doi: 10.1158/0008-5472.CAN-11-3934.

Honma, N., Horii, R., Iwase, T., Saji, S., Younes, M., Takubo, K., Matsuura, M., Ito, Y., Akiyama, F. and Sakamoto, G. (2008). Clinical importance of estrogen receptor-beta evaluation in breast cancer patients treated with adjuvant tamoxifen therapy. *J Clin Oncol* 26, 3727-3734, doi: 10.1200/JCO.2007.14.2968.

Horn, D., Hess, J., Freier, K., Hoffmann, J. and Freudlsperger, C. (2015). Targeting EGFR-PI3K-AKT-mTOR signaling enhances radiosensitivity in head and neck squamous cell carcinoma. *Expert Opin Ther Targets* 19, 795-805, doi: 10.1517/14728222.2015.1012157.

Hsu, L. H., Chu, N. M. and Kao, S. H. (2017). Estrogen, Estrogen Receptor and Lung Cancer. *Int J Mol Sci* 18, doi: 10.3390/ijms18081713.

Hynes, N. E. and Lane, H. A. (2005). ERBB receptors and cancer: the complexity of targeted inhibitors. *Nat Rev Cancer* 5, 341-354, doi: 10.1038/nrc1609.

Ichikawa, A., Ando, J. and Suda, K. (2008). G1 arrest and expression of cyclin-dependent kinase inhibitors in tamoxifen-treated MCF-7 human breast cancer cells. *Hum Cell* 21, 28-37, doi: 10.1111/j.1749-0774.2008.00048.x.

Isaacsson Velho, P. H., Castro, G., Jr. and Chung, C. H. (2015). Targeting the PI3K Pathway in Head and Neck Squamous Cell Carcinoma. *Am Soc Clin Oncol Educ Book*, 123-128, doi: 10.14694/EdBook_AM.2015.35.123.

Ishida, H., Wada, K., Masuda, T., Okura, M., Kohama, K., Sano, Y., Nakajima, A., Kogo, M. and Kamisaki, Y. (2007). Critical role of estrogen receptor on anoikis and invasion of squamous cell carcinoma. *Cancer Sci* 98, 636-643, doi: 10.1111/j.1349-7006.2007.00437.x.

Javelot, H., Messaoudi, M., Garnier, S. and Rougeot, C. (2010). Human opiorphin is a naturally occurring antidepressant acting selectively on enkephalin-dependent delta-opioid pathways. *J Physiol Pharmacol* 61, 355-362.

- Jeng, J. H., Chang, M. C. and Hahn, L. J. (2001). Role of areca nut in betel quid-associated chemical carcinogenesis: current awareness and future perspectives. *Oral Oncol* 37, 477-492.
- Jiang, X., Zhou, J., Giobbie-Hurder, A., Wargo, J. and Hodi, F. S. (2013). The activation of MAPK in melanoma cells resistant to BRAF inhibition promotes PD-L1 expression that is reversible by MEK and PI3K inhibition. *Clin Cancer Res* 19, 598-609, doi: 10.1158/1078-0432.CCR-12-2731.
- Jie, H. B., Schuler, P. J., Lee, S. C., Srivastava, R. M., Argiris, A., Ferrone, S., Whiteside, T. L. and Ferris, R. L. (2015). CTLA-4(+) Regulatory T Cells Increased in Cetuximab-Treated Head and Neck Cancer Patients Suppress NK Cell Cytotoxicity and Correlate with Poor Prognosis. *Cancer Res* 75, 2200-2210, doi: 10.1158/0008-5472.CAN-14-2788.
- Jordan, V. C., Collins, M. M., Rowsby, L. and Prestwich, G. (1977). A monohydroxylated metabolite of tamoxifen with potent antioestrogenic activity. *J Endocrinol* 75, 305-316.
- Kakavand, H., Rawson, R. V., Pupo, G. M., Yang, J. Y. H., Menzies, A. M., Carlino, M. S., Kefford, R. F., Howle, J. R., Saw, R. P. M., Thompson, J. F., Wilmott, J. S., Long, G. V., Scolyer, R. A. and Rizos, H. (2017). PD-L1 Expression and Immune Escape in Melanoma Resistance to MAPK Inhibitors. *Clin Cancer Res*, doi: 10.1158/1078-0432.CCR-16-1688.
- Kantorowitz, D. A., Thompson, H. J. and Furmanski, P. (1993). Effect of conjoint administration of tamoxifen and high-dose radiation on the development of mammary carcinoma. *Int J Radiat Oncol Biol Phys* 26, 89-94.
- Kawamura, J., Shimada, Y., Kitaichi, H., Komoto, I., Hashimoto, Y., Kaganoi, J., Miyake, M., Yamasaki, S., Kondo, K. and Imamura, M. (2007). Clinicopathological significance of aminopeptidase N/CD13 expression in human gastric carcinoma. *Hepatogastroenterology* 54, 36-40.
- Kiyohara, C. and Ohno, Y. (2010). Sex differences in lung cancer susceptibility: a review. *Gend Med* 7, 381-401, doi: 10.1016/j.genm.2010.10.002.
- Koffler, J., Holzinger, D., Sanhueza, G. A., Flechtenmacher, C., Zaoui, K., Lahrmann, B., Grabe, N., Plinkert, P. K. and Hess, J. (2013). Submaxillary gland androgen-regulated protein 3A expression is an unfavorable risk factor for the survival of oropharyngeal squamous cell carcinoma patients after surgery. *Eur*

Arch Otorhinolaryngol 270, 1493-1500, doi: 10.1007/s00405-012-2201-6.

Koppikar, P., Lui, V. W., Man, D., Xi, S., Chai, R. L., Nelson, E., Tobey, A. B. and Grandis, J. R. (2008). Constitutive activation of signal transducer and activator of transcription 5 contributes to tumor growth, epithelial-mesenchymal transition, and resistance to epidermal growth factor receptor targeting. *Clin Cancer Res* 14, 7682-7690, doi: 10.1158/1078-0432.CCR-08-1328.

Kostareli, E., Holzinger, D. and Hess, J. (2012). New Concepts for Translational Head and Neck Oncology: Lessons from HPV-Related Oropharyngeal Squamous Cell Carcinomas. *Front Oncol* 2, 36, doi: 10.3389/fonc.2012.00036.

Koung Jin Suh, J. H. S., Jin Won Kim, Song-Hee Han, Hye Seung Lee, Ahrum Min, Mi Hyun Kang, Ji Eun Kim, Ji-Won Kim, Se Hyun Kim, Jeong-Ok Lee¹, Yu Jung Kim¹, Keun-Wook Lee¹, Jee Hyun Kim¹, Soo-Mee Bang¹, Seock-Ah Im^{3,4} and Jong Seok Lee¹ (2017). EGFR or HER2 inhibition modulates the tumor microenvironment by suppression of PD-L1 and cytokines release. *Oncotarget*, doi: doi.org/10.18632/oncotarget.19194.

Kuniyasu, H., Luo, Y., Fujii, K., Sasahira, T., Moriwaka, Y., Tatsumoto, N., Sasaki, T., Yamashita, Y. and Ohmori, H. (2010). CD10 enhances metastasis of colorectal cancer by abrogating the anti-tumoural effect of methionine-enkephalin in the liver. *Gut* 59, 348-356, doi: 10.1136/gut.2009.178376.

Lai, A. C. and Crews, C. M. (2017). Induced protein degradation: an emerging drug discovery paradigm. *Nat Rev Drug Discov* 16, 101-114, doi: 10.1038/nrd.2016.211.

Lai, S. Y., Childs, E. E., Xi, S., Coppelli, F. M., Gooding, W. E., Wells, A., Ferris, R. L. and Grandis, J. R. (2005). Erythropoietin-mediated activation of JAK-STAT signaling contributes to cellular invasion in head and neck squamous cell carcinoma. *Oncogene* 24, 4442-4449, doi: 10.1038/sj.onc.1208635.

Lai, S. Y. and Johnson, F. M. (2010). Defining the role of the JAK-STAT pathway in head and neck and thoracic malignancies: implications for future therapeutic approaches. *Drug Resist Updat* 13, 67-78, doi: 10.1016/j.drug.2010.04.001.

Lee, C. I., Goodwin, A. and Wilcken, N. (2017). Fulvestrant for hormone-sensitive metastatic breast cancer. *Cochrane Database Syst Rev* 1, CD011093, doi: 10.1002/14651858.CD011093.pub2.

Lee, Y., Shin, J. H., Longmire, M., Wang, H., Kohrt, H. E., Chang, H. Y. and Sunwoo, J.

- B. (2016). CD44+ Cells in Head and Neck Squamous Cell Carcinoma Suppress T-Cell-Mediated Immunity by Selective Constitutive and Inducible Expression of PD-L1. *Clin Cancer Res* 22, 3571-3581, doi: 10.1158/1078-0432.CCR-15-2665.
- Leemans, C. R., Braakhuis, B. J. and Brakenhoff, R. H. (2011). The molecular biology of head and neck cancer. *Nat Rev Cancer* 11, 9-22, doi: 10.1038/nrc2982.
- Lewis, A., Kang, R., Levine, A. and Maghami, E. (2015). The New Face of Head and Neck Cancer: The HPV Epidemic. *Oncology (Williston Park)* 29, 616-626.
- Licitra, L., Mesia, R., Rivera, F., Remenar, E., Hitt, R., Erfan, J., Rottey, S., Kaweckki, A., Zabolotnyy, D., Benasso, M., Storkel, S., Senger, S., Stroh, C. and Vermorken, J. B. (2011). Evaluation of EGFR gene copy number as a predictive biomarker for the efficacy of cetuximab in combination with chemotherapy in the first-line treatment of recurrent and/or metastatic squamous cell carcinoma of the head and neck: EXTREME study. *Ann Oncol* 22, 1078-1087, doi: 10.1093/annonc/mdq588.
- Liu, L., Mayes, P. A., Eastman, S., Shi, H., Yadavilli, S., Zhang, T., Yang, J., Seestaller-Wehr, L., Zhang, S. Y., Hopson, C., Tsvetkov, L., Jing, J., Zhang, S., Smothers, J. and Hoos, A. (2015). The BRAF and MEK Inhibitors Dabrafenib and Trametinib: Effects on Immune Function and in Combination with Immunomodulatory Antibodies Targeting PD-1, PD-L1, and CTLA-4. *Clin Cancer Res* 21, 1639-1651, doi: 10.1158/1078-0432.CCR-14-2339.
- Lukits, J., Remenar, E., Raso, E., Ladanyi, A., Kasler, M. and Timar, J. (2007). Molecular identification, expression and prognostic role of estrogen- and progesterone receptors in head and neck cancer. *Int J Oncol* 30, 155-160.
- Luo, Y., Fujii, K., Ohmori, H., Sasahira, T., Moriwaka, Y., Isobe, M. and Kuniyasu, H. (2009). Antisense phosphorothioate oligodeoxynucleic acid for CD10 suppresses liver metastasis of colorectal cancer. *Pathobiology* 76, 267-273, doi: 10.1159/000228903.
- Lyford-Pike, S., Peng, S., Young, G. D., Taube, J. M., Westra, W. H., Akpeng, B., Bruno, T. C., Richmon, J. D., Wang, H., Bishop, J. A., Chen, L., Drake, C. G., Topalian, S. L., Pardoll, D. M. and Pai, S. I. (2013). Evidence for a role of the PD-1:PD-L1 pathway in immune resistance of HPV-associated head and neck squamous cell carcinoma. *Cancer Res* 73, 1733-1741, doi: 10.1158/0008-5472.CAN-12-2384.
- Maguer-Satta, V., Besancon, R. and Bachelard-Cascales, E. (2011). Concise review:

neutral endopeptidase (CD10): a multifaceted environment actor in stem cells, physiological mechanisms, and cancer. *Stem Cells* 29, 389-396, doi: 10.1002/stem.592.

Marquez-Garban, D. C., Chen, H. W., Fishbein, M. C., Goodglick, L. and Pietras, R. J. (2007). Estrogen receptor signaling pathways in human non-small cell lung cancer. *Steroids* 72, 135-143, doi: 10.1016/j.steroids.2006.11.019.

Marur, S., D'Souza, G., Westra, W. H. and Forastiere, A. A. (2010). HPV-associated head and neck cancer: a virus-related cancer epidemic. *Lancet Oncol* 11, 781-789, doi: 10.1016/S1470-2045(10)70017-6.

Meniawy, T. M., Lake, R. A., McDonnell, A. M., Millward, M. J. and Nowak, A. K. (2016). PD-L1 on peripheral blood T lymphocytes is prognostic in patients with non-small cell lung cancer (NSCLC) treated with EGFR inhibitors. *Lung Cancer* 93, 9-16, doi: 10.1016/j.lungcan.2015.12.006.

Messaoudi, M., Desor, D., Nejdi, A. and Rougeot, C. (2004). The endogenous androgen-regulated sialorphin modulates male rat sexual behavior. *Horm Behav* 46, 684-691, doi: 10.1016/j.yhbeh.2004.06.012.

Mizerska-Dudka, M. and Kandefler-Szerszen, M. (2015). Opioids, Neutral Endopeptidase, its Inhibitors and Cancer: Is There a Relationship among them? *Arch Immunol Ther Exp (Warsz)* 63, 197-205, doi: 10.1007/s00005-014-0311-0.

Molinolo, A. A., Amornphimoltham, P., Squarize, C. H., Castilho, R. M., Patel, V. and Gutkind, J. S. (2009). Dysregulated molecular networks in head and neck carcinogenesis. *Oral Oncol* 45, 324-334, doi: 10.1016/j.oraloncology.2008.07.011.

Mountzios, G., Rampias, T. and Psyrri, A. (2014). The mutational spectrum of squamous-cell carcinoma of the head and neck: targetable genetic events and clinical impact. *Ann Oncol* 25, 1889-1900, doi: 10.1093/annonc/mdu143.

Murugan, A. K., Hong, N. T., Fukui, Y., Munirajan, A. K. and Tsuchida, N. (2008). Oncogenic mutations of the PIK3CA gene in head and neck squamous cell carcinomas. *Int J Oncol* 32, 101-111.

Nagpal, J. K., Mishra, R. and Das, B. R. (2002). Activation of Stat-3 as one of the early events in tobacco chewing-mediated oral carcinogenesis. *Cancer* 94, 2393-2400, doi: 10.1002/cncr.10499.

- Nardella, C., Clohessy, J. G., Alimonti, A. and Pandolfi, P. P. (2011). Pro-senescence therapy for cancer treatment. *Nat Rev Cancer* 11, 503-511, doi: 10.1038/nrc3057.
- Nefedova, Y. and Gabrilovich, D. I. (2007). Targeting of Jak/STAT pathway in antigen presenting cells in cancer. *Curr Cancer Drug Targets* 7, 71-77.
- Negrini, S., Gorgoulis, V. G. and Halazonetis, T. D. (2010). Genomic instability--an evolving hallmark of cancer. *Nat Rev Mol Cell Biol* 11, 220-228, doi: 10.1038/nrm2858.
- Niyazi, M., Niyazi, I. and Belka, C. (2007). Counting colonies of clonogenic assays by using densitometric software. *Radiat Oncol* 2, 4, doi: 10.1186/1748-717X-2-4.
- Nose, N., Sugio, K., Oyama, T., Nozoe, T., Uramoto, H., Iwata, T., Onitsuka, T. and Yasumoto, K. (2009). Association between estrogen receptor-beta expression and epidermal growth factor receptor mutation in the postoperative prognosis of adenocarcinoma of the lung. *J Clin Oncol* 27, 411-417, doi: 10.1200/JCO.2008.18.3251.
- Nose, N., Uramoto, H., Iwata, T., Hanagiri, T. and Yasumoto, K. (2011). Expression of estrogen receptor beta predicts a clinical response and longer progression-free survival after treatment with EGFR-TKI for adenocarcinoma of the lung. *Lung Cancer* 71, 350-355, doi: 10.1016/j.lungcan.2010.06.009.
- Ock, C. Y., Kim, S., Keam, B., Kim, M., Kim, T. M., Kim, J. H., Jeon, Y. K., Lee, J. S., Kwon, S. K., Hah, J. H., Kwon, T. K., Kim, D. W., Wu, H. G., Sung, M. W. and Heo, D. S. (2016). PD-L1 expression is associated with epithelial-mesenchymal transition in head and neck squamous cell carcinoma. *Oncotarget* 7, 15901-15914, doi: 10.18632/oncotarget.7431.
- Osborne, C. K., Coronado-Heinsohn, E. B., Hilsenbeck, S. G., McCue, B. L., Wakeling, A. E., McClelland, R. A., Manning, D. L. and Nicholson, R. I. (1995). Comparison of the effects of a pure steroidal antiestrogen with those of tamoxifen in a model of human breast cancer. *J Natl Cancer Inst* 87, 746-750.
- Osborne, C. K., Schiff, R., Fuqua, S. A. and Shou, J. (2001). Estrogen receptor: current understanding of its activation and modulation. *Clin Cancer Res* 7, 4338s-4342s; discussion 4411s-4412s.
- Osborne, C. K., Shou, J., Massarweh, S. and Schiff, R. (2005). Crosstalk between estrogen receptor and growth factor receptor pathways as a cause for

endocrine therapy resistance in breast cancer. *Clin Cancer Res* 11, 865s-870s.

- Osborne, C. K., Wakeling, A. and Nicholson, R. I. (2004). Fulvestrant: an oestrogen receptor antagonist with a novel mechanism of action. *Br J Cancer* 90 *Suppl* 1, S2-6, doi: 10.1038/sj.bjc.6601629.
- Oshimori, N., Oristian, D. and Fuchs, E. (2015). TGF-beta promotes heterogeneity and drug resistance in squamous cell carcinoma. *Cell* 160, 963-976, doi: 10.1016/j.cell.2015.01.043.
- Ozanne, B., Richards, C. S., Hendler, F., Burns, D. and Gusterson, B. (1986). Over-expression of the EGF receptor is a hallmark of squamous cell carcinomas. *J Pathol* 149, 9-14, doi: 10.1002/path.1711490104.
- Pai, S. I. and Westra, W. H. (2009). Molecular pathology of head and neck cancer: implications for diagnosis, prognosis, and treatment. *Annu Rev Pathol* 4, 49-70, doi: 10.1146/annurev.pathol.4.110807.092158.
- Paulsen, G. H., Strickert, T., Marthinsen, A. B. and Lundgren, S. (1996). Changes in radiation sensitivity and steroid receptor content induced by hormonal agents and ionizing radiation in breast cancer cells in vitro. *Acta Oncol* 35, 1011-1019.
- Piattelli, A., Fioroni, M., Iezzi, G., Perrotti, V., Stellini, E., Piattelli, M. and Rubini, C. (2006). CD10 expression in stromal cells of oral cavity squamous cell carcinoma: a clinic and pathologic correlation. *Oral Dis* 12, 301-304, doi: 10.1111/j.1601-0825.2005.01196.x.
- Platet, N., Cathiard, A. M., Gleizes, M. and Garcia, M. (2004). Estrogens and their receptors in breast cancer progression: a dual role in cancer proliferation and invasion. *Crit Rev Oncol Hematol* 51, 55-67, doi: 10.1016/j.critrevonc.2004.02.001.
- Poeta, M. L., Manola, J., Goldwasser, M. A., Forastiere, A., Benoit, N., Califano, J. A., Ridge, J. A., Goodwin, J., Kenady, D., Saunders, J., Westra, W., Sidransky, D. and Koch, W. M. (2007). TP53 mutations and survival in squamous-cell carcinoma of the head and neck. *N Engl J Med* 357, 2552-2561, doi: 10.1056/NEJMoa073770.
- Qiu, W., Schonleben, F., Li, X., Ho, D. J., Close, L. G., Manolidis, S., Bennett, B. P. and Su, G. H. (2006). PIK3CA mutations in head and neck squamous cell carcinoma. *Clin Cancer Res* 12, 1441-1446, doi: 10.1158/1078-0432.CCR-05-2173.

- Quon, H., Liu, F. F. and Cummings, B. J. (2001). Potential molecular prognostic markers in head and neck squamous cell carcinomas. *Head Neck* 23, 147-159.
- Ratanaphan, A. (2012). A DNA repair BRCA1 estrogen receptor and targeted therapy in breast cancer. *Int J Mol Sci* 13, 14898-14916, doi: 10.3390/ijms131114898.
- Ratovitski, E., Trink, B. and Sidransky, D. (2006). p63 and p73: teammates or adversaries? *Cancer Cell* 9, 1-2, doi: 10.1016/j.ccr.2005.12.027.
- Reed, A. L., Califano, J., Cairns, P., Westra, W. H., Jones, R. M., Koch, W., Ahrendt, S., Eby, Y., Sewell, D., Nawroz, H., Bartek, J. and Sidransky, D. (1996). High frequency of p16 (CDKN2/MTS-1/INK4A) inactivation in head and neck squamous cell carcinoma. *Cancer Res* 56, 3630-3633.
- Ritprajak, P. and Azuma, M. (2015). Intrinsic and extrinsic control of expression of the immunoregulatory molecule PD-L1 in epithelial cells and squamous cell carcinoma. *Oral Oncol* 51, 221-228, doi: 10.1016/j.oraloncology.2014.11.014.
- Rocco, J. W., Leong, C. O., Kuperwasser, N., DeYoung, M. P. and Ellisen, L. W. (2006). p63 mediates survival in squamous cell carcinoma by suppression of p73-dependent apoptosis. *Cancer Cell* 9, 45-56, doi: 10.1016/j.ccr.2005.12.013.
- Roesch-Ely, M., Nees, M., Karsai, S., Ruess, A., Bogumil, R., Warnken, U., Schnolzer, M., Dietz, A., Plinkert, P. K., Hofele, C. and Bosch, F. X. (2007). Proteomic analysis reveals successive aberrations in protein expression from healthy mucosa to invasive head and neck cancer. *Oncogene* 26, 54-64, doi: 10.1038/sj.onc.1209770.
- Roman-Blas, J. A., Castaneda, S., Largo, R. and Herrero-Beaumont, G. (2009). Osteoarthritis associated with estrogen deficiency. *Arthritis Res Ther* 11, 241, doi: 10.1186/ar2791.
- Rosenberg, P. S., Socie, G., Alter, B. P. and Gluckman, E. (2005). Risk of head and neck squamous cell cancer and death in patients with Fanconi anemia who did and did not receive transplants. *Blood* 105, 67-73, doi: 10.1182/blood-2004-04-1652.
- Rosenthal, E. L. and Matrisian, L. M. (2006). Matrix metalloproteases in head and neck cancer. *Head Neck* 28, 639-648, doi: 10.1002/hed.20365.
- Rothenberg, S. M. and Ellisen, L. W. (2012). The molecular pathogenesis of head and neck squamous cell carcinoma. *J Clin Invest* 122, 1951-1957.

- Rougeot, C., Messaoudi, M., Hermitte, V., Rigault, A. G., Blisnick, T., Dugave, C., Desor, D. and Rougeon, F. (2003). Sialorphin, a natural inhibitor of rat membrane-bound neutral endopeptidase that displays analgesic activity. *Proc Natl Acad Sci U S A* *100*, 8549-8554, doi: 10.1073/pnas.1431850100.
- Sailasree, R., Abhilash, A., Sathyan, K. M., Nalinakumari, K. R., Thomas, S. and Kannan, S. (2008). Differential roles of p16INK4A and p14ARF genes in prognosis of oral carcinoma. *Cancer Epidemiol Biomarkers Prev* *17*, 414-420, doi: 10.1158/1055-9965.EPI-07-0284.
- Schaaij-Visser, T. B., Graveland, A. P., Gauci, S., Braakhuis, B. J., Buijze, M., Heck, A. J., Kuik, D. J., Bloemena, E., Leemans, C. R., Slijper, M. and Brakenhoff, R. H. (2009). Differential Proteomics Identifies Protein Biomarkers That Predict Local Relapse of Head and Neck Squamous Cell Carcinomas. *Clin Cancer Res* *15*, 7666-7675, doi: 10.1158/1078-0432.CCR-09-2134.
- Schache, A. G., Liloglou, T., Risk, J. M., Folia, A., Jones, T. M., Sheard, J., Woolgar, J. A., Helliwell, T. R., Triantafyllou, A., Robinson, M., Sloan, P., Harvey-Woodworth, C., Sisson, D. and Shaw, R. J. (2011). Evaluation of human papilloma virus diagnostic testing in oropharyngeal squamous cell carcinoma: sensitivity, specificity, and prognostic discrimination. *Clin Cancer Res* *17*, 6262-6271, doi: 10.1158/1078-0432.CCR-11-0388.
- Schuller, D. E., Abou-Issa, H. and Parrish, R. (1984). Estrogen and progesterone receptors in head and neck cancer. *Arch Otolaryngol* *110*, 725-727.
- Schwartz, A. G., Prysak, G. M., Murphy, V., Lonardo, F., Pass, H., Schwartz, J. and Brooks, S. (2005). Nuclear estrogen receptor beta in lung cancer: expression and survival differences by sex. *Clin Cancer Res* *11*, 7280-7287, doi: 10.1158/1078-0432.CCR-05-0498.
- Senorale-Pose, M., Jacqueson, A., Rougeon, F. and Rosinski-Chupin, I. (1998). Acinar cells are target cells for androgens in mouse submandibular glands. *J Histochem Cytochem* *46*, 669-678, doi: 10.1177/002215549804600512.
- Sharma, P. and Allison, J. P. (2015). The future of immune checkpoint therapy. *Science* *348*, 56-61, doi: 10.1126/science.aaa8172.
- Shiah, S. G., Shieh, Y. S. and Chang, J. Y. (2016). The Role of Wnt Signaling in Squamous Cell Carcinoma. *J Dent Res* *95*, 129-134, doi: 10.1177/0022034515613507.

- Siegfried, J. M., Gubish, C. T., Rothstein, M. E., Henry, C. and Stabile, L. P. (2012). Combining the multitargeted tyrosine kinase inhibitor vandetanib with the antiestrogen fulvestrant enhances its antitumor effect in non-small cell lung cancer. *J Thorac Oncol* 7, 485-495, doi: 10.1097/JTO.0b013e31824177ea.
- Siegfried, J. M., Hershberger, P. A. and Stabile, L. P. (2009). Estrogen receptor signaling in lung cancer. *Semin Oncol* 36, 524-531, doi: 10.1053/j.seminoncol.2009.10.004.
- Skinner, H. D., Giri, U., Yang, L. P., Kumar, M., Liu, Y., Story, M. D., Pickering, C. R., Byers, L. A., Williams, M. D., Wang, J., Shen, L., Yoo, S. Y., Fan, Y. H., Molkenkine, D. P., Beadle, B. M., Meyn, R. E., Myers, J. N. and Heymach, J. V. (2017). Integrative Analysis Identifies a Novel AXL-PI3 Kinase-PD-L1 Signaling Axis Associated with Radiation Resistance in Head and Neck Cancer. *Clin Cancer Res* 23, 2713-2722, doi: 10.1158/1078-0432.CCR-16-2586.
- Skov, B. G., Fischer, B. M. and Pappot, H. (2008). Oestrogen receptor beta over expression in males with non-small cell lung cancer is associated with better survival. *Lung Cancer* 59, 88-94, doi: 10.1016/j.lungcan.2007.07.025.
- Slaughter, D. P., Southwick, H. W. and Smejkal, W. (1953). Field Cancerization in Oral Stratified Squamous Epithelium - Clinical Implications of Multicentric Origin. *Cancer* 6, 963-968, doi: 10.1002/1097-0142(195309)6:5<963::Aid-Cncr2820060515>3.0.Co;2-Q.
- Smeets, S. J., Brakenhoff, R. H., Ylstra, B., van Wieringen, W. N., van de Wiel, M. A., Leemans, C. R. and Braakhuis, B. J. (2009). Genetic classification of oral and oropharyngeal carcinomas identifies subgroups with a different prognosis. *Cell Oncol* 31, 291-300, doi: 10.3233/CLO-2009-0471.
- Song, J. I. and Grandis, J. R. (2000). STAT signaling in head and neck cancer. *Oncogene* 19, 2489-2495, doi: 10.1038/sj.onc.1203483.
- Sorensen, K. D., Abildgaard, M. O., Haldrup, C., Ulhoi, B. P., Kristensen, H., Strand, S., Parker, C., Hoyer, S., Borre, M. and Orntoft, T. F. (2013). Prognostic significance of aberrantly silenced ANPEP expression in prostate cancer. *Br J Cancer* 108, 420-428, doi: 10.1038/bjc.2012.549.
- Stabile, L. P., Dacic, S., Land, S. R., Lenzner, D. E., Dhir, R., Acquafondata, M., Landreneau, R. J., Grandis, J. R. and Siegfried, J. M. (2011). Combined analysis of estrogen receptor beta-1 and progesterone receptor expression

identifies lung cancer patients with poor outcome. *Clin Cancer Res* 17, 154-164, doi: 10.1158/1078-0432.CCR-10-0992.

Stabile, L. P., Lyker, J. S., Gubish, C. T., Zhang, W., Grandis, J. R. and Siegfried, J. M. (2005). Combined targeting of the estrogen receptor and the epidermal growth factor receptor in non-small cell lung cancer shows enhanced antiproliferative effects. *Cancer Res* 65, 1459-1470, doi: 10.1158/0008-5472.CAN-04-1872.

Stewart, H. J. (1992). The Scottish trial of adjuvant tamoxifen in node-negative breast cancer. Scottish Cancer Trials Breast Group. *J Natl Cancer Inst Monogr*, 117-120.

Stransky, N., Egloff, A. M., Tward, A. D., Kostic, A. D., Cibulskis, K., Sivachenko, A., Kryukov, G. V., Lawrence, M. S., Sougnez, C., McKenna, A., Shefler, E., Ramos, A. H., Stojanov, P., Carter, S. L., Voet, D., Cortes, M. L., Auclair, D., Berger, M. F., Saksena, G., Guiducci, C., Onofrio, R. C., Parkin, M., Romkes, M., Weissfeld, J. L., Seethala, R. R., Wang, L., Rangel-Escareno, C., Fernandez-Lopez, J. C., Hidalgo-Miranda, A., Melendez-Zajgla, J., Winckler, W., Ardlie, K., Gabriel, S. B., Meyerson, M., Lander, E. S., Getz, G., Golub, T. R., Garraway, L. A. and Grandis, J. R. (2011). The mutational landscape of head and neck squamous cell carcinoma. *Science* 333, 1157-1160, doi: 10.1126/science.1208130.

Suh, Y., Amelio, I., Guerrero Urbano, T. and Tavassoli, M. (2014). Clinical update on cancer: molecular oncology of head and neck cancer. *Cell Death Dis* 5, e1018, doi: 10.1038/cddis.2013.548.

Swanson, M. S., Kokot, N. and Sinha, U. K. (2016). The Role of HPV in Head and Neck Cancer Stem Cell Formation and Tumorigenesis. *Cancers (Basel)* 8, doi: 10.3390/cancers8020024.

Swick, A. D., Prabakaran, P. J., Miller, M. C., Javaid, A. M., Fisher, M. M., Sampene, E., Ong, I. M., Hu, R., Iida, M., Nickel, K. P., Bruce, J. Y., Wheeler, D. L. and Kimple, R. J. (2017). Cotargeting mTORC and EGFR Signaling as a Therapeutic Strategy in HNSCC. *Mol Cancer Ther* 16, 1257-1268, doi: 10.1158/1535-7163.MCT-17-0115.

Syrjanen, S. (2005). Human papillomavirus (HPV) in head and neck cancer. *J Clin Virol* 32 Suppl 1, S59-66, doi: 10.1016/j.jcv.2004.11.017.

Szturz, P. and Vermorken, J. B. (2017). Immunotherapy in head and neck cancer: aiming at EXTREME precision. *BMC Med* 15, 110, doi: 10.1186/s12916-017-0879-4.

- Tabor, M. P., Brakenhoff, R. H., Ruijter-Schippers, H. J., Kummer, J. A., Leemans, C. R. and Braakhuis, B. J. (2004). Genetically altered fields as origin of locally recurrent head and neck cancer: a retrospective study. *Clin Cancer Res* 10, 3607-3613, doi: 10.1158/1078-0432.CCR-03-0632.
- Tian, X. Z., Chen, J., Xiong, W., He, T. and Chen, Q. (2009). Effects and underlying mechanisms of human opiorphin on colonic motility and nociception in mice. *Peptides* 30, 1348-1354, doi: 10.1016/j.peptides.2009.04.002.
- Tong, Y., Tar, M., Melman, A. and Davies, K. (2008). The opiorphin gene (ProL1) and its homologues function in erectile physiology. *BJU Int* 102, 736-740, doi: 10.1111/j.1464-410X.2008.07631.x.
- Tong, Y., Tar, M., Monrose, V., DiSanto, M., Melman, A. and Davies, K. P. (2007). hSMR3A as a marker for patients with erectile dysfunction. *J Urol* 178, 338-343, doi: 10.1016/j.juro.2007.03.004.
- Traynor, A. M., Schiller, J. H., Stabile, L. P., Kolesar, J. M., Eickhoff, J. C., Dacic, S., Hoang, T., Dubey, S., Marcotte, S. M. and Siegfried, J. M. (2009). Pilot study of gefitinib and fulvestrant in the treatment of post-menopausal women with advanced non-small cell lung cancer. *Lung Cancer* 64, 51-59, doi: 10.1016/j.lungcan.2008.07.002.
- Vassilakopoulou, M., Psyrris, A. and Argiris, A. (2015). Targeting angiogenesis in head and neck cancer. *Oral Oncol* 51, 409-415, doi: 10.1016/j.oraloncology.2015.01.006.
- Venuti, A. and Paolini, F. (2012). HPV detection methods in head and neck cancer. *Head Neck Pathol* 6 *Suppl* 1, S63-74, doi: 10.1007/s12105-012-0372-5.
- Vogelstein, B., Lane, D. and Levine, A. J. (2000). Surfing the p53 network. *Nature* 408, 307-310, doi: 10.1038/35042675.
- Wakeling, A. E. (2000). Similarities and distinctions in the mode of action of different classes of antioestrogens. *Endocr Relat Cancer* 7, 17-28.
- Wakeling, A. E., Dukes, M. and Bowler, J. (1991). A potent specific pure antiestrogen with clinical potential. *Cancer Res* 51, 3867-3873.
- Wang, J., Yang, Q., Haffty, B. G., Li, X. and Moran, M. S. (2013). Fulvestrant radiosensitizes human estrogen receptor-positive breast cancer cells. *Biochem*

Biophys Res Commun 431, 146-151, doi: 10.1016/j.bbrc.2013.01.006.

Wang, T. H., Hsia, S. M., Shih, Y. H. and Shieh, T. M. (2017). Association of Smoking, Alcohol Use, and Betel Quid Chewing with Epigenetic Aberrations in Cancers. *Int J Mol Sci* 18, doi: 10.3390/ijms18061210.

Wardley, A. M. (2002). Fulvestrant: a review of its development, pre-clinical and clinical data. *Int J Clin Pract* 56, 305-309.

Warnakulasuriya, S. (2009). Global epidemiology of oral and oropharyngeal cancer. *Oral Oncol* 45, 309-316, doi: 10.1016/j.oraloncology.2008.06.002.

Wazer, D. E., Tercilla, O. F., Lin, P. S. and Schmidt-Ullrich, R. (1989). Modulation in the radiosensitivity of MCF-7 human breast carcinoma cells by 17 β -estradiol and tamoxifen. *Br J Radiol* 62, 1079-1083, doi: 10.1259/0007-1285-62-744-1079.

Whiteside, T. L. (2017). Head and Neck Carcinoma Immunotherapy: Facts and Hopes. *Clin Cancer Res*, doi: 10.1158/1078-0432.CCR-17-1261.

Wilmott, J. S., Long, G. V., Howle, J. R., Haydu, L. E., Sharma, R. N., Thompson, J. F., Kefford, R. F., Hersey, P. and Scolyer, R. A. (2012). Selective BRAF inhibitors induce marked T-cell infiltration into human metastatic melanoma. *Clin Cancer Res* 18, 1386-1394, doi: 10.1158/1078-0432.CCR-11-2479.

Wisner, A., Dufour, E., Messaoudi, M., Nejd, A., Marcel, A., Ungeheuer, M. N. and Rougeot, C. (2006). Human Opiorphin, a natural antinociceptive modulator of opioid-dependent pathways. *Proc Natl Acad Sci U S A* 103, 17979-17984, doi: 10.1073/pnas.0605865103.

Xi, S., Zhang, Q., Gooding, W. E., Smithgall, T. E. and Grandis, J. R. (2003). Constitutive activation of Stat5b contributes to carcinogenesis in vivo. *Cancer Res* 63, 6763-6771.

Yamamoto, R., Nishikori, M., Tashima, M., Sakai, T., Ichinohe, T., Takaori-Kondo, A., Ohmori, K. and Uchiyama, T. (2009). B7-H1 expression is regulated by MEK/ERK signaling pathway in anaplastic large cell lymphoma and Hodgkin lymphoma. *Cancer Sci* 100, 2093-2100, doi: 10.1111/j.1349-7006.2009.01302.x.

Yan, F., Pang, J., Peng, Y., Molina, J. R., Yang, P. and Liu, S. (2016). Elevated Cellular PD1/PD-L1 Expression Confers Acquired Resistance to Cisplatin in Small Cell Lung Cancer Cells. *PLoS One* 11, e0162925, doi:

10.1371/journal.pone.0162925.

- Yang, W., Song, Y., Lu, Y. L., Sun, J. Z. and Wang, H. W. (2013). Increased expression of programmed death (PD)-1 and its ligand PD-L1 correlates with impaired cell-mediated immunity in high-risk human papillomavirus-related cervical intraepithelial neoplasia. *Immunology* 139, 513-522, doi: 10.1111/imm.12101.
- Yarden, Y. and Sliwkowski, M. X. (2001). Untangling the ErbB signalling network. *Nat Rev Mol Cell Biol* 2, 127-137, doi: 10.1038/35052073.
- Yoon, Y. K., Kim, H. P., Han, S. W., Hur, H. S., Oh, D. Y., Im, S. A., Bang, Y. J. and Kim, T. Y. (2009). Combination of EGFR and MEK1/2 inhibitor shows synergistic effects by suppressing EGFR/HER3-dependent AKT activation in human gastric cancer cells. *Mol Cancer Ther* 8, 2526-2536, doi: 10.1158/1535-7163.MCT-09-0300.
- Zhu, X., Zhang, F., Zhang, W., He, J., Zhao, Y. and Chen, X. (2013). Prognostic role of epidermal growth factor receptor in head and neck cancer: a meta-analysis. *J Surg Oncol* 108, 387-397, doi: 10.1002/jso.23406.

8. Supplements

Supplement 8-1. Univariate Cox regression models for progression-free and disease-specific survival

Risk factor	Progression-free survival			Disease-specific survival		
	HR	95% CI	p-value	HR	95% CI	p-value
Gender female vs male ¹	1.111	0.626-1.973	0.719	1.139	0.627-2.069	0.668
Age [years] ≥58 vs <58 ¹	0.647	0.403-1.039	0.072	0.715	0.433-1.180	0.189
T status T3-4 vs T1-2 ¹	1.831	1.097-3.055	0.021	2.189	1.238-3.871	0.007
N status N+ vs N0 ¹	0.981	0.486-1.980	0.957	1.090	0.518-2.296	0.820
Pathological grading G3 vs G1-2 ¹	1.074	0.627-1.840	0.795	0.985	0.551-1.762	0.961
Clinical staging IV vs I-III ¹	1.394	0.814-2.387	0.226	1.842	0.998-3.401	0.051
Alcohol current vs never/former ¹	1.073	0.563-2.043	0.831	1.187	0.603-2.337	0.620
Tobacco current vs never/former ¹	2.868	1.466-5.617	0.002	2.606	1.284-5.290	0.008
HPV status ² related vs non-related ¹	0.264	0.120-0.577	0.001	0.282	0.121-0.655	0.003
Subgroup ESR2 ^{pos} SMR3A ^{high} vs ESR2 ^{pos} SMR3A ^{low,1}	2.514	1.333-4.739	0.004	2.442	1.260-4.730	0.008
Subgroup All others vs ESR2 ^{pos} SMR3A ^{low,1}	2.492	1.469-4.230	0.001	2.307	1.319-4.036	0.003

HR = Hazard ratio, CI = confidence interval, ¹reference group, ²related = viral DNA⁺RNA⁺, non-related = viral DNA⁺RNA⁻ or viral DNA⁻ according to Holzinger et al., 2012.

Supplement 8-2. Multivariable Cox regression models for progression-free and disease-specific survival (N=66)

Risk factor	Progression-free survival			Disease-specific survival		
	HR	95% CI	p-value	HR	95% CI	p-value
Gender female vs male ¹	1.109	0.506-2.427	0.796	1.042	0.476-2.280	0.919
Age [years] ≥58 vs <58 ¹	0.618	0.295-1.296	0.209	0.624	0.280-1.394	0.250
Clinical staging IV vs. I-III ¹	1.530	0.745-3.142	0.247	1.966	0.909-4.251	0.086
Alcohol current vs never/former ¹	1.166	0.493-2.760	0.726	1.490	0.612-3.631	0.380
Tobacco current vs never/former ¹	2.016	0.720-5.646	0.182	1.799	0.639-5.011	0.268
HPV status ² related vs non-related ¹	0.429	0.130-1.480	0.184	0.415	0.124-1.388	0.153
Therapy RCT vs RT ¹	0.700	0.308-1.591	0.395	0.713	0.295-1.725	0.453
Subgroup ESR2 ^{pos} SMR3A ^{high} vs ESR2 ^{pos} SMR3A ^{low,1}	1.965	0.960-4.025	0.065	1.988	0.912-4.333	0.084

N=66 cases were included based on complete clinical data, HR = Hazard ratio, CI = confidence interval, ¹reference group, ²related = viral DNA⁺RNA⁺, non-related = viral DNA⁺RNA⁻ or viral DNA⁻ according to Holzinger et al., 2012.

Supplement 8-3. Multivariable Cox regression models for progression-free and disease-specific survival (N=103)

Risk factor	Progression-free survival			Disease-specific survival		
	HR	95% CI	p-value	HR	95% CI	p-value
Gender female vs male ¹	1.004	0.554-1.822	0.999	0.959	0.519-1.770	0.893
Age [years] ≥58 vs <58 ¹	0.686	0.421-1.118	0.130	0.719	0.426-1.213	0.216
Clinical staging IV vs. I-III ¹	1.544	0.876-2.721	0.133	2.039	1.081-3.843	0.028
Alcohol current vs never/former ¹	1.077	0.516-1.965	0.983	1.237	0.623-2.455	0.544
Tobacco current vs never/former ¹	1.855	0.922-3.734	0.083	1.783	0.854-3.722	0.124
HPV status ² related vs non-related ¹	0.298	0.134-0.659	0.003	0.308	0.130-0.727	0.007
Therapy RCT vs RT ¹	0.928	0.543-1.584	0.783	0.943	0.532-1.675	0.842
Subgroup All others vs ESR2 ^{pos} SMR3A ^{low,1}	1.877	1.075-3.277	0.027	1.561	0.872-2.796	0.134

N=103 cases were included based on complete clinical data, HR = Hazard ratio, CI = confidence interval, ¹reference group, ²related = viral DNA⁺RNA⁺, non-related = viral DNA⁺RNA⁻ or viral DNA⁻ according to Holzinger et al., 2012.

9. Curriculum vitae

Personal information

Name: Chao Rong
Date of birth: 03/11/1986
Place of birth: Hefei, China
Marital status: Happily married
Address: Oberdorfstr. 8, 69124 Heidelberg

Education

9.2004 - 6.2009	Bachelor of Medicine	Anhui Medical University, China
9.2009 - 7.2012	Master of Medicine	Anhui Medical University, China
9.2012 - 8.2014	Master of Science	Medical Faculty Mannheim, University of Heidelberg, Germany
9.2014 - Present	doctoral candidate	Medical Faculty Heidelberg, University of Heidelberg, Germany

Academic Training

12.2007- 12.2008	Clinical practice in PLA 105 hospital, Hefei, China
4.2010 - 9.2011	Graduate Student Researcher, School of Pharmacy, Anhui Medical University, China
12.2013 - 8.2014	Work for Master thesis at Department of Radiotherapy and Radiation Oncology, Medical Faculty Mannheim, University of Heidelberg, Germany
9.2014 - present	Work as a doctoral researcher in Section Experimental & Translational Head and Neck Oncology, Department of Otolaryngology, Medical Faculty Heidelberg, University of Heidelberg, Germany

10. Acknowledgements

First of all, I am especially grateful to my mentor Prof. Dr. Jochen Hess for providing the opportunity to perform my PhD thesis in the section Experimental and Translational Head and Neck Oncology, Department of Otolaryngology, Head and Neck Surgery at the University Hospital Heidelberg. Many thanks for his many creative ideas and conceptual design of this study, as well as his helpful and encouraging discussions. Appreciate heartily his patience and endurance when reviewing my dissertation, as well as his warmhearted encouragement and advice for my life and near future career.

I also wish to thank Prof. Dr. Peter Angel, head of Division of Signal Transduction and Growth Control at German Cancer Research Center, for kindly permitting me to perform experiments and access to the equipment and resources of his laboratory. I would like to thank Prof. Dr. Peter Plinkert, Director of Department of Otolaryngology, Head and Neck Surgery at the University Hospital Heidelberg, for providing excellent clinical documents and specimens in this study. I wish to thank Prof. Dr. Weber Klaus-Josef from Department of Radiation Oncology, for his valuable introduction and helpful support for irradiation.

Moreover, I appreciate many adorable colleagues who greatly contributed to my thesis during this time. Especially to all the technicians (Antje Schuhmann, Nataly Henfling, Ines Kaden, Leoni Erdinger and Ingeborg Vogt) for excellent technical assistance; Dr. Julia Thierauf, Dr. Adriana Jou, Dr. Annette Affolter, Dr. Jennifer Grünow, Marie, Tillmann, Steffen, Alexandra, Julia, Kathrin, Natalia, Katrin, Fasolt: many thanks for fruitful discussion on research and being awesome coworkers.

All former lab members have been never forgotten. Especially, Dr. Sarika Sharma, Dr.

Carola Schrader, Dr. Pilar Bayo-Zaera, Dr. Babitha George, Andre, Britta. Thanks for meeting you in the great team.

I would like to express my thanks to the group of friends in the master program of Mannheim Medical Faculty, who arrived in Germany together with me five years ago. Despite them not being listed here, I wish to appreciate my friends for making the years of study abroad a truly unique and unforgettable period in my life. Special thanks also go to the PhD fellowship support from China Scholarship Council.

Finally, I would like to express my gratefulness to my parents, who always support and love me. My thesis work would not have been achieved without the unconditional support of my wife, Xiaojuan Cao, who has been there for me all the time.

